Interactions driving Chaperone-assisted Assembly of Proteasome Core particles

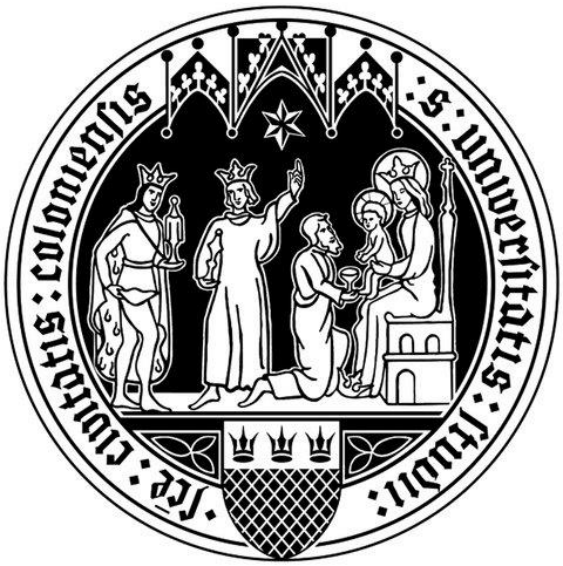

Inaugural-Dissertation

zur

Erlangung des Doktorgrades

der Mathematisch-Naturwissenschaftlichen Fakultät

der Universität zu Köln

vorgelegt von

Jessica Zimmermann

aus Mechernich

Köln, 2023

Berichterstatter: Prof. Dr. R. Jürgen Dohmen
(Gutachter)

Prof. Dr. Kay Hofmann

Tag der mündlichen Prüfung: 20.10.2023

Table of Contents

List of Figures

List of Tables

Abstract

The ubiquitin-proteasome system (UPS) of eukaryotic cells provides an essential proteolytic control system, malfunctions of which are linked to various human diseases. The central component of the UPS is the 26S proteasome, a protease complex composed of a catalytic 20S core particle (CP) and one or two attached 19S regulatory particles (RP). Proteasome assembly is a conserved ordered process involving different intermediates and chaperones associated, which was thought to be initiated by the formation of rings comprising seven distinct α subunits. A critical intermediate in CP assembly is the 15S precursor complex (PC) containing all α and β subunits except for β7, as well as the chaperones Ump1 and Pba1-Pba2. Although the crystal structure of the mature 20S CP is already known, the step-wise process of proteasome formation is still not completely understood. The present study reveals important aspects concerning early assembly intermediates for the formation of the 15S precursor complex, the dimerization of such complexes into 20S CPs as well as specific interactions important during proteasome assembly and maturation. Using an integrated approach comprising codon adaptation and gene fusion technologies, it was possible to obtain distinct yeast proteasome components in sufficient quantities to be used for specific antibody production. In contrast to the α-ring as an early assembly intermediate, we identified two complementary complexes containing distinct subsets of α and β subunits, Complex I (α1-α4, β2-β4, Ump1) and Complex II (α5-α7, Pba3-Pba4), which constitute preliminary assembly intermediates for the formation of the 15S precursor complex, a process likely facilitated by Pba1-Pba2. With the help of *in vitro* binding experiments, these studies identified a novel function of the Ump1 N-terminus in the recruitment of Pro-β7 to the 15S PC complexes to drive their dimerization. Furthermore, the incorporation of the β7 subunit into the complex was confirmed to be the critical step in dimerization of 15S PCs followed by active site maturation of the catalytic subunits leading to proteolytically active 20S PCs and the degradation of Ump1.

1 Introduction

1.1 Intracellular protein degradation

Living systems undergo a continual turnover at all levels of organization, from populations of whole organisms to populations of molecules within cells that are continually degraded and replaced by new synthesis (Schoenheimer, 1942). Besides the function of adaptation and other cellular processes, a controlled regulation of proteins is important for the removal of abnormal proteins, which might arise by mutations, errors in gene expression, denaturation, or chemical modification (Goldberg and Wittes, 1966; Woese, 1970). Irreversible accumulation of abnormal proteins has been linked to the development of aging-related diseases that include neurodegenerative disorders such as amyotrophic lateral sclerosis (Cozzi and Ferrari, 2022), Parkinson's disease (Ho *et al.*, 2020) or Alzheimer's disease (Morawe *et al.*, 2012), metabolic disorders (Sooparb *et al.*, 2004; Kimura *et al.*, 2015) or even cancer (Frankland-Searby and Bhaumik, 2012; Fulop *et al.*, 2013). To maintain a balance between folding efficiency, misfolding, protein degradation and aggregation, the cell possesses two main components contributing to proteostasis: molecular chaperones and intracellular proteolytic systems (Frankowska *et al.*, 2022). While chaperones promote folding, assembly and trafficking of newly synthesized proteins counteracting misfolding and aggregation of nascent proteins, proteolytic machineries are responsible for the degradation of misfolded or malfunctioning proteins (Saibil, 2013). Apart from a group of free cytoplasmic proteases including calpains, caspases, and the desintegrase and metalloproteinase (ADAM) families, the main intracellular proteolytic systems responsible for protein turnover are the ubiquitin-proteasome system (UPS) and the autophagy-lysosome pathway (ALP) (Figure 1.1) (Horvitz, 1999; Sorimachi *et al.*, 2011; Kaushik and Cuervo, 2015; Mullooly *et al.*, 2016).

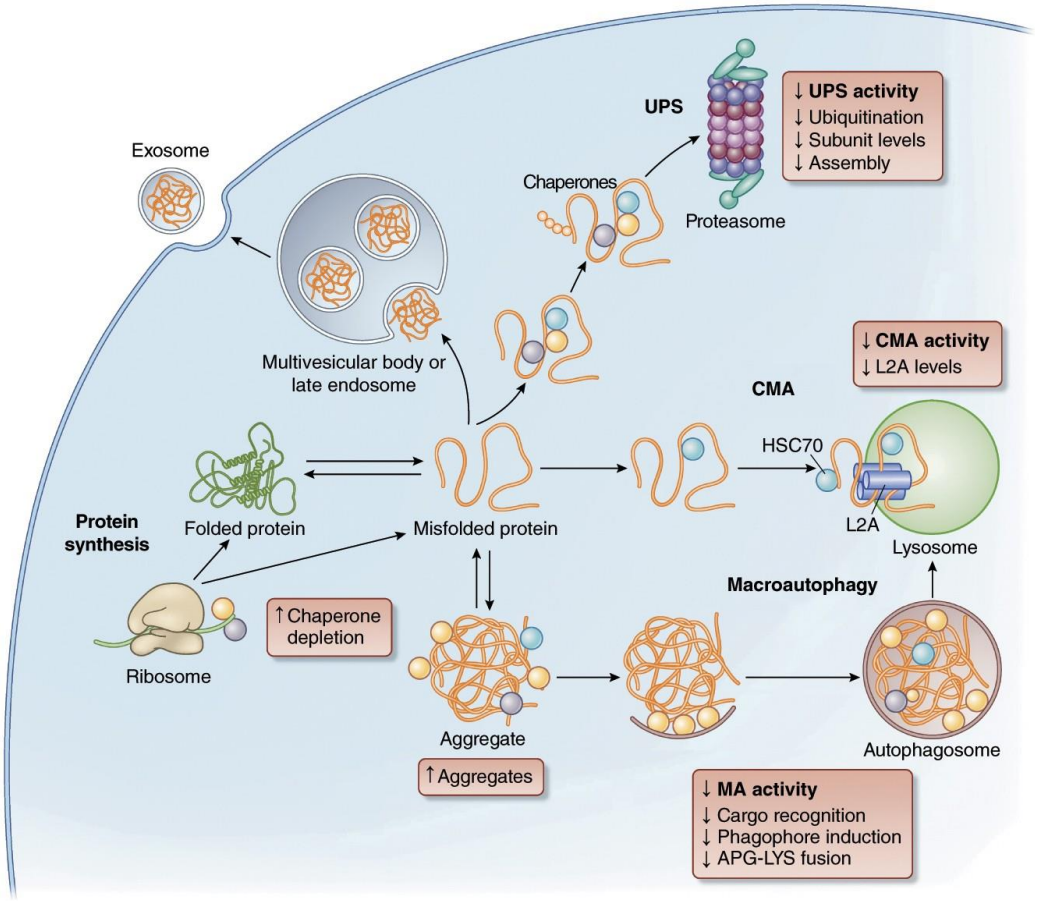

Figure 1.1 – Intracellular proteostasis systems and their changes with age. Intracellular proteostasis is maintained by chaperones and two proteolytic systems, the ubiquitin-proteasome system (UPS) and autophagy. *De novo* synthesized proteins and unfolded proteins are folded with the help of chaperones (blue, yellow and gray circles). If folding is not possible, proteins are targeted for degradation by the proteasome or lysosomes. For chaperone-mediated autophagy (CMA), single soluble proteins are carried through a membrane transporter to the lysosomal lumen. Oligomers and insoluble aggregates, however, can only be eliminated from the cytosol by degradation in lysosomes through macroautophagy (MA) or expulsion outside the cell by means of small vesicles (exosomes). Red boxes indicate changes with age in different steps or components of the proteostasis networks. APG-LYS, autophagosome-lysosome; HSC70, heat-shock cognate protein of 70 kDa; L2A, lysosome-associated membrane protein type 2A (Figure taken from Kaushik and Cuervo, 2015).

In contrast to the proteasome, which only degrades proteins, the lysosomal system can digest different macromolecules, aggregates, or even extracellular material (Galluzzi *et al.*, 2017). Thereby three possible ways of autophagic degradation can be distinguished (Galluzzi *et al.*, 2017). Whereas microautophagy relies on the direct uptake of cytosolic cargo through a lysosomal membrane invagination (Farré and Subramani, 2004; Uttenweiler and Mayer, 2008), macroautophagy involves the incorporation of cytoplasmic material by the phagophore, a *de-novo* generated vesicle (Yang and Klionsky, 2010). After the formation of double membrane vesicles around the cargo, these autophagosomes fuse with the lysosome to generate autolysosomes, and the content of the vesicle is degraded (Amaya *et al.*, 2015).

In contrast to micro- and macroautophagy, chaperone-mediated autophagy (CMA) is targeted against single proteins which are delivered to the lysosomal lumen to be degraded in a selective manner (Kaushik and Cuervo, 2012). The ubiquitin-proteasome system preferentially degrades soluble and polyubiquitylated naturally short-lived, damaged or otherwise abnormal proteins (Hershko and Ciechanover, 1992). The main machinery in this system is the 26S proteasome, which is responsible for the ATP-dependent degradation of 80 % of cellular proteins. Thus it is not surprising that malfunctions within the UPS have been associated with a variety of human diseases, and the proteasome has become an important therapeutic target for anti-cancer treatment (Hershko and Ciechanover, 1986; Crawford *et al*., 2011; Chitra *et al*., 2012; Kaplan *et al.*, 2017).

1.2 The ubiquitin-proteasome system

To ensure that a protein is functioning properly, it is subjected to a process referred to as protein quality control (Amm *et al*., 2014). In this process, a rapid and efficient recognition of unfolded or misfolded proteins is essential to prevent the formation of insoluble aggregates and consequential potential damage to the cellular homeostasis (Gottesman *et al*., 1997). Improperly folded proteins are either retained and subjected to additional rounds of folding cycles facilitated by molecular chaperones or eventually targeted for degradation by the ubiquitin-proteasome system (UPS) (Hartl and Hayer-Hartl, 2009). The UPS exerts quality control not only on proteins in the cytosol, which is, together with the endoplasmic reticulum (ER), the primary location for *de novo* protein synthesis, but also in the nucleus and at the ER (Amm *et al*., 2014). The cytosolic and nuclear protein quality control can be directly linked to components of the UPS. Chaperones and degradation machineries regulate whether unfolded proteins are targeted for either refolding or degradation in a direct cross-talk, a mechanism known as the protein triage (Arndt *et al*., 2007). In contrast to the cytosol and the nucleus, the identification of misfolded proteins in the ER initially takes place in complete isolation of the UPS. As many of these proteins are secretory and cell surface proteins, being exposed to the stringent extracellular milieu, folding is more complicated (Sitia and Braakman, 2003). Besides retention for additional folding cycles, not properly folded proteins are targeted back to the cytosol in a ubiquitin-dependent process known as endoplasmic reticulum-associated degradation (ERAD) (Ellgaard and Helenius, 2003;

Vembar and Brodsky, 2008). In the UPS, substrate proteins are identified and then targeted for degradation by the proteasome, which is able to destruct almost any polypeptide (Hershko and Ciechanover, 1998). To ensure targeting specificity, the UPS relies on the attachment of ubiquitin to the substrate, a process which is performed by an E1-E2-E3 cascade of enzymes (Hershko, 1996). However, degradation is not the only possible fate for ubiquitin tagged proteins. Ubiquitylation also regulates certain biological processes without a link to protein degradation. Examples include DNA repair, the initiation of the inflammatory response, morphogenesis, and transcriptional control, (Hochstrasser, 1996; Hershko and Ciechanover, 1998; Peters *et al*., 1998).

1.2.1 Ubiquitylation pathway

Ubiquitin (Ub) is a small protein with a molecular weight of about 8.5 kDa, and ubiquitylation is among the major post-translational modifications (PTM) of proteins (Xu and Jaffrey, 2013). As the amino acid sequence of ubiquitin variants differs in only 3 of 76 residues between organisms, ubiquitin is the most conserved known protein in eukaryotes (Ozkaynak *et al*., 1984). Ubiquitylation, which is usually the covalent attachment of the carboxyl terminus of ubiquitin to an ε-amino group of a substrate lysine through an isopeptide linkage, is an enzymatic reaction generally carried out by a cascade of three different classes of enzymes: the ubiquitin-activating enzyme (E1), one of several ubiquitin-conjugating enzymes (E2), and one of many different ubiquitin-protein ligases (E3) (Finley *et al.*, 2012). The reaction is initiated by Uba1, which is the only known ubiquitin-activating enzyme in *Saccharomyces cerevisiae* and essential for viability. A thioester bond is formed between the C-terminal glycine of ubiquitin and a cysteine residue of Uba1, leading to an intermediate state under consumption of ATP with subsequent release of AMP and pyrophosphate (Finley *et al.*, 2012). In the second step, activated ubiquitin is transferred to an active site cysteine residue within one of eleven ubiquitin-conjugating enzymes in yeast (Finley *et al.*, 2012). Finally, the formation of isopeptide bonds between ε-amino groups of lysine residues in substrate proteins and the activated carboxyl group of ubiquitin is catalyzed by one of many ubiquitin-ligases (with 60-100 members in yeast), mediating the high selectivity of ubiquitylation by direct interaction with substrates (Figure 1.2) (Varshavsky, 2012).

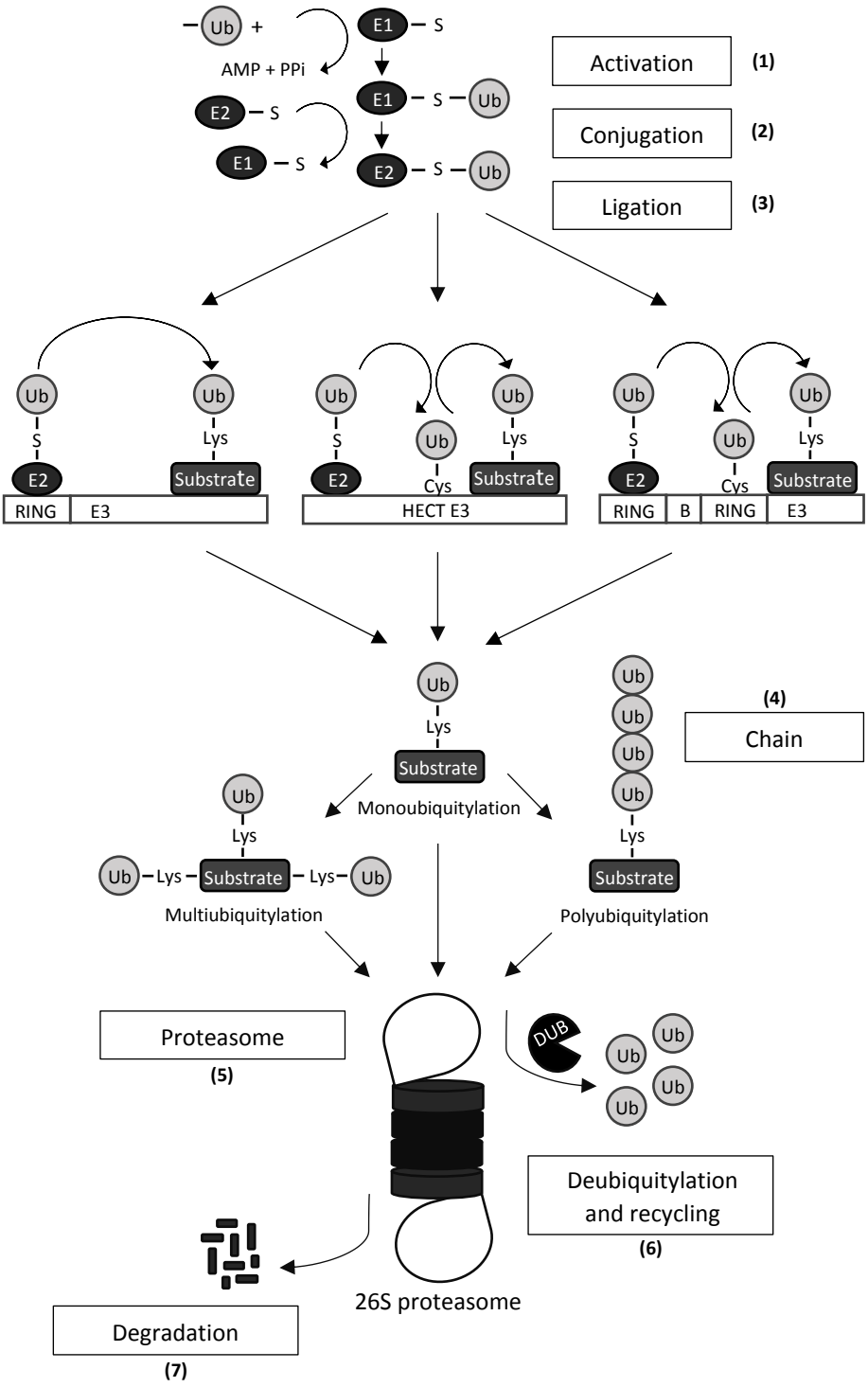

Figure 1.2 – The ubiquitin-proteasome system. (1) Ubiquitin (Ub) is activated in an ATP-dependent reaction by ubiquitin-activating enzyme (E1), (2) conjugated to an E2 enzyme, and (3) subsequently transferred to a lysine (Lys) residue of the substrate protein through three different classes of ubiquitin ligases (E3). HECT-type and RBR-type E3 transfer ubiquitin onto the substrate through an intermediate step whereby the ubiquitin is transferred onto its own cysteine (Cys) residue whereas the RING-type E3 promote transfer of ubiquitin directly from the E2-Ub complex onto the Lys residue of the substrate protein. Thioester linkage is denoted by -S-. (4) Mono-, multi-, or polyubiquitylated substrates modified at one or several lysine (Lys) residues are (5) targeted to the proteasome where (6) ubiquitin moieties are removed and recycled by deubiquitylating (DUB) activities, and (7) the substrate is unfolded and degraded by the 26S proteasome.

E3 enzymes can be typically assigned into three major classes: RING (Really Interesting New Gene) domain E3s, HECT (Homologous to the E6-AP Carboxyl Terminus) domain E3s and RBR (RING-Between-RING) family E3s (Berndsen and Wolberger, 2014). RING and RBR ligases have the common feature of zinc binding domains, which mediate binding to the E2 enzyme. RING E3 ligases mediate direct transfer of ubiquitin from the E2 enzyme to the substrate, simultaneously binding both the E2~Ub thioester and the substrate (Metzger *et al.*, 2013). In the case of HECT E3 ligases, ubiquitin is first transferred from the E2 to an E3-internal cysteine residue and an intermediate thioester linkage is formed. Afterwards, ubiquitin is transferred to a lysine residue of the substrate to create an isopeptide bond (Huibregtse *et al.*, 1995). RBR-type ligases however, feature characteristics of both RING and HECT domain E3s. The E2 enzyme is recognized in a similar way to the canonical RING-type ligases, but ubiquitylation occurs via an ubiquitin-thioester intermediate involving a cysteine residue in the second RING domain of the same ligase (Gundogdu and Walden, 2019).

The fate of ubiquitylated proteins is decided by the nature of the ubiquitin modification. While monoubiquitylation describes the attachment of a single ubiquitin molecule to a substrate protein, multiubiquitylation involves the binding of multiple single ubiquitin molecules to several acceptor lysine residues in one protein. Both ubiquitylation types often mediate proteasome-independent functions such as protein binding, subcellular localization, intracellular trafficking, and modulation of activity (Hicke, 2001; Kravtsova-Ivantsiv *et al*., 2009; Ziv *et al.*, 2011). Polyubiquitylation involves the formation of ubiquitin–ubiquitin conjugates, in which any of the seven lysine residues of ubiquitin (K6, K11, K27, K29, K33, K48, and K63) can serve as an isopeptide bond acceptor in yeast and mammals. The resulting chains define distinct signals. The best-studied type is the K48-linked ubiquitin chain, which is critical for protein degradation and essential for viability. In contrast, K63-linked chains are mainly implicated in DNA repair mechanisms and trafficking of membrane proteins, and K11-linked ubiquitin chains are assumed to be involved in the ERAD pathway (Peng *et al.*, 2003; Tagwerker *et al.*, 2006; Meierhofer *et al.*, 2008; Dikic *et al*., 2009; Xu *et al.*, 2009; Komander and Rape, 2012). Overall, besides its proteolytic functions, ubiquitylation plays important roles in the regulation of a substrate's activity, its interactions with other proteins, or its localization (Komander and Rape, 2012).

1.2.2 Deubiquitylation

Like other post-translational modifications, ubiquitylation is a reversible process. Ubiquitin can be removed from a substrate protein by peptidases called deubiquitylating enzymes (DUBs) (Komander et al., 2009). Besides removing ubiquitin from substrate proteins, DUBs are also responsible for the processing of ubiquitin precursors and the editing of ubiquitin chains. Proteins related to DUBs act on ubiquitin-like proteins (UBLs) such as the small ubiquitin-like modifier (SUMO) and their conjugates (Van Der Veen and Ploegh, 2012). Prominent examples are the SENP (Sentrin/SUMO-specific protease) proteins which process SUMO precursors and SUMO conjugates (Huang *et al.*, 2015). Based on sequence and domain conservation, DUBs are classified into seven families: ubiquitin-specific proteases (USPs/UBPs), ubiquitin c-terminal hydrolases (UCHs), Machado-Josephin domain-containing proteases (MJDs), ovarian tumor proteases (OTUs), zinc finger with UFM1-specific peptidase domain protein protease (ZUFSP), motif-interacting with ubiquitin-containing novel DUB family (MINDYs) and the JAB1, MPN, MOV34 family (JAMMs) (Hermanns and Hofmann, 2019; Suresh *et al*., 2020). While JAMMs are zinc metallopeptidases, the other DUB families and SENPs are cysteine peptidases (Harrigan *et al.*, 2018). All DUB families besides MJDs and ZUFSPs are conserved in *Saccharomyces cerevisiae* comprising 22 putative DUB genes encoded in the genome (Suresh *et al*., 2020). The only DUB activity essential for viability in yeast is mediated by the Rpn11 subunit of the proteasome lid subcomplex (Amerik and Hochstrasser, 2004). Together with Ubp6, it has an interesting functional interplay in regulating substrate degradation at the proteasome as well as the biogenesis and stability of the RP subcomplex (Verma *et al.*, 2002; Bashore *et al.*, 2015).

1.2.3 Degradation signals for ubiquitin-mediated proteolysis

The ubiquitin-proteasome system degrades a wide range of proteins in a highly selective manner enabled by specific degradation signals (degrons) within the protein (Ravid and Hochstrasser, 2008). Degrons are usually defined as minimal elements within a protein that are sufficient for recognition and degradation by a proteolytic apparatus. They can be regulated either signal-dependent, or by protein folding and assembly, as it often occurs in protein quality control (Ravid and Hochstrasser, 2008). One important example is the N-end

rule pathway, according to which protein half-life is determined by its N-terminal amino acid residue. This destabilizing residue, called the N-degron, was the first degradation signal component described in *S. cerevisiae* (Varshavsky, 1996). Whereas amino terminal residues such as alanine, cysteine or methionine are highly stabilizing residues, arginine, lysine, leucine, phenylalanine, tryptophan, tyrosine, histidine, isoleucine, asparagine, aspartic acid and glutamic acid are rather destabilizing N-terminal residues. Exposure of these residues is usually a result of post-translational events such as endoproteolytic cleavage (Varshavsky, 1996). A specific type of ubiquitin ligases, the N-recognin Ubr1, recognizes the destabilizing N-terminus and targets the protein for proteasomal degradation (Bartel *et al.*, 1990). Many other degradation pathways mediated by distinct E3 ligases exist in the cell. For instance, a variety of degrons are formed by post-translation modification, such as phosphorylation, or exposure of hydrophobic patches, that were hidden in the normally correctly folded structure, and which are recognized by ubiquitin ligases with distinct substrate recognition modes (Johnson *et al.*, 1998; Finley *et al.*, 2012). Another interesting degron variant formed by post-translational modification is recognized by the small ubiquitin-related modifier (SUMO)-targeted ubiquitin ligases (STUbLs) (Perry *et al.*, 2008). These E3 enzymes contain SUMO interacting motifs that mediate binding to SUMOylated substrate proteins for ubiquitylation (Finley *et al.*, 2012).

1.3 The 26S proteasome

Two major proteasome species coexist in most cells: the 20S core particle (CP) as a standalone complex that does not rely on ubiquitin as a degradation signal but can degrade substrates with a considerable unstructured stretch, and the 20S complex as a core complex that forms together with the regulatory particles or activators the highly regulated 26S proteasome (Sahu and Glickman, 2021). The 26S proteasome is a giant multimeric protease complex of ~2.5 MDa that is found in both nucleus and cytoplasm of eukaryotic cells and is essential for viability (Baumeister *et al.*, 1998). In general, proteasomes are organized in an ATP-independent barrel-shaped 20S catalytic core particle, flanked by one or two ATP-dependent 19S regulatory particles (RP) (Figure 1.3) (Matias *et al.*, 2010; Huang *et al.*, 2016). While the RP is mainly responsible for recognition, deubiquitylation, unfolding and translocation of substrate proteins into the CP, the proteolytic active sites are localized within

an interior chamber of the core particle (Saeki and Tanaka, 2012). Substrates are routed from the RP to the CP through a narrow substrate translocation channel, which can exist in open and closed states, ensuring strictly controlled access of substrate proteins thereby minimizing nonspecific proteolysis (Finley *et al.*, 2012).

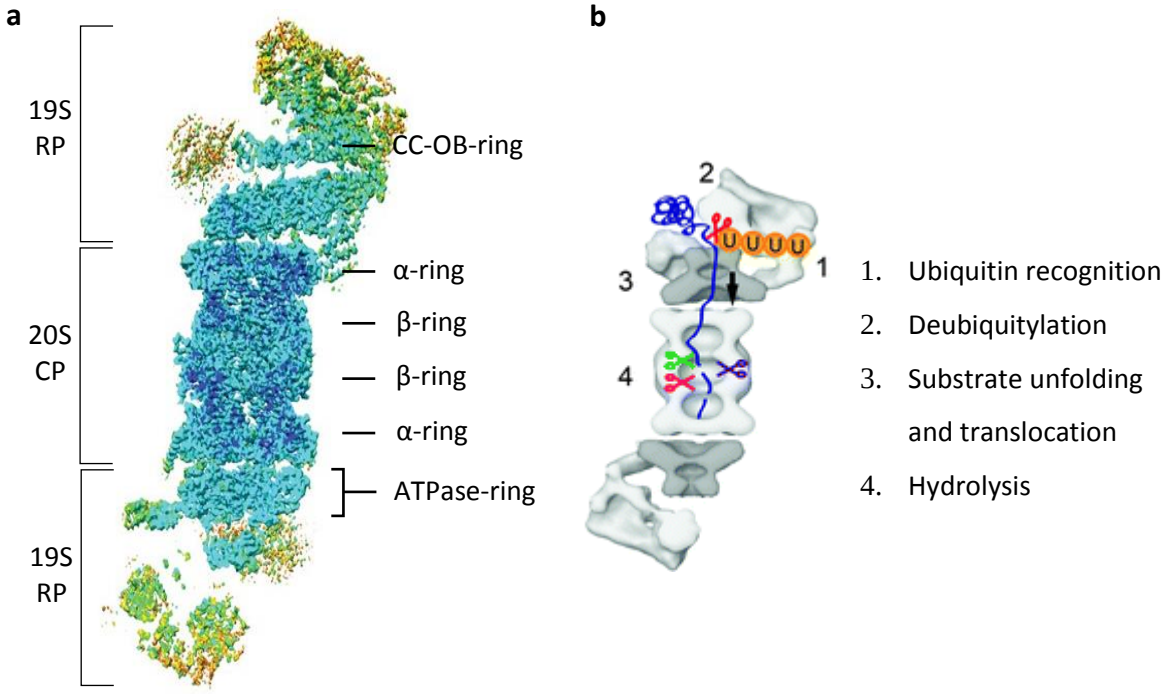

Figure 1.3 – Structure and function of the 26S proteasome. (a) Cryo-EM structure and **(b)** model based upon electron microscopy images with a cut open view of the proteasome, composed of an 20S core particle (CP) flanked by two 19S regulatory particles (RP). The CP is formed by four stacked rings with two outer α- and two inner β-rings. The 19S ATPase subunits form a double ring structure, called the CC-OB-ring and the ATPase-ring. Polyubiquitin chains with four or more ubiquitin (U) are recognized by the proteasome, unfolded, translocated into the CP bearing the proteolytic active sites, and degraded into small peptides. Concomitantly, the polyubiquitin chains are disassembled by deubiquitylating activities. Figures adapted from Huang *et al.*, 2016 (a) and Saeki and Tanaka, 2012 (b).

1.3.1 The 19S regulatory particle

The regulatory particle (RP), also known as PA700 is the major activator of the 20S proteasome, enabling the degradation of ubiquitin tagged proteins (Chu-Ping *et al.*, 1994). 19S RPs can attach at either one or both sides of a single 20S catalytic core particle to form the 26S or the 30S proteasome, respectively (Yoshimura *et al.*, 1993). In *S. cerevisiae*,

15 essential and 4 non-essential subunits form the two subcomplexes of the 19S, the base and the lid (Figure 1.4) (Glickman *et al.*, 1998).

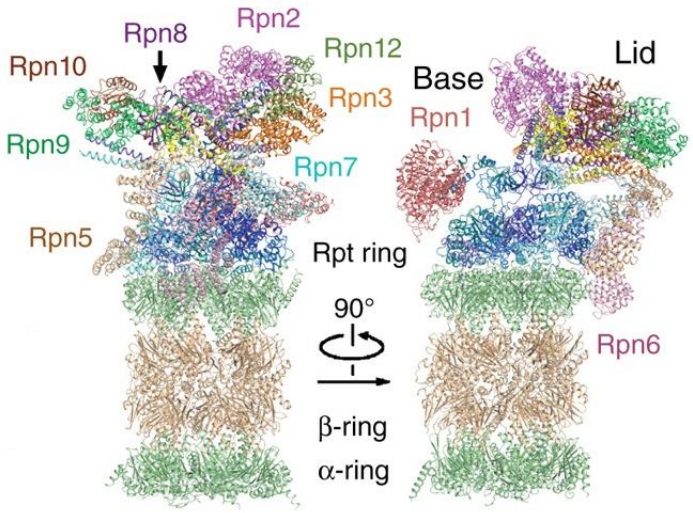

Figure 1.4 – Architecture of the 19S regulatory particle. Cartoon representation of the human proteasome in two perpendicular views, showing various subunits in different colors (Figure taken from Huang *et al.*, 2016).

Aside from opening the gate into the 20S CP and unfolding of the substrate proteins, the base-subcomplex is assumed to provide substrate interaction sites and translocates proteins into the core particle (Lander *et al.*, 2012). It contains six ATPase subunits (Rpt1-6, Regulatory particle ATPase) that belong to the family of so called AAA+ (ATPases associated with various cellular activities) proteins (Beyer, 1997). These proteins form hexameric rings and are characterized by a highly conserved nucleotide binding module of 220-250 amino acids (Kunau *et al.*, 1993). ATP binding and hydrolysis are necessary to exert a pulling force on substrate proteins, unfold them, and translocate the polypeptides through the narrow central pore into the peptidase chamber (Lander *et al.*, 2012). Gate opening requires ATP binding and structural rearrangements of the 20S CP α subunit N-termini mediated by the insertion of specific C-terminal HbYX motifs (hydrophobic/tyrosine/unspecific residue) of the 19S ATPase subunits into pockets formed between the α subunits (Matyskiela and Martin, 2013). Although only three of the six ATPases, Rpt2, Rpt3 and Rpt5, contain HbYX sequences, crosslinking studies suggested that the tails of Rpt1, Rpt4 and Rpt6 might also dock into α-pockets, interacting with the core as well (Tian *et al.*, 2011). Besides Rpt1-6, the base contains four non-ATPase subunits:

Rpn1, Rpn2, and the ubiquitin chain receptors Rpn10 and Rpn13 (Lander *et al.*, 2012). While proteins with single chains of K48-linked ubiquitin are targeted for degradation almost exclusively through binding to Rpn10, Rpn1 can act as a co-receptor with Rpn10 for K63 chains and for certain other chain types (Martinez-Fonts *et al.*, 2020). Additional ubiquitin shuttle receptors, Rad23, Dsk2 and Ddi1, share an Ub association domain (UBA) and an Ub-like domain (UBL) (Elsasser *et al.*, 2002; Gomez *et al.*, 2011). The about 55 residue comprising UBA domain occurs in subsets of the E2, E3 and UBP superfamilies and is necessary for binding to ubiquitin domains (Hofmann and Bucher, 1996). The Ub-like domain is important for binding the base subcomplex via Rpn1, which specifically recognizes the leucine-rich-repeat-like (LRR-like) domain of the UBLs (Elsasser *et al.*, 2002; Gomez *et al.*, 2011).

The lid subcomplex is composed of nine non-ATPase subunits, Rpn3, Rpn5-9, Rpn11, Rpn12 and Rpn15/Sem1 in yeast and contacts the base at many different points via different subunits (Lander *et al.*, 2012). The deubiquitylating (DUB) Rpn11 subunit contains an MPN (Mpr1/Pad1 N-terminal) domain that provides metalloprotease activity, which removes ubiquitin from substrates and is essential for efficient substrate degradation (Verma *et al.*, 2002; Yao and Cohen, 2002). A subset of MPN domain proteins such as Rpn11 and Csn5/Jab1 contain a highly conserved MPN+ motif, which is critical for Rpn11 function, but does not occur outside of this subfamily (Maytal-Kivity *et al.*, 2002).

The regulatory particle is the only proteasome activator that is known to stimulate degradation of ubiquitylated protein substrates (Rechsteiner and Hill, 2005). However, three other evolutionarily conserved protein complexes, PA28 (proteasome activator of apparent subunit molecular weight 28 kDa, also known as REG (11S regulator)), PI31 and PA200, exist, which do not recognize ubiquitylated proteins or use ATP, but were shown to specifically bind to and activate 20S proteasomes against model peptide substrates (Hill *et al.*, 2002; Ustrell *et al.*, 2002; Zaiss *et al.*, 2002). One 20S CP can interact at both ends with either two identical or two different regulators, resulting in hybrid proteasomes (Tanahashi *et al.*, 2000). PA28 family members, which are found in higher eukaryotes, but are apparently absent from yeasts, exist as homo- or heteromeric complexes of seven ~28 kDa subunits (Rechsteiner and Hill, 2005). In mammals, PA28 has a broad tissue distribution and is expressed in three isoforms termed PA28α, β, γ (Hill *et al.*, 2002). PI31 (PSMF1), which acts *in vitro* as an inhibitor of proteasome activity, was shown to rather function as a selective

modulator *in vivo* by controlling immunoproteasome formation and maintaining an effective intracellular balance between constitutive and immunoproteasome in the absence/presence of infection (Zaiss *et al.*, 2002).

Unlike the 11S and 19S activators, which use multiple C-termini to bind in pockets between α subunits, mammalian PA200 and its yeast homolog Blm10 are single chain proteins of 1843 and 2143 residues (~200/250 kDa), respectively (Ustrell *et al.*, 2002; Sadre-Bazzaz *et al.*, 2010). These large, internally repetitive proteins are mainly nuclear and were shown to activate proteasomal hydrolysis of model peptides, but not folded proteins (Ustrell *et al.*, 2002). Blm10 is predominantly found within hybrid Blm10-CP-RP complexes, activating the CP by opening the axial channel into its proteolytic chamber (Schmidt *et al.*, 2005). The crystal structure of a proteasome-Blm10 complex (Figure 1.5) revealed that Blm10 forms a closed dome on the top of the CP and that its C-terminal HbYX motif interacts via α6-Lys66 in the pocket formed between the α5 and α6 subunits (Sadre-Bazzaz *et al.*, 2010).

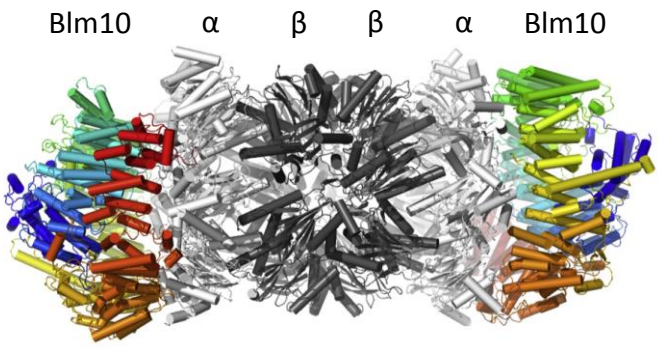

Figure 1.5 – Structure of the Blm10-Proteasome complex. Cartoon side view representation of the Blm10-20S proteasome complex. 20S CP subunits of the α- and β-ring are represented in white (α subunits) and gray (β subunits). Blm10 is highlighted in rainbow colors from N-terminus in blue to C-terminus in red. Figure adapted from Sadre-Bazzaz *et al*., 2010.

1.3.2 The 20S core particle

The 20S core particle is a highly conserved, barrel-shaped complex composed of four stacked heptameric rings, two outer α- and two inner β-rings each consisting of seven subunits (Kunjappu and Hochstrasser, 2014). Whereas the outer rings form a narrow substrate entry channel, the two inner rings create an internal chamber containing the

proteolytic active sites responsible for protein cleavage (Budenholzer *et al.*, 2017). In contrast to CPs of simpler organisms like archaea and bacteria, which consist of homo-heptameric α- and β-rings, more complex organisms such as eukaryotes possess CPs composed of 14 distinct α and β subunits with specific functions and unique positions within the ring (Figure 1.6) (Löwe *et al.*, 1995; Groll *et al.*, 1997; Unno *et al.*, 2002).

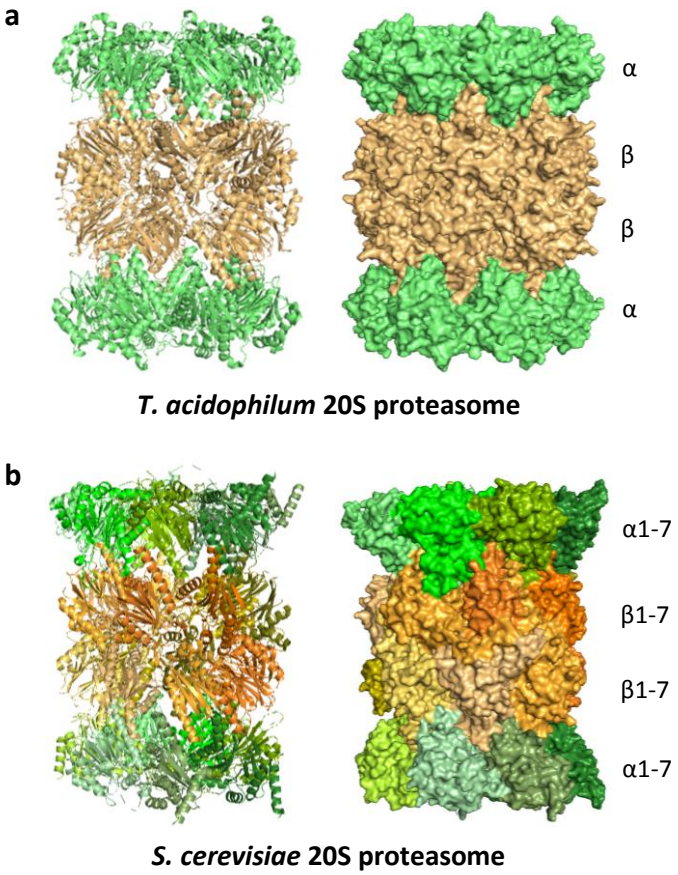

Figure 1.6 – Structural comparison between a prokaryotic and a eukaryotic 20S proteasome. Side view ribbon (left) and surface (right) representation of the crystal structure from *Thermoplasma acidophilum* (a; PDB code 1PMA) and *S. cerevisiae* (b; PDB code 2F16) 20S proteasome. For *T. acidophilum*, identical α and β subunits are shown in green and orange, respectively. In the case of *S. cerevisiae*, the 14 individual α and β subunits are highlighted in different shades of green and orange, respectively. The crystal structure representations were prepared using PyMOL (http://pymol.org).

In *S. cerevisiae*, these subunits are encoded by a family of related but distinct genes, which have similar amino acid sequences as well as molecular weights, and can be divided into an α-type and a β-type group (Table 1.1) (Baumeister *et al.*, 1998). Except for Pre9/α3, all proteasomal core particle subunits are essential for cell viability (Emori *et al.*, 1991). *PRE9*

deletion is not lethal because in mutant proteasomes, the missing α3 subunits are replaced with additional copies of Pre6/α4, resulting in 20S CPs bearing two α4 subunits per α-ring (Velichutina *et al.*, 2004). As anticipated from their sequence similarity, α- and β-type subunits share a similar overall protein structure with a central five-stranded β sandwich flanked on either side by α-helices, helix H1-2 on one side and H3-5 on the other (Baumeister *et al.*, 1998). However, the main difference between α- and β-type subunits in eukaryotes is an additional highly conserved N-terminal extension (H0) of the α-type subunits, forming a dense network in the center of the heptameric ring to restrict unregulated access to the internal chamber (Baumeister *et al.*, 1998; Groll *et al.*, 2000). In particular the N-terminal residues of the α3 subunit seem to have an important role in closing the pore by making contact with the N-terminal residues of the other six α subunits, as a deletion of the N-terminal residues 2-10 (α3ΔN) is sufficient to open the pore (Figure 1.7) (Groll *et al.*, 2000).

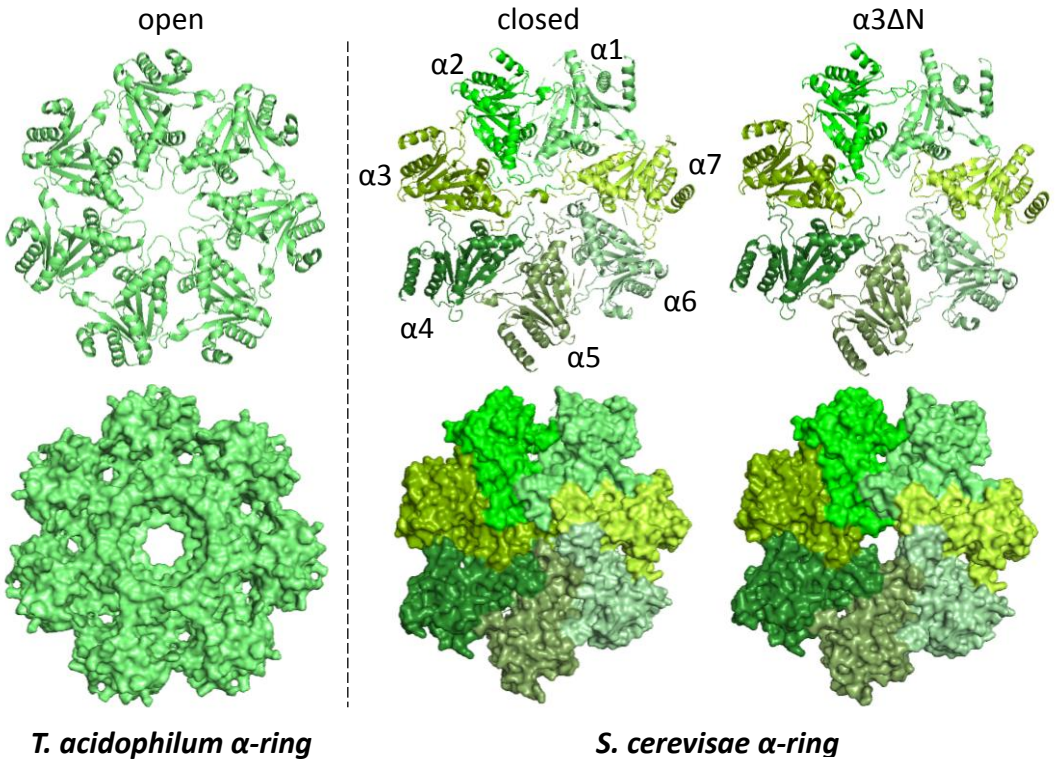

Figure 1.7 – The 20S CP pore. Top view ribbon (top) and surface (bottom) representation of the 20S CP α-ring from *T. acidophilum* and *S. cerevisiae* crystal structure. Left: *T. acidophilum* α-ring where the N-terminal residues are not ordered and are not given in the presented structure (PDB code 1PMA). Middle: *S. cerevisiae* wild-type α-ring in closed conformation (PDB code 2F16). Right: *S. cerevisiae* open 20S CP gate conformation after deletion of nine N-terminal residues in subunit α3 (α3ΔN; PDB code 1G0U). The figure was prepared using PyMOL.

The opening of this pore in the normal 20S CP is mediated by binding of the 19S RP, and requires structural rearrangement of the α-tail segments (Groll *et al.*, 2000). Furthermore, the cryo-EM structure of recombinant human 20S shows that binding of PA200 induces proteasome α-ring conformational rearrangements, resulting in global allosteric structure adjustments that extend to the proteasome β subunits and lead to the modulation of the proteolytic activity (Toste Rêgo and da Fonseca, 2019). In prokaryotic 20S CPs, this structural features do not seem to occur, as these domains were not detectable in the crystal structure of the archaeal *T. acidophilum* proteasome (Figure 1.7) (Löwe *et al.*, 1995).

The β subunits of the core particle contain also unique extensions. Five of the seven β subunits are synthesized as precursors with propeptides, which are proteolytically processed during proteasome maturation (Frentzel *et al.*, 1994; Chen and Hochstrasser, 1995; Seemüller *et al.*, 1995). The pro-forms of Pre3/β1, Pup2/β2 and Pre2/β5 are fully processed and cleaved between Gly(-1) and Thr1, Pre7/β6 between His(-10) and Gln(-9) and Pre4/β7 between Asn(-9) and Thr(-8) (Groll *et al.*, 1997). Pup3/β3 and Pre1/β4 are not synthesized as pro-proteins (Groll *et al.*, 1997). Each of the β subunit propeptides exhibits a distinct number of amino acids and consequently a different length and function in *S. cerevisiae* (Table 1.1). Important functions are for instance the prevention of unspecific proteolysis before the 20S CP assembly is completed and the protection of the N-terminal threonine residue against cytosolic N-α-acetyltransferases (*NAT1*) (Arendt and Hochstrasser, 1999; Marques *et al.*, 2009). Moreover, these propeptides are also suggested to be involved in proteasome assembly (see chapter 1.4.3.4) (Arendt and Hochstrasser, 1999).

Table 1.1 – The *Saccharomyces cerevisiae* 20S proteasome subunits. Nomenclature, standard and systematic chromosomal locus names, molecular weight (kDa) and amino acid (a.a.) length of proteasomal subunits are shown (http://www.yeastgenome.org/). The molecular weight and length of mature/processed subunits are indicated in brackets.

Subunit nomenclature	Standard name	Systematic name	Molecular weight (kDa)	Length (a.a.)
α1	Scl1	YGL011C	28.0	252
α2	Pre8	YML092C	27.2	250
α3	Pre9	YGR135W	28.7	258
α4	Pre6	YOL038W	28.4	254
α5	Pup2	YGR253C	28.6	260
α6	Pre5	YMR314W	25.6	234
α7	Pre10	YOR362C	31.5	288
β1	Pre3	YJL001W	23.5 (21.5)	215 (196)
β2	Pup1	YOR157C	28.3 (25.1)	261 (232)

β3	Pup3	YER094C	22.6	205
β4	Pre1	YER012W	22.5	198
β5	Pre2	YPR103W	31.6 (23.3)	287 (212)
β6	Pre7	YBL041W	26.9 (24.9)	241 (222)
β7	Pre4	YFR050C	29.4 (25.9)	266 (233)

While in prokaryotic 20S proteasomes, each β subunit is catalytically active, in eukaryotes, only three distinct β subunits are active: β1 preferentially cleaves after acidic residues (caspase-like or post-acidic activity), β2 after basic residues (tryptic activity) and β5 after hydrophobic residues (chymotryptic activity) (Groll *et al.*, 2005). To minimize non-specific substrate cleavage, the N-terminal catalytic active sites are localized inside the inner chamber of the CP (Groll *et al.*, 1997). Upon auto-catalytic cleavage of the prosequence, the active-site residue Thr1, responsible for the hydrolysis of substrate peptide bonds, is exposed and the β subunit becomes active (Brannigan *et al.*, 1995; Seemüller *et al.*, 1995). This process occurs during 20S CP assembly and is termed β subunit maturation (Chen and Hochstrasser, 1996; Seemüller *et al.*, 1996). The processing of the inactive subunits β6 and β7, however, is not auto-catalytic, instead their propeptides are cleaved by the neighboring active β subunits (Heinemeyer *et al.*, 1997).

In addition to Thr1, the active site region also contains the critical residues Asp17 and Lys33 (Marques *et al.*, 2009; Matias *et al.*, 2010). These conserved residues are only present in the active subunits β1, β2 and β5 and are known to be critical for propeptide removal by intramolecular autolysis and proteolytic site structural integrity (Ditzel *et al.*, 1998; Heinemeyer *et al.*, 2004). The absence of one of these critical residues in the active site region is enough to abolish the catalytic activity, explaining why β3, β4, β6 and β7 are catalytically inactive (Heinemeyer *et al.*, 1997).

During β subunit propeptide processing, the intramolecular autolysis of the Gly(-1)-Thr1 bond is initiated by the adoption of a γ turn conformational change extending from Leu-2 to Thr1 in the propeptide. In this position, a water molecule deprotonates the hydroxyl group of the Thr1 residue to enhance its nucleophilicity, which is then able to perform a nucleophilic attack onto the Gly1 carbonyl carbon atom located on the inner side of the γ turn. This nucleophilic attack results in the release of the propeptide from the mature β subunit and exposure of a free N-terminal Thr1 residue through several intermediate states (Ditzel *et al.*, 1998; Marques *et al.*, 2009).

The catalytic mechanism of the active sites involves the deprotonation of the Thr1 hydroxyl group, enabling a nucleophilic attack onto the carbonyl carbon of a peptide bond. In this process, an active site neighbor water molecule mediates the proton transfer between Thr1-O γ and Thr1-N atoms during substrate binding (Heinemeyer *et al.*, 2004; Marques *et al.*, 2009). Unlike traditional proteases, the proteasome digests the substrate all the way to small peptides ranging from 3-15 amino acid residues in length, until they are sufficiently small to pass the proteasome's gates. These peptides only exist for a few seconds in the cell, because cytosolic peptidases quickly trim them down into single amino acids that are reutilized for new protein synthesis (Vabulas and Hartl, 2005; Marques *et al.*, 2009). Although it was assumed that the different active sites of the proteasome function independently, it has been suggested that the active β subunits can indeed cooperate in substrate degradation (Djaballah and Rivett, 1992; Stein *et al.*, 1996).

Additionally to the widely conserved proteasome described before, vertebrates possess tissue-specific proteasomes, called immunoproteasome, thymoproteasome and spermatoproteasome (Abi Habib *et al.*, 2022; Watanabe *et al.*, 2022). In these specialized proteasomes, the constitutive β1, β2 and β5 catalytic subunits are replaced by β1i/LMP2, β2i/MECL1 and β5i/LMP7 in the case of immunoproteasomes, and β1i, β2i and β5t in thymoproteasomes (Murata *et al.*, 2018). The expression of the immunoproteasome is highest in immune cells and IFN-γ-stimulated cells, and is thought to contribute to the maintenance of the immune system function by producing peptides suitable for antigen presentation to Major Histocompatibility Complex (MHC) class I (Borissenko and Groll, 2007). The thymoproteasome (expressed in the thymus), however, contributes to CD8+ T cell differentiation by using its specific protein cleavage activity to produce specialized MHC class I-binding peptides in cTECs (Murata *et al.*, 2007; Huber *et al.*, 2012). The spermatoproteasome contains an alternative α4 subunit, the α4s or PSMA8. This subunit is found in mammalian testes and apparently does not modify the catalytic activities of the proteasome (Abi Habib *et al.*, 2022).

1.4 Assembly of the 20S proteasome

An important field of proteasome research concerns its assembly and regulation. Not only the assembly of the 19S RPs, but also the assembly pathway of the 20S CP is fairly well

understood by now. Due to a higher complex subunit composition and organization, the mechanism of 20S CP assembly found in eukaryotic cells is more intricate than in prokaryotic cells (Budenholzer *et al.*, 2017).

1.4.1 Assembly of prokaryotic proteasomes

Most prokaryotic proteasomes are formed by only two distinct subunits, α and β, which are capable of allowing self-assembly without the help of additional factors (Maupin-Furlow *et al.*, 2006). In contrast to α subunits, β subunits are not able to form rings by themselves but mature 20S proteasomes are formed when both α and β subunits are co-expressed, suggesting that α-rings represent starting platforms on which β subunits are arranged (Zwickl *et al.*, 1994). The ability of self-assembly is enabled by a long N-terminal helix that facilitates the contact surface interaction between neighboring α subunits, which is not present in β subunits (Löwe *et al.*, 1995). Although these findings indicate that archaeal 20S CPs do not require assembly chaperones, two factors named PbaA and PbaB were found in *Methanococcus maripaludis*, that are thought to be homologs of the eukaryotic chaperones Pba1 and Pba2 (see chapter 1.4.3.2) (Kusmierczyk *et al.*, 2011). Similar to Pba1 and Pba2, PbaA forms a complex with PbaB and binds with its conserved HbYX motif to the same surface pocket in the α-ring that is bound by proteasomal activators (Kusmierczyk *et al.*, 2011). However, the basic functional properties of PbaA and PbaB in archaeal 20S CP assembly still remain unclear. By contrast, in the eubacterium *Rhodococcus*, no formation of ring structures was observed, likely because of the substantially smaller contact region between α subunits (Zühl *et al.*, 1997). Instead, α and β subunits form dimers that subsequently assemble into half- proteasome precursor complexes (Zühl *et al.*, 1997). While the propeptides of the *Rhodococcus* β subunits are important for correct proteasome assembly, the *Mycobacterium tuberculosis* propeptides do not play a role (Zühl *et al.*, 1997; Kwon *et al.*, 2004; Hu *et al.*, 2006; Lin *et al.*, 2006). *In vitro* experiments revealed that *Rhodococcus* proteasome β subunits possess three distinct regions in the propeptide, from which region I accelerates dimerization and autocatalytic activation, while the more structured region II nucleates half CP formation, and the flexible part in region III inhibits dimerization (Suppahia *et al.*, 2020). Finally, two immature half-proteasomes, composed by a heptameric α-ring and a heptameric β-ring, interact and the propeptides are auto-catalytically removed, yielding a mature proteasome (Ditzel *et al.*, 1998).

1.4.2 Assembly of eukaryotic proteasomes

Given the abundance and subunit complexity of the eukaryotic proteasome, the assembly of this complex must be carefully arranged to ensure its correct formation. Therefore, CP biogenesis is assisted by many factors, such as the intrinsic self-assembly properties of subunits, dedicated assembly chaperones, and the N- and C-terminal extensions of specific subunits (Budenholzer *et al.*, 2017).

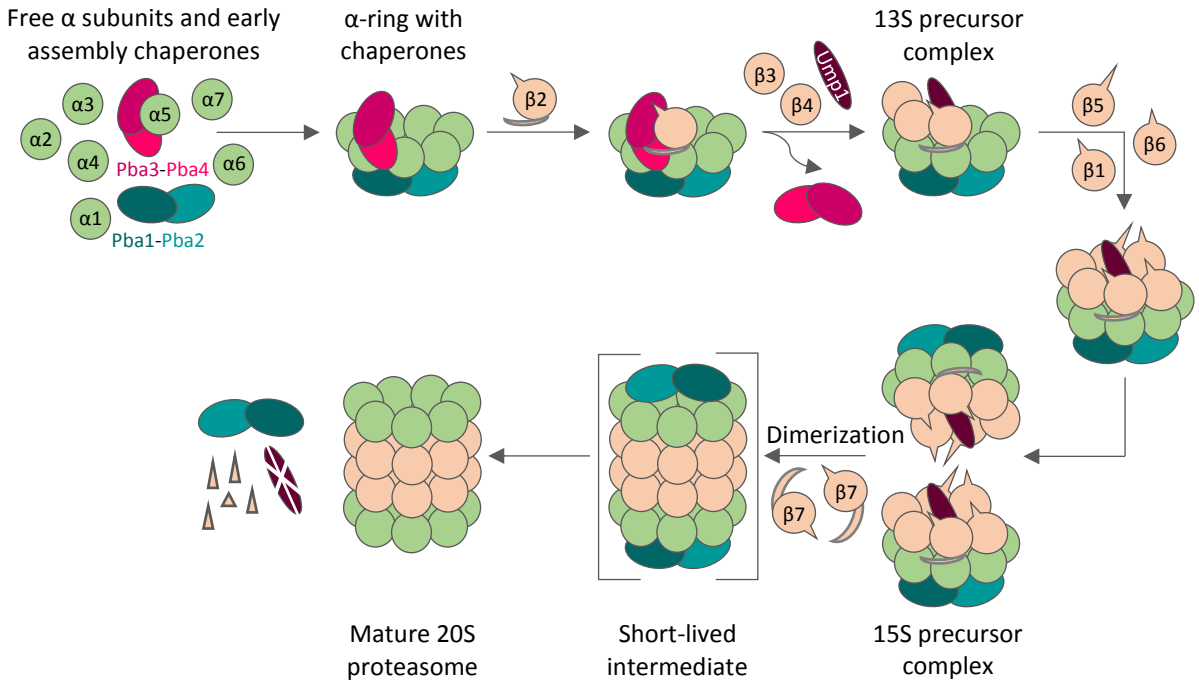

Figure 1.8 – Currently prevailing α-ring model. Schematic representation showing the different α (light green) and β subunits (light orange), as well as the chaperones involved in the assembly of the 20S CPs in *S. cerevisiae*. The heterodimers Pba1-Pba2 (dark green and green) and Pba3-Pba4 (dark pink and pink) are assisting in the formation of the α-ring, which serves as platform for the β subunits. The first subunit that joins the α-ring is β2. Afterwards, Ump1 and β3 are assembled to the complex. The incorporation of β4 is enabled by dissociation of Pba3-Pba4. The intermediate consisting of a complete α-ring, β2, β3, β4 and Ump1 is called 13S precursor complex. After incorporation of β5, β6 and β1, the complex is called 15S PC or half-proteasome. The last subunit entering the complex is β7. The C-terminal extension of β7 reaches into the other half of the 20S CP to stabilize the nascent proteasome which is short-lived (shown in brackets) and promotes dimerization of two 15S PCs. The nascent proteasome is activated by autocatalytic maturation of the β subunits (propeptides are drawn as little extensions), Ump1 is degraded, and Pba1-Pba2 is released.

The current model prevailing in the literature assumes that assembly of the 20S proteasome is initiated with the formation of heptameric α-rings containing the subunits α1-α7, which serve as platforms for subsequent incorporation of β subunits (Figure 1.8) (Ramos and Dohmen, 2008; Murata *et al.*, 2009; Tomko and Hochstrasser, 2013). The theory of the α-

ring model is supported by the ability of prokaryotic α subunits to self-assemble into ring structures and the observation that also recombinant eukaryotic subunits such as *Trypanosoma brucei* α5 and human α7 can self-assemble into homo-heptameric rings (Zwickl *et al.*, 1994; Gerards *et al.*, 1997; Yao *et al.*, 1999). However, whether hetero-heptameric or simpler α-rings are real common assembly intermediates *in vivo* is still not clear (Budenholzer *et al.*, 2017). More recently, the CP subunits α1, α2 and α4 were shown to form small complexes dependent on chaperones of the Hsp70/Ssa and Hsp110/Sse families, indicating that these chaperones are important for the correct folding of individual subunits and/or to prevent unproductive homomeric interactions of these α subunits and thereby increase the efficiency of CP assembly (Matias *et al.*, 2022).

As correct placing of all the different subunits seems to be a much more complex process in eukaryotes, this task is aided by the heterodimeric chaperones Pba1-Pba2 and Pba3-Pba4 in *S. cerevisiae* (Le Tallec *et al.*, 2007; Kusmierczyk *et al.*, 2008). The first β subunit that is assembled on the α-ring platform containing the assembly chaperones is β2 (Hirano *et al.*, 2008). Afterwards, the maturation factor Ump1 as well as β3 are incorporated and Pba3-Pba4 is released from the complex to enable the incorporation of β4 in a position where the chaperone was located before (Hirano *et al.*, 2006; Yashiroda *et al.*, 2008). The assembly intermediate at this stage is called 13S precursor complex (PC) (Li *et al.*, 2007). Upon incorporation of the subunits β5, β6 and β1, the complex contains all α subunits, the β subunits β1-β6, the maturation factor Ump1 as well as the dimeric-chaperone Pba1-Pba2, and is referred to as 15S precursor complex or half proteasome (Hirano *et al.*, 2008; Marques *et al.*, 2009). Dimerization of two 15S PCs is triggered by the incorporation of the β7 subunit, whose C-terminal extension reaches out into the other half stabilizing the newly formed 20S PC, which is short-lived (Ramos *et al.*, 2004; Li *et al.*, 2007). The fact that β7 incorporation is the rate-limiting step in proteasome assembly was shown in several studies (Ramos *et al.*, 2004; Li *et al.*, 2007; Marques *et al.*, 2007). The assembly process is finalized by autocatalytic cleavage of the proteolytic subunits β1, β2 and β5 propeptides to expose the active sites. This triggers processing of β6 and β7 propeptides as well as degradation of Ump1, the first substrate of the newly formed active CP. At the same time the Pba1-Pba2 heterodimer is released and recycled (Chen and Hochstrasser, 1996; Ramos *et al.*, 1998; Groll *et al.*, 1999; Hirano *et al.*, 2005; Kock *et al.*, 2015). These events likely trigger important conformational changes that lead to further stabilization of the resulting 20S CP

and tightening of the α-ring opening to restrict access into the mature CP (Ramos *et al.*, 1998; Kock *et al.*, 2015; Wani *et al.*, 2015). This gate can then only be opened through binding of regulatory particles thus protecting the cell from uncontrolled protein degradation (Groll *et al.*, 2000).

1.4.3 Chaperones involved in eukaryotic 20S CP formation

The assistance of proteasome-specific assembly chaperones is required to ensure successful proteasome biogenesis. These chaperones, Ump1, Pba1-Pba2 and Pba3-Pba4, as well as the N- and C-terminal extensions of specific subunits aid the specific and efficient assembly of the 20S core particle by promoting different steps of this pathway and are described in the following sections.

Table 1.2 – Proteasome assembly chaperones in yeast and human. Standard, gene and systematic names, as well as molecular weight (kDa), amino acid (a.a.) residue number and human orthologue names of yeast proteasome assembly chaperones are shown (http://www.yeastgenome.org/).

Yeast standard name	Yeast gene name	Systematic name	Molecular weight (kDa)	Length (a.a.)	Human orthologue standard name
Ump1	*UMP1*/*RNS2*	YBR173C	16.8	148	hUMP1/POMP
Pba1	*PBA1*/*POC1*	YLR199C	30.7	276	PAC1
Pba2	*PBA2*/*POC2*/*ADD66*	YKL206C	30.7	267	PAC2
Pba3	*PBA3*/*POC3*/*DMP2*/*IRC25*	YLR021W	20.1	179	PAC3
Pba4	*PBA4*/*POC4*/*DMP1*	YPL144W	16.6	148	PAC4

1.4.3.1 Maturation factor Ump1

Ump1 is a 16.8 kDa protein that was first discovered in a genetic screen for mutants defective in ubiquitin-mediated proteolysis (Ramos *et al.*, 1998). Despite low sequence similarity, both yeast Ump1p and its human homologue hUmp1/POMP (proteasome maturation protein) associate specifically with proteasome precursor complexes, while being absent from mature 20S proteasomes (Ramos *et al.*, 1998; Burri *et al.*, 2000; Witt *et al.*, 2000). In 15S PCs, Ump1 is encased within the cavity of the complex, contacting subunits at the interface of the α- and β-rings (Sá-Moura *et al.*, 2013; Kock *et al.*, 2015). Cross-linking experiments suggest that the N-terminus of Ump1 is located near the interface of β6 and the incoming β7 subunit, possibly able to sense the arrival of β7 in the complex (Kock *et al.*, 2015). The ability to bind

multiple subunits during proteasome assembly may be accomplished by the flexibility of the Ump1 N-terminal domain providing a checkpoint that prevents early dimerization of precursor complexes until their assembly is completed (Li *et al.*, 2007; Sá-Moura *et al.*, 2013). The propeptides of β5 and β6, as well as the β7 C-terminal extension might contribute to overcome this checkpoint after incorporation of β7, leading to positional or conformational changes of Ump1 (Ramos *et al.*, 1998; Sá-Moura *et al.*, 2013). Upon assembly of 20S proteasomes, autocatalytic maturation of the subunit propeptides is enabled and Ump1 is degraded by the active proteasome, thereby becoming its first substrate (Groll *et al.*, 1997; Ramos *et al.*, 1998).

Although deletion of *UMP1* is not lethal in *S. cerevisiae*, cells are impaired in growth and hypersensitive to a variety of stresses. They accumulate proteasome precursors and assembled 20S CPs with incompletely processed β subunits (Ramos *et al.*, 1998). Hence, Ump1 was identified as a proteasome assembly chaperone that coordinates the dimerization of half proteasomes and maturation of active sites (Ramos *et al.*, 1998). Biochemical, biophysical and structural analysis of recombinant yeast Ump1 showed that Ump1 is an intrinsically unstructured protein with little secondary elements, that might become structured only upon interaction with the proteasome subunits (Sá-Moura *et al.*, 2013; Uekusa *et al.*, 2014). Cryo-electron microscopy and crosslinking analyses identified Ump1 to make multiple contacts with α7 and α1-α4, being positioned opposite from the α4-α6 side, at a location occupied by Pba3-Pba4 at an earlier stage of assembly (Schnell *et al.*, 2021). A steric clash between Ump1 and Pba4 in the vicinity of α4 explains why Pba3-Pba4 has to exit the complex before Ump1 can be incorporated (Kock *et al.*, 2015; Schnell *et al.*, 2021). Structurally, Ump1 consists of seven α-helices with intervening loops of variable length, with its N-terminus being situated near β5 and β6 and winding around the β-ring towards β2-β4 (Schnell *et al.*, 2021).

Based on yeast complementation and biochemical assays, Ump1 was assumed to possess at least two functionally distinct domains. The C-terminal region comprising residues 51-141 mediates the physical interaction between Ump1 and the proteasome precursor complexes. Notably, amino acid residues 68-72 seem to be essential for this interaction. The N-terminal domain of the first 50 residues was suggested to be essential for the formation of functional 20S particles, maybe by interacting with the propeptide of one or more β subunits (Burri *et al.*, 2000). In contrast to yeast Ump1, hUmp1 appears to be essential for viability

(Le Tallec *et al.*, 2007; Hirano *et al.*, 2008; Yashiroda *et al.*, 2008). hUmp1 directly binds to α-rings *in vitro*. This interaction is independent of β subunits and appears to be essential in recruiting β2 as the first β subunit (Fricke *et al.*, 2007; Hirano *et al.*, 2008). Furthermore, it has been reported to play a role in the trafficking of precursor complexes, since it can bind to membranes and recruit those complexes to the endoplasmic reticulum (ER). In fact, the ER is where most of the proteasome assembly in mammalian cells seems to occur (Fricke *et al.*, 2007). By contrast, studies in *S. cerevisiae* suggested that Ump1-containing precursor complexes are imported from the cytoplasm into the nucleus, where the assembly is completed (Lehmann *et al.*, 2002).

1.4.3.2 Assembly chaperone Pba1-Pba2

The yeast proteasome biogenesis associated proteins Pba1 and Pba2, similar to the human PAC1 an PAC2 (proteasome assembly chaperones), function together as a heterodimer and were found to be associated with assembly intermediates (Hirano *et al.*, 2005; Le Tallec *et al.*, 2007; Li *et al.*, 2007). While the deletion of *PAC1* and *PAC2*, which stabilize each other *in vivo*, leads to slow cell growth and misassembled intermediates in mammals, knockdown of the metabolically stable Pba1-Pba2 results in no obvious growth defect in yeast (Hirano *et al.*, 2005; Le Tallec *et al.*, 2007; Li *et al.*, 2007). Both Pba1 and Pba2 have a C-terminal HbYX (hydrophobic-tyrosine-any amino acid) motif, which is found in several proteasome activators and is required for interaction with the α-pocket of two adjacent α subunits (Kusmierczyk *et al.*, 2011). X-ray crystallography of a complex between the mature 20S CP from *S. cerevisiae* and recombinantly expressed Pba1 and Pba2 revealed that Pba1 C-terminal residues bind the α5/α6-pocket and that Pba2 C-terminal residues interact with the α6/α7-pocket (Figure 1.9 b) (Stadtmueller *et al.*, 2012). As the deletion of *PBA1* leads to a substantial reduction in the levels of α5 and α6 subunits in immature CPs, Pba1-Pba2 probably contributes to the incorporation of these subunits (Wani *et al.*, 2015). The 3D structures of Pba1 and Pba2 are quite similar, consisting of a β sheet of four parallel strands, extended by anti-parallel strands and flanked on either side by two α-helices. They mainly differ in loop regions connecting structured parts and their C-terminal regions (Stadtmueller *et al.*, 2012). While the C-terminal region of Pba1 is quite short and consists of a helical region that interacts with α5, the C-terminus of Pba2 is longer and more unstructured with

several loops and two short helices interacting with α7 (Figure 1.9 a) (Stadtmueller *et al.*, 2012).

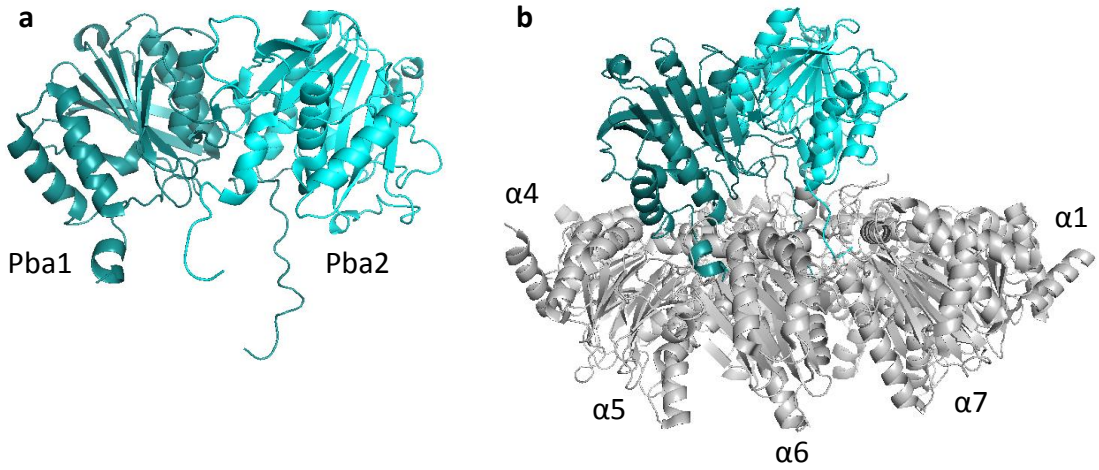

Figure 1.9 – Structure of Pba1-Pba2. (a) Structure of the heterodimeric chaperone pair Pba1-Pba2. Figure was prepared from the pre-15S structure, omitting all other subunits (PDB code 7LS6). **(b)** Structure of the complete α-ring in complex with Pba1-Pba2, which sits on the outer surface of α5, α6 and α7 with the HbYX motif of Pba1 docked in between α5 and α6, the HbYX motif of Pba2 docked in between α6 and α7, and the N-terminus of Pba1 transiting through the α-ring pore (PDB code 7LS6). The figure was prepared using PyMOL.

Pba1-Pba2 forms a cup-like structure over the center of the proteasome α-ring pore, which is functionally closed in this structure (Stadtmueller *et al.*, 2012). After opening the CP gate, the Pba1-Pba2 N-terminus enters the pore and blocks it to prevent access of substrates to the CP interior. This explains the preferential association of Pba1-Pba2 with immature CP and their release from the CP upon completion of assembly (Schnell *et al.*, 2021). Tight binding of Pba1-Pba2 to CP precursors prevents their association with the RP, allowing RP-CP interaction only after proper processing of the CP to its mature form. This potentially leads to an affinity switch triggering the expulsion of Pba1-Pba2 or the displacement by other activators with higher affinity (Wani *et al.*, 2015). Cryo-EM data revealed, that Pba1 makes contacts with Ump1 and the β5 propeptide by accessing the CP interior. Likely, the affinity of Pba1 for mature CP is reduced upon cleavage of the β5 propeptide and degradation of Ump1, disrupting these interactions (Schnell *et al.*, 2021). After 20S CP maturation, the Pba1-Pba2 heterodimer is not degraded like Ump1 but is expelled from the α-ring by a restructuring event that organizes the β-ring and leads to tightening of the α-ring opening. It is then recycled for a new round of proteasome assembly (Kock *et al.*, 2015).

1.4.3.3 Assembly chaperone Pba3-Pba4

Similar to Pba1 and Pba2, yeast Pba3 and Pba4 form a heterodimer and were shown to interact most strongly with α5 subunits early in proteasome assembly (Kusmierczyk *et al.*, 2008; Yashiroda *et al.*, 2008). The accumulation of polyubiquitylated proteins, a decreased proteasome activity and accumulation of CP assembly intermediates upon deletion of *PBA3* and/or *PBA4* support the role of Pba3-Pba4 as a proteasome assembly chaperone (Budenholzer *et al.*, 2017). Pba3 and Pba4 share a high degree of structural similarity, consisting of a six-stranded anti-parallel β sheet and two α-helices (Yashiroda *et al.*, 2008). In the dimer, they form an αββα sandwich structure, which resembles greatly those of proteasome subunits (Figure 1.10) (Yashiroda *et al.*, 2008).

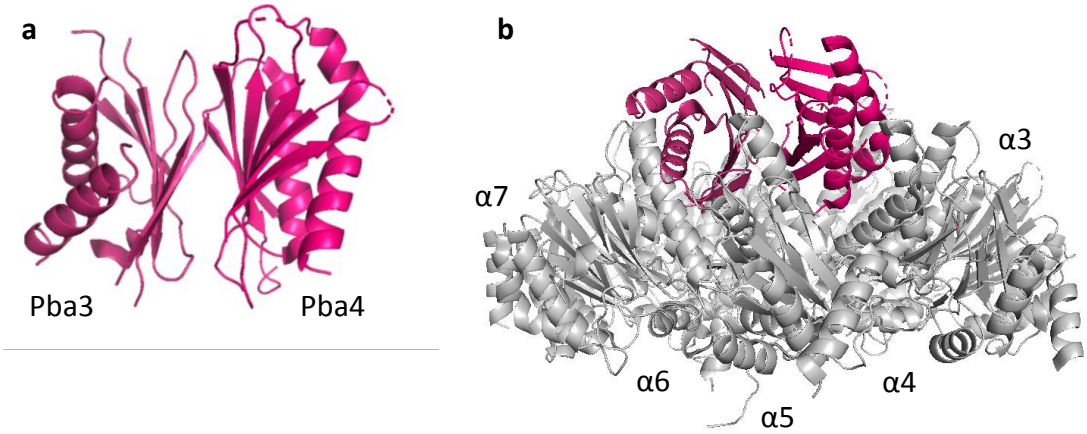

Figure 1.10 – Structure of Pba3-Pba4. (a) Structure of the heterodimeric chaperone pair Pba3-Pba4. Figure was generated from the Pba3-Pba4-α5 structure with α5 omitted (PDB code 2Z5C). **(b)** Composite structure of the complete α-ring in complex with Pba3-Pba4, which occupies the undersurface of α4-α6. Figure was generated by modeling the Pba3-Pba4-α5 structure (PDB code 2Z5C; α5 omitted) onto pre-15S (PDB code 7LS6; β-subunits, Ump1 and Pba1-Pba2 omitted). The figure was prepared using PyMOL.

Structural and biochemical studies showed that the Pba3-Pba4 complex binds directly to the α5 subunit and that this binding also occurs when α5 is associated with α6 and α7 (Kusmierczyk *et al.*, 2008; Yashiroda *et al.*, 2008). The Pba3-Pba4-α5 complex is therefore thought to serve as a starting point for proteasome assembly (Kusmierczyk *et al.*, 2008; Yashiroda *et al.*, 2008). In contrast to Pba1-Pba2, Pba3-Pba4 is predicted to be located close to the center of the α-ring, in a position where the β4 subunit will be assembled later (Takagi *et al.*, 2014). A strong steric clash between Pba3-Pba4 and the β4 subunit was suggested, explaining why Pba3-Pba4 must dissociate from the complex prior to β4 incorporation and

its absence in 13S intermediates (all α subunits, β2, β3, β4, Pba1-Pba2 and Ump1) (Li *et al.*, 2007; Takagi *et al.*, 2014).

1.4.3.4 β subunits N- or C-terminal extensions

Besides the assistance of proteasome-specific assembly chaperones, the N-terminal propeptides and C-terminal extensions of several β subunits have the ability to act as intramolecular chaperones to promote the formation of mature 20S proteasomes (Hirano *et al.*, 2008). All three subunits β1, β2 and β5 bearing the active-sites have N-terminal propeptides that play some role in subunit processing and assembly of the CP (Arendt and Hochstrasser, 1999). The most prominent CP intramolecular chaperone is the 75 amino acid residues long N-terminal propeptide of β5 (β5pro), which is essential for proteasome biogenesis in both yeast and human (Chen and Hochstrasser, 1996; Hirano *et al.*, 2008). β5pro is not only necessary for the incorporation of β5 itself, but functions together with Ump1 in promoting propeptide cleavage during proteasome maturation and has a similar role as the C-terminal tail of β7 in facilitating dimerization of two half-proteasomes (Li *et al.*, 2007, Li *et al*., 2016). As it was proposed before, cryo-EM data revealed that both the β2 and β5 propeptides contact Ump1, indicating a supportive role of Ump1 in positioning of these subunits (Schnell *et al.*, 2021). Interestingly, the lethality due to β5pro deletion can be rescued by an additional deletion of *UMP1*, suggesting that the propeptide of β5 is necessary to induce a change in the position or conformation of Ump1 that is required for the progression and completion of the CP assembly and maturation (Ramos *et al.*, 1998). A similar inhibitory role of Ump1 was detected upon truncating nine residues of the β6 N-terminal extension (NTE), which is in line with the notion that Ump1 functions as an assembly checkpoint, thus blocking proteasome dimerization and maturation until particular β subunit N-terminal extensions are present and the β7 subunit is incorporated (Li *et al.*, 2007). Compared to the β5 propeptide, the two other active subunits propeptides contribute in a much smaller degree to yeast proteasome assembly (Arendt and Hochstrasser, 1999). Deletion of β1 or β2 propeptides is not lethal, but cause defects in β5 processing and, in the case of β2, makes cells hypersensitive to higher temperatures (Jäger *et al.*, 1999). However, when β1 and β2 propeptides are simultaneously deleted, a severe growth defect and reduction of proteasome levels can be observed, implying that the two propeptides could have an overlapping role in proteasome assembly (Arendt and Hochstrasser, 1999).

Both β2 and β7 subunits have long C-terminal extensions, which were shown to interact with adjacent subunits (Groll *et al.*, 1997). β2 is the first β subunit to join the complex, and uses its unusually long C-terminal tail (~30 amino acid residues) to help dictate the directionality and specificity of proteasome assembly (Ramos *et al.*, 2004; Hirano *et al.*, 2008). Being required for incorporation of the β3 subunit, β2 is essential for progression of proteasome assembly and cell viability in yeast (Ramos *et al.*, 2004; Hirano *et al.*, 2008). In the mature proteasome, the β2 tail is wrapped around the neighboring β3 subunit and makes contact with β4 (Figure 1.11 a) (Ramos *et al.*, 2004; Hirano *et al.*, 2008). β7 is the last subunit that is inserted in the complex and uses its long C-terminal extension (CTE) to promote half-mer dimerization. It intercalates between β1 and β2 in the opposing β-ring and clamps the two half-proteasomes together (Figure 1.11 b) (Ramos *et al.*, 2004; Li *et al.*, 2007; Marques *et al.*, 2007). β7 incorporation is the rate limiting step in 20S CP assembly *in vivo* and its CTE appears to be important to stabilize the nascent dimer (Ramos *et al.*, 2004; Li *et al.*, 2007; Marques *et al.*, 2007). Although its role is conserved in both yeast and mammals, a deletion comprising the entire β7 CTE (19 amino acid residues) proved to be lethal only in mammals, whereas it leads to the accumulation of proteasome assembly intermediates and active-site autocatalytic processing defects in yeast cells (Marques *et al.*, 2009).

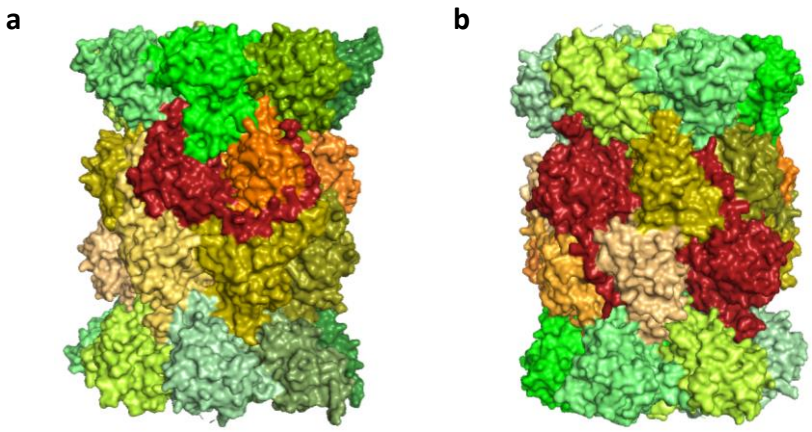

Figure 1.11 – Surface representations of β2 and β7 subunits C-terminal extensions in *S. cerevisiae*. (a) The long C-terminal extension (CTE) of β2 wraps around the neighboring β3 subunit. β2 is highlighted in red. **(b)** The β7 CTE intercalates between the β1 and β2 subunits on the opposing ring of the mature CP. β7 is highlighted in red. The figure was prepared with PDB code 2F16 using PyMOL.

1.5 Expression regulation of proteasome subunit genes by Rpn4

Apart from controlling proteasome function by regulation of interaction partners or facultative subunits, the essential genes encoding the subunits of house-keeping proteasomes are under a coordinated transcriptional control (Mannhaupt *et al.*, 1999; Meiners *et al.*, 2003; Lundgren *et al.*, 2005). In yeast, the transcriptional activator Rpn4 was shown to bind a common element (GGTGGCAAA), present in the promoters of nearly all genes encoding proteasome subunits. These PACE (Proteasome Associated Control Elements) are required for normal expression of proteasome genes (Mannhaupt *et al.*, 1999). Furthermore, Rpn4 was not only demonstrated to be a transcriptional activator of proteasome genes but also a proteasome substrate, indicating an Rpn4-mediated feedback regulation of proteasome gene expression (Xie and Varshavsky, 2001a). In addition to the regulation of proteasome genes, Rpn4 is also responsible for the expression of *UBA1*, *UBI4*, *CDC48* and several hundred other genes related to stress responses and DNA damage repair (Figure 1.12) (Mannhaupt *et al.*, 1999; Jelinsky *et al.*, 2000; Fleming *et al.*, 2002).

Cellular Rpn4 concentrations are controlled at the level of *RPN4* gene transcription, and post-translationally at the level of Rpn4 protein stability. *RPN4* transcription is activated by HSF (heat-shock transcription factor), Yap1 (Yeast AP-1), involved in response to oxidative stress and DNA damage, and multidrug resistance-related transcription factors Pdr1 and Pdr3 (Mamnun *et al.*, 2002; Owsianik *et al.*, 2002; Hahn *et al.*, 2006). Therefore, Rpn4 is an important stress-response mediator, which is reflected by a higher stress sensitivity of *rpn4*Δ cells (London *et al.*, 2004; Wang *et al.*, 2010a). Rpn4 has an extremely short half-life of two minutes and its turnover rate depends on the intracellular level of functional and available proteasome (Xie and Varshavsky, 2001a). Rpn4 is subject to Ubr2-Rad6-mediated ubiquitin-dependent degradation by the proteasome, but additionally, Rpn4 stability involves a ubiquitin-independent targeting pathway that is not yet understood in detail (Ju and Xie, 2004). Inhibition of proteasome function leads to stabilization of Rpn4 and thereby to an up-regulation of its target genes (Dohmen *et al.*, 2007).

In contrast to most proteasome subunits genes, which are recognized by Rpn4 via their authentic PACE sequence in the promoter, some subunit genes such as *PRE5*/α6, *PUP1*/β2, *RPN8, RPN10, RPN13* and *SEM1* do have octamer PACE-like sequences (AGTGGCAA or GGTGGCGA) (Leggett *et al.*, 2002; Mannhaupt and Feldmann, 2007). The proteasome

assembly chaperones Ump1, Pba1, Pba2, Nas2, Hsm3, Rpn14 and Nas6, however, have neither PACE nor PACE-like sequences in their promoters, but minimal hexamer PACE-core sequences ((A/G)GTGGC) (Shirozu *et al*., 2015). Pba3 and Pba4 even do not contain any of those alternatives. This system of sequence variations facilitates a differential and sensitive regulation of gene expression and therefore maintenance of proteostasis under conditions of cellular stress (Shirozu *et al*., 2015).

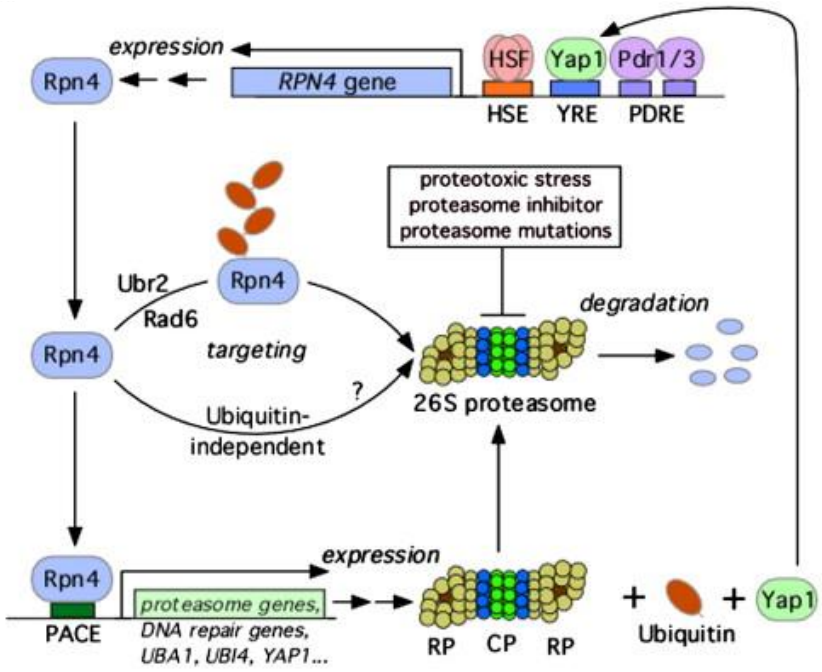

Figure 1.12 – Regulation of proteasome subunit gene expression by Rpn4. Regulatory circuits involving Rpn4 are illustrated. The elements HSE, YRE and PDRE of the Rpn4 gene promoter are recognized by the transcriptional activators HSF, Yap1 and Pdr1/3, respectively. Rpn4 itself stimulates expression of proteasome subunit genes as well as of genes involved in ubiquitylation, DNA repair and other stress responses. Rpn4 is a short-lived protein and its stability is controlled by the 26S proteasome in an ubiquitin-dependent manner mediated by Ubr2-Rad6 and a ubiquitin–independent manner which is not yet understood in details. Inhibition of proteasome function leads to stabilization of Rpn4 and in turn to an up-regulation of its target genes. Figure from Dohmen *et al*., 2007.

1.6 Aim of the study

The eukaryotic 20S CP assembly is a step-wise process involving different intermediates and is still not fully understood. To analyze and demonstrate the presence and participation of yeast proteasome subunits and associated assembly chaperones in distinct assembly steps during 20S complex formation as well as to prove particular protein-protein interactions, their specific detection would be a useful tool.

The expression levels of proteasome genes are regulated by the transcriptional activator Rpn4, which binds PACE and PACE-like sequences. This discovery was an indication that proteasome subunits might not be synthesized in stoichiometric amounts, as it has been assumed, but can be regulated individually. Therefore, the aim was to analyze the expression level of different 20S proteasome subunits and to which extent the protein levels are influenced by Rpn4-mediated regulation.

According to the literature, the assembly of the proteasome is thought to be initiated with formation of an α-ring. However, in our studies in *Saccharomyces cerevisiae*, a preliminary complex containing distinct subsets of α and β subunits (α1-α4 and β2-β4) as well as the maturation factor Ump1 was identified. This complex was termed Complex I and was shown to accumulate in cells lacking functional Pba1-Pba2 assembly chaperones. Based on these findings, our model suggests that a complementary complex, namely Complex II exists, that contains the subunits α5, α6 and α7 as well as the chaperones Pba1-Pba2 and Pba3-Pba4. To confirm the existence of such a complex and to determine whether Complex II is a real precursor complex occurring in yeast, the aim was to assemble this complex *in vitro.*

Another critical intermediate in 20S assembly is the 15S precursor complex containing all α and β subunits except for β7, as well as the chaperones Ump1 and Pba-Pba2. Although deletion of *UMP1* is not lethal in *S. cerevisiae*, Ump1 is important for efficient 20S proteasome assembly and correct maturation of the active sites. Cross-linking experiments suggested that the N-terminus of Ump1 is located near the interface of the incoming β7 subunit and Ump1 inhibits the dimerization of half-proteasomes until β7 is incorporated, whose C-terminal extension helps to overcome Ump1 inhibition (Kock *et al.*, 2015). Therefore, the aim of this study was to identify functional domains of the Ump1 proteasome

assembly chaperone and the interactions they engage in. Specifically, the role of the Ump1 N-terminal domain was intended to be analyzed.

As mentioned above, the β7 subunit is thought to be the last subunit to be incorporated into the complex, thereby triggering the dimerization of two such complexes. This process and subsequent events such as the maturation of the active sites (β1, β2 and β5), the degradation of Ump1, becoming the first substrate of the mature 20S core particle, and the release of Pba1-Pba2, were aimed to be proven *in vitro*.

In short, mainly it was aimed to:

1. Purify the yeast 20S proteasome components α5, α6, α7, Pba1-Pba2 and Pba3-Pba4 from *E. coli*
2. Produce specific antibodies against α5, α6 and Pba3-Pba4 (as well as β1, β5, β6, β7)
3. Investigate whether 20S CP subunits are produced stoichiometrically *in vivo*
4. Examine the influence of Rpn4 on the regulation of different proteasome subunits genes using produced antibodies
5. Assemble Complex II *in vitro*
6. Identify functional domains of the Ump1 proteasome assembly chaperone
7. Analyze the importance of the β7 propeptide and C-terminus for the interaction with Ump1
8. Demonstrate β7-driven dimerization of 15S PCs into 20S proteasomes resulting in subsequent events such as active site maturation, Ump1 degradation, and Pba1-Pba2 release *in vitro*

2 Results

2.1 Production of antibodies against yeast proteasome components

The specific detection of untagged yeast proteasome subunits and associated assembly chaperones would be a useful tool to analyze and demonstrate their presence and participation in distinct assembly steps during proteasome formation as well as to study particular protein-protein interactions. Therefore, the aim was to produce antibodies against the subunits α5 and α6, and the heterodimeric chaperone pair Pba3-Pba4.

2.1.1 Expression and purification of yeast proteasome components from *E. coli*

For the production of specific antibodies and *in vitro* downstream applications, it was necessary to obtain the respective proteins in adequate amounts and a soluble and pure form. Plasmids expressing the yeast proteasome subunits α5 and α6 as well as the assembly chaperone pair Pba3-Pba4 in *E. coli* were established. Pba3 and Pba4 were expressed from the same plasmid under control of the same promoter but containing individual translation initiation sites (Shine-Dalgarno-Sequence). To increase the yield of heterologous protein expression, yeast genes were adapted for *E. coli* by codon optimization. Furthermore, constructs contained human SUMO1 (small-ubiquitin-related modifier 1), a useful gene fusion technology, to enhance the expression and solubility of heterologous proteins (Wang *et al.*, 2010), and an N-terminal polyhistidin tag (8His) to enable for selective affinity purification (Figure 2.1 a). Pba4 was additionally tagged with an HA tag on the C-terminus. Using this method, all proteasome components were efficiently expressed in *E. coli* and yielded adequate soluble amounts (Figure 2.1 b, compare total (T) and soluble (SL) protein amounts). The empty vector control (EV) revealed specificity of the detected bands, as no

corresponding protein was present in this sample. Crude extracts of *E. coli* cells were used to purify these subunits by consecutive Ni^{2+}-NTA and TALON affinity chromatographies. The 8His-SUMO1 tag was cleaved using Senp1 (Sentrin-specific protease 1, see 2.1.2) enzyme to obtain the representative protein. Samples of the input (IN), the elution after Ni-NTA chromatography (E) and the concentrated material after cleavage of the 8His-SUMO1 tag (C) were analyzed by SDS-PAGE, followed by Coomassie staining to verify the efficiency of the purification (Figure 2.1 c). All proteasome components were obtained in high amounts (approximately 20-40 mg) and purity, and a soluble form. Even though proteins were observed to lose some of their solubility during purification, most likely due to cleavage of the solubility tag (SUMO1), sufficient amounts of soluble, pure proteins of all yeast proteasome components were obtained for the production of antisera and for downstream applications such as assembly and interaction studies regarding proteasome formation.

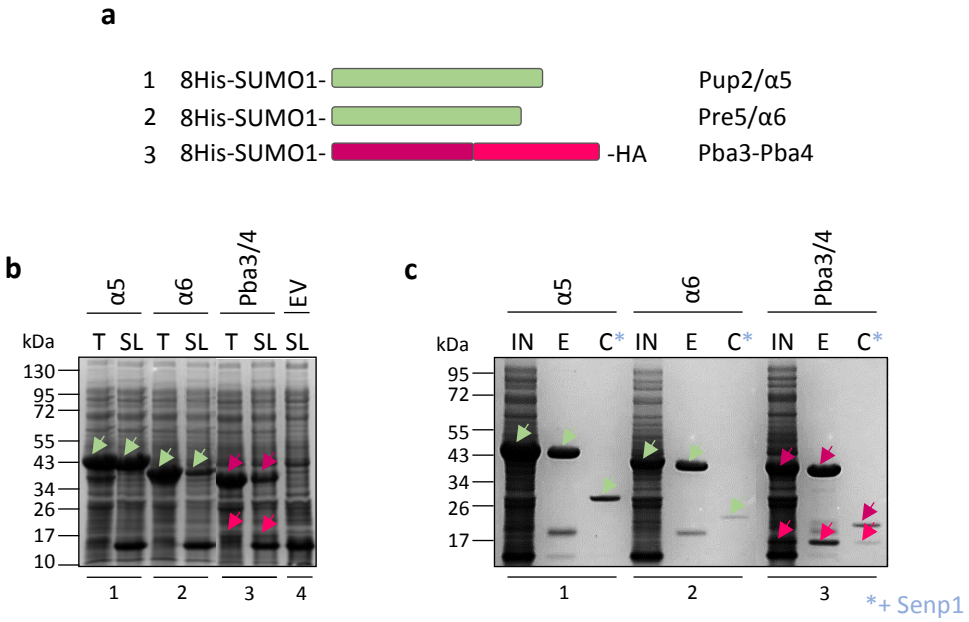

Figure 2.1 – Expression and purification of yeast proteasome components. (a) Schematic representation of produced proteasome subunits Pup2/α5 (plasmid pJZ20), Pre5/α6 (plasmid pJZ21) and the chaperone pair Pba3-Pba4 (plasmid pJZ23) fused to small ubiquitin-related modifier 1 (SUMO1) and 8His. Pba4 additionally contains an HA tag on the C-terminus. **(b)** Comparison of total (T) and soluble (SL) protein amounts (0.2 OD) of 8His-SUMO1 tagged proteins in *E. coli* analyzed by 12 % SDS-PAGE followed by Coomassie staining. The empty vector (EV) serves as control. Specific proteins are indicated by arrows. **(c)** Proteasome components were purified using consecutive Ni^{2+}-NTA and TALON affinity chromatographies. The 8His-SUMO1 tag was cleaved during the procedure using Senp1. Samples of the input (IN), the elution after Ni-NTA chromatography (E) and the concentrated material after cleaving off SUMO1 (C) were analyzed by 12 % SDS-PAGE and Coomassie staining. Loaded material corresponds to 0.2 OD of cells. Purified proteins were yielded in concentrations between ~20-30 mg/ml.

2.1.2 Expression and purification of Senp1

As described above, to obtain required proteins in adequate amounts and a soluble representative form, they were expressed as fusions to human SUMO1, which was meant to be cleaved during the purification process using Senp1. Therefore, Senp1 was expressed in *E. coli* from a pET plasmid containing an N-terminal polyhistidin tag (6His) (Hermanns *et al.*, 2018). Proteins were purified from crude extracts by Ni^{2+}-NTA chromatography and steps were analyzed by SDS-PAGE, followed by Coomassie staining (Figure 2.2 a). Senp1 purification was very efficient, obtaining the protein in high amounts (~50 mg) and a very pure form. To analyze Senp1 activity, a test protein fused to 8His-SUMO1 was mixed with increasing amounts of the protease. A sample without Senp1 served as a negative control. After a 30 min incubation on ice, samples were analyzed by SDS-PAGE and western blotting (Figure 2.2 b). Already minimal amounts of the enzyme were sufficient to cleave 50-80 % of the tagged protein, indicating that the purified Senp1 is highly active and efficient in cleaving SUMO1.

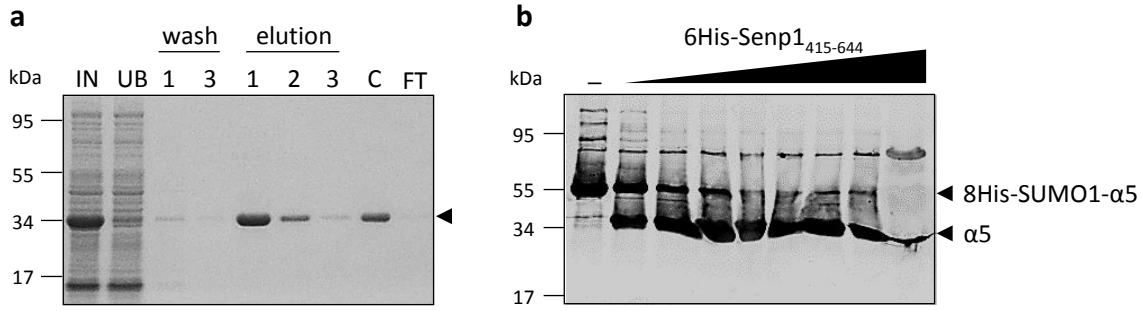

Figure 2.2 – Purification and activity of Senp1 enzyme produced in *E. coli*. (a) 6His tagged $Senp1_{415-644}$ was purified from *E. coli* cells using a Ni-NTA packed gravity flow column. Steps of the Ni-chromatography (input (IN), unbound material (UB), multiple washing- and elution steps as well as concentrated material (C) and flow through (FT) after the spin column concentration) were analyzed by 12 % SDS-PAGE and Coomassie staining. Loaded material corresponds to 0.2 OD of cells. The arrowhead points to the specific band for 6His-$Senp1_{415-644}$ (~31 kDa). Purified proteins were obtained in a final concentration of ~115 mg/ml. **(b)** To test the activity of the protease, previously purified 8His-SUMO1-α5 was mixed with different amounts of Senp1, starting with 10 µl from right to serial diluted amounts (1:10 steps) to the left. A sample without addition of Senp1 served as a control. Samples were incubated on ice for 30 min and analyzed by SDS-PAGE and anti-α5 western blotting. Arrowheads indicate non-cleaved and cleaved (8His-SUMO1)-α5.

2.1.3 Production of antisera against proteasome components

To produce antisera against the subunits α5 and α6 and the assembly chaperone pair Pba3-Pba4, the purified proteins (see 2.1.1) were sent to an external company for immunization

of rabbits. To ensure the highest possible specificity of the antisera, pre-immune blood sera of six different rabbits were first tested concerning unspecific background cross-reactivity to yeast proteins. Therefore, boiled extracts from wild-type (WT) yeast cells were separated by SDS-PAGE and after western blotting, each lane was probed with the individual rabbit blood sera in two different concentrations (1:1000 and 1:5000). Subsequent to washing and incubation with anti-rabbit secondary antibody, the membrane was developed and signals were analyzed (Figure 2.3 a).

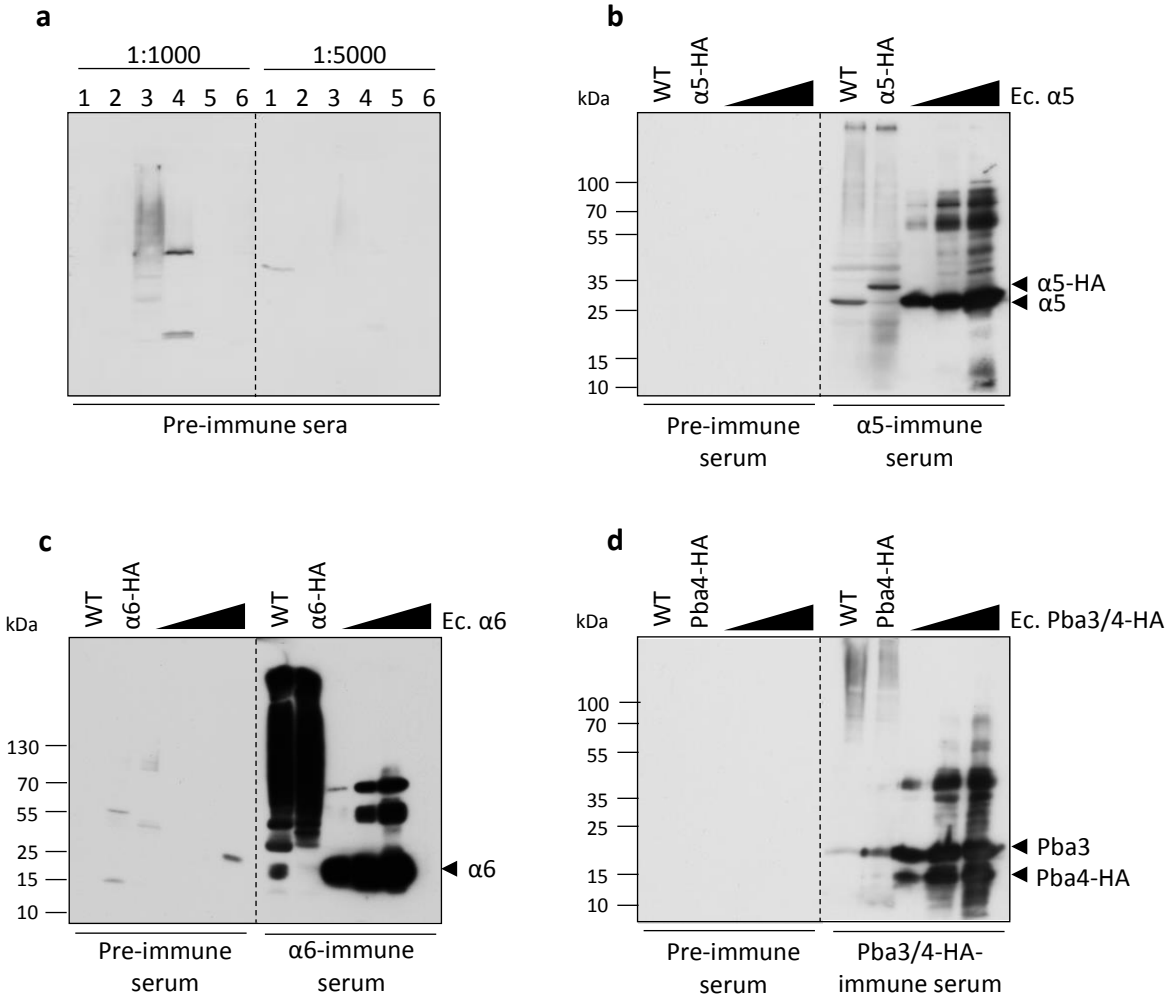

Figure 2.3 – Pre-immune and immune sera test. (a) Boiled extracts from wild-type (WT) yeast cells (JD47-13C) were probed with blood sera from 6 different rabbits in the dilutions 1:1000 and 1:5000 to test cross-reactivity with unspecific yeast proteins. The exposure was intentionally done for a long time (overnight). **(b)**, **(c)**, **(d)** Comparison of pre-immune sera and specific protein immune sera from immunization day 61. 1 OD cells of WT (JD47-13C) and Ha tagged proteins α5 (JM9), α6 (JM10) and Pba4 (FP16) from yeast boiled extracts as well as different concentrations (0.1 µg, 1 µg and 5 µg from left to right) of the corresponding proteins purified from *E. coli* were analyzed by 12 % SDS-PAGE and western blotting. Samples were either probed with the respective pre-immune serum (left) or the specific protein immune serum (right) of α5 **(b)**, α6 **(c)** or Pba3/4-HA **(d)**.

Although the analyzed extract was the same for all tested rabbit blood sera, some pre-immune sera detected unspecific signals (rabbit 1, 3 and 4). As the pre-immune sera of rabbit 2, 5 and 6 showed no cross-reaction with unspecific proteins, even after a long exposure time overnight, these rabbits were chosen for immunization (Table 2.1). Samples of 10 mg/ml in 100 µl of the desired antigen in buffer (50 mM Tris-HCl pH 7.4, 150 mM NaCl, 5 mM $MgCl_2$, 20 mM imidazole) were sent for antibody production. The immunization process was performed by the company Pineda Antikörper-Service in Berlin (http://www.pineda-abservice.de).

Table 2.1 – Rabbits chosen for immunization with respective antigen.

Labeling	Antigen	Immunized rabbit
A5	Pup2/α5	rabbit 5
A6	Pre5/α6	rabbit 6
P34	Pba3/4-HA	rabbit 2

To check for the specificity of the produced antisera, pre-immune sera and corresponding protein immune sera from immunization day 61 were compared. Therefore, wild-type yeast and cells expressing the desired antigen together with an HA tag as well as different concentrations of the corresponding protein purified from *E. coli* were analyzed (Figure 2.3 b-d). In contrast to the pre-immune sera, which barely detected any signal (Figure 2.3 b-d left), the antisera did clearly detect a huge specific signal for the individual proteasome components purified from *E. coli* (Figure 2.3 b-d right). For α5, a distinct band was visible in the wild-type yeast sample, which shifted upwards when α5 was tagged with HA (Figure 2.3 b). However, the α6 antisera detected the α6 subunit only in wild-type yeast cells, but not when the protein was fused to HA on the N-terminus (Figure 2.3 c). The immune serum against Pba3/Pba4-HA seemed to recognize mainly Pba3 in both the WT and the HA tagged yeast cells. Pba4 and HA were not explicitly detected in yeast boiled extracts (Figure 2.3 d). In contrast, for proteins purified from *E. coli*, Pba3 and Pba4-HA were detected by the antiserum. As for all immune sera, a quite high background of unspecific signals was visible for both the *E. coli* purified proteins and the yeast boiled extracts, a purification of the immune sera was necessary to improve the specificity of the antibody and reduce the signal to noise ratio.

2.1.4 Specificity improvement of antibodies against proteasome components

To reduce unspecific background signals detected by the immune sera, the aim was to purify the antibodies by a rather indirect method using deletion or shut-off yeast strains. As *PUP2*/α5 and *PRE5*/α6 are essential genes in *S. cerevisiae*, they cannot be deleted. Therefore, yeast strains were used expressing these subunits under control of the galactose-inducible promoter P_{GALS} (Mumberg *et al*., 1994). After cells were grown in galactose, they were shifted to glucose medium overnight to repress synthesis of the α5 and α6 proteins. *PBA3* however is not essential and could be deleted. Boiled extracts of these strains were loaded on SDS-PAGE and proteins were transferred to a PVDF membrane. The respective antiserum was incubated with the membrane to remove material binding nonspecifically to other yeast proteins. Finally, the supernatant with the unbound material was aliquoted and stored at -80 °C for further usage.

The efficiency of the generated antibodies was tested by comparing the antisera before and after the purification procedure. Wild-type yeast (WT) and cells expressing the desired antigen together with an HA tag as well as the mentioned strains with a repression or deletion of the distinct gene and the corresponding protein purified from *E. coli* were analyzed using SDS-PAGE and western blotting (Figure 2.4). For α5 a clear signal was visible in the yeast extract, which slightly shifted upwards when the protein was tagged with HA and disappeared in cells that repress this protein. After the purification of the antiserum nearly no unspecific signal was detected (Figure 2.4 a, compare before (left) and after (right) purification). An α6-specific signal could be detected in wild-type cells, but was absent when the protein was tagged with HA. In comparison to the antiserum before the purification, the unspecific background was obviously reduced and the α6-signal could be distinguished more easily from the other bands. However, the α6 antibody still detected a lot of unspecific material, especially in the upper part of the membrane (Figure 2.4 b). Originally, the antibody against Pba3/Pba4-HA was intended to be specific against both of the heterodimeric chaperone proteins, Pba3 and Pba4. As the purification of the antiserum was done using a *pba3*Δ strain, the antibody mainly detected Pba3. Similar to α5, a nice shift was visible when the protein was tagged with HA and the signal disappeared in the *pba3*Δ cells, confirming the specificity of the antibody. In the *pba3*Δ cells, another prominent band appeared. Besides the deletion of *PBA3*, this strain expresses a HA tagged version of α5. As

the size fits perfectly, it can be concluded that the antibody not only detects Pba3 but recognizes HA tagged proteins in yeast. After purification of the antiserum, barely any unspecific signal was visible for the Pba3 antibody (Figure 2.4 c). All together it can be said that specific antibodies were generated for the proteasome components α5, α6 and Pba3(-Pba4-HA). Especially for purified *E. coli* proteins these antibodies are highly efficient and specific, but also in yeast boiled extracts, the distinct proteins can be specifically detected.

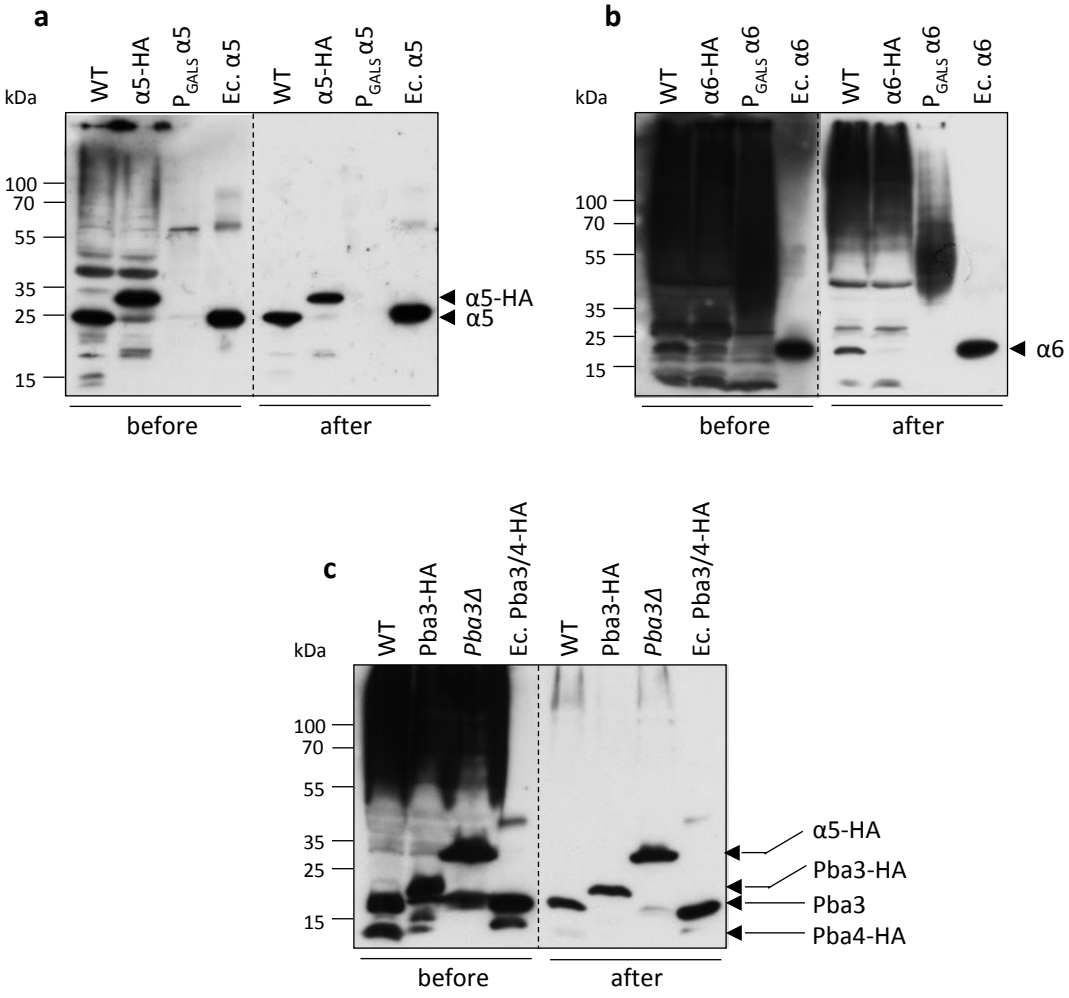

Figure 2.4 – Specificity of produced α subunit and Pba3/Pba4-HA antibodies. Comparison of antisera before and after the purification procedure for anti-α5 **(a)**, anti-α6 **(b)** and anti-Pba3 **(c)** antibodies. 2 OD boiled extracts from wild-type (JD47-13C), α5-HA (JM9), α6-HA (JM10), Pba3-HA (PG28) and P$_{GALS}$*PUP2*/α5 *PRE10*/α7-HA (PR57), P$_{GALS}$*PRE5*/α6 *PUP2*/α5-HA (PR65), *pba3*Δ *PUP2*/α5-HA (PR123) as well as the corresponding proteins purified from *E. coli* were analyzed by SDS-PAGE and western blotting. Antisera before (left) and after (right) purification were compared (concentration 1:5000 for anti-α5 and anti-Pba3 and 1:1000 for anti-α6).

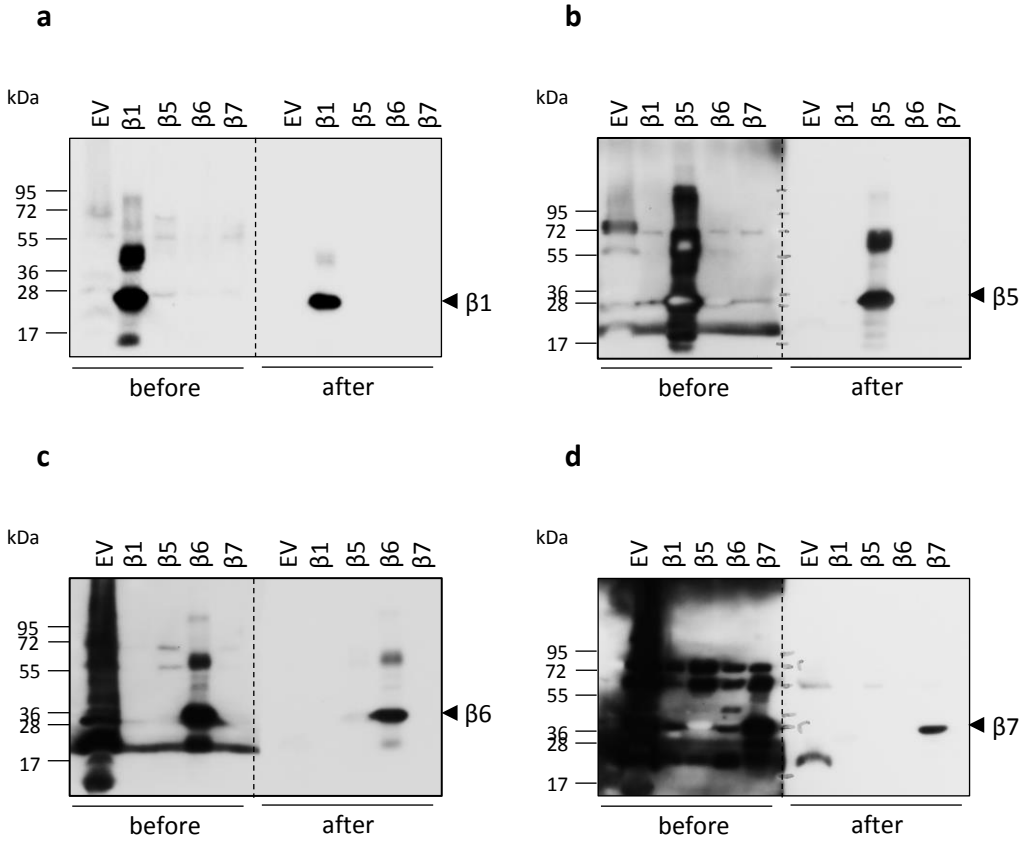

Figure 2.5 – Specificity of produced β subunit antibodies. Comparison of antisera before and after the affinity purification for anti-β1 **(a)**, anti-β5 **(b)**, anti-β6 **(c)**, and anti-β7 **(d)** antibodies. 1 OD boiled extracts of the empty vector (EV) and 14 µg of the proteins purified from *E. coli* were analyzed by SDS-PAGE and western blotting. Antisera before (left) and after (right) the purification were compared (concentration 1:5000).

Besides antibodies against α5, α6 and Pba3/Pba4-HA, antisera for a specific detection of the proteasome subunits β1, β5, β6 and β7 were produced. Untagged yeast proteins were expressed in *E. coli* and purified as described above. Afterwards, proteins were sent to Pineda Antikörper-Service for immunization of rabbits (see also M.Sc. thesis Jessica Zimmermann, 2018). This time polyclonal antibodies were affinity purified from the serum. 250 µg of the purified target protein was loaded on SDS-PAGE, transferred to a PVDF membrane and stained in Ponceau S solution. The band specific for the target protein was cut and incubated with the serum at 4 °C overnight. The next day, antibodies were eluted from the membrane using Glycine buffer pH 2.8 and the antibody solution was transferred for neutralization to Tris buffer pH 8.1 containing 10 % BSA and 6.5 % NaN_3. Finally, antibodies were aliquoted and stored at -80 °C for further usage. Efficiency of the purification was tested by comparing the antisera before and after the procedure. Therefore,

an empty vector control (EV) and the *E. coli* purified proteins were analyzed by SDS-PAGE and western blotting (Figure 2.5). All antibodies detected a specific signal for the distinct β subunits purified from *E. coli*. When proteins were detected using the serum, the unspecific background was much higher, especially for the empty vector sample. In contrast, the affinity purified antibodies did detect mainly one specific band. In case of β7, the unspecific background was pretty high when the serum was used. After the purification, still some unspecific signals were detected for the empty vector sample. In general, the antibodies were highly efficient and specific for the detection of purified *E. coli* proteins. For yeast protein extracts, however, hardly any specific signal was detected. The unspecific background was extremely high, both before and after the affinity purification (data not shown). When alternatively the same method was used to remove non-specific antibodies from the serum as it was done to improve the specificity of the α5, α6 and Pba3/Pba4-HA antibodies, the results did not get better.

Together with the antibodies, which were already present in the laboratory, a large selection for 20S proteasome-specific detection is available. These antibodies against α5, α6, α7, β1, β2, β5, β6 and β7 will be a useful tool for the analysis of distinct proteasome assembly steps and to study particular protein-protein interactions.

2.2 Rpn4-mediated expression regulation of 20S proteasome subunits

The expression levels of proteasome genes are regulated by the transcriptional activator Rpn4, which binds PACE and PACE-like sequences in their promoters. The discovery of such distinct elements was an indication that proteasome subunits might not be synthesized in stoichiometric amounts, as it has been assumed, but can be regulated differently. Therefore, the aim was to analyze the expression level of different 20S proteasome subunits, and to study to which extent their levels are influenced by Rpn4-mediated regulation.

2.2.1 The expression level of 20S CP α subunits is higher than for β subunits

To compare the abundances of the different 20S proteasome subunits on protein level, C-terminally 2xHA tagged proteins were used. Yeast strains were grown to an OD_{600} of about

0.8-1, cells were harvested and proteins were extracted by boiling in Laemmli lysis buffer. Subunits were analyzed by SDS-PAGE and anti-HA western blotting (Figure 2.6).

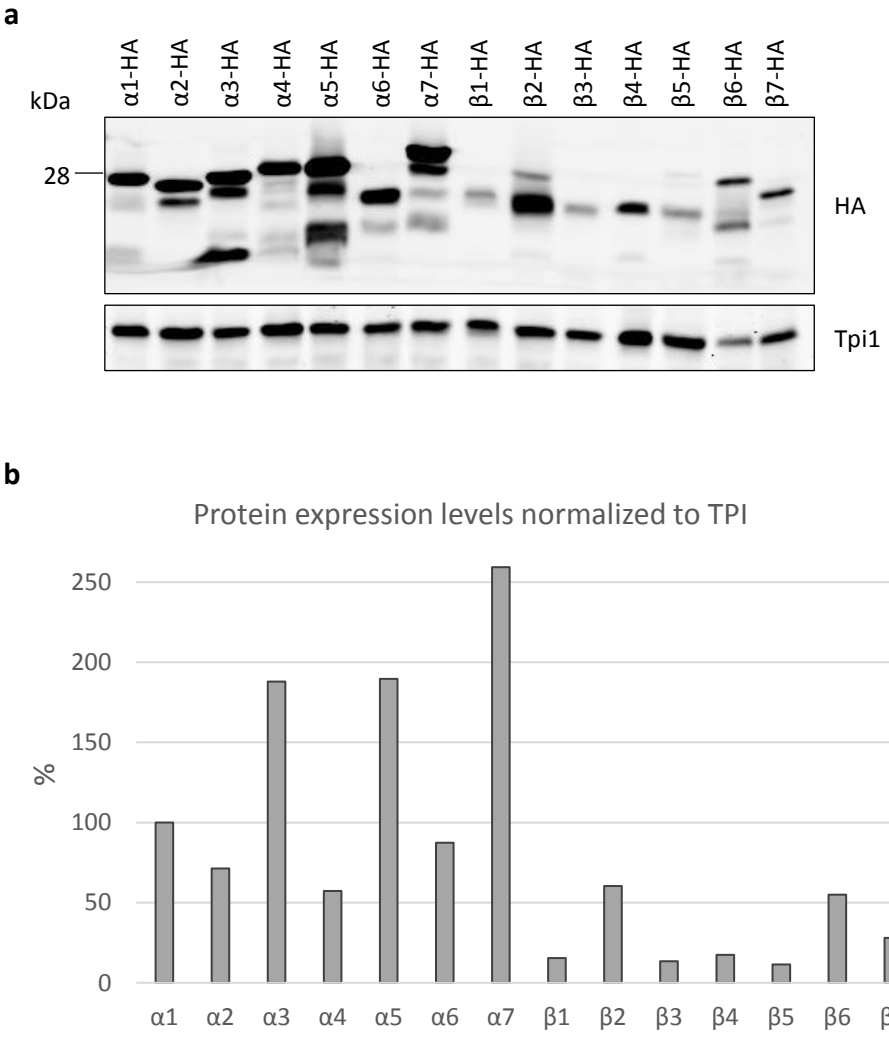

Figure 2.6 – Protein expression levels of 20S proteasome subunits. (a) *S. cerevisiae* strains were grown in SD medium at 30 °C until an OD_{600} ~0.8-1 was reached. 15 µl boiled extracts of cells containing different C-terminally 2xHA tagged subunits (α1/*SCL1*-2HA (JD2701), α2/*PRE8*-2HA (JD2702), α3/*PRE9*-2HA (CM257), α4/*PRE6*-2HA (JD2704), α5/*PUP2*-2HA (JD2705), α6/*PRE5*-2HA (CM273), α7/*PRE10*-2HA (JD2707), β1/*PRE3*-2HA (FP6), β2/*PUP1*-2HA (JD139), β3/*PUP3*-2HA (CM61), β4/*PRE1*-2HA (JD71), β5/*PRE2*-2HA (JD138), β6/*PRE7*-2HA (MN36) and β7/*PRE4*-2HA (SS4)) were analyzed by SDS-PAGE and western blotting. HA tagged subunits were detected by anti-HA (3F10) antibody. Tpi1 served as an internal loading control. **(b)** Relative expression levels of proteasome subunits normalized to corresponding Tpi1 levels in percent were calculated by setting α1-2HA protein levels as 100 %.

Interestingly, α subunits were present at strikingly higher levels than β subunits. Especially α3, α5 and α7 were detected in high relative amounts between 190-260 % compared to α3, which was set as 100 %. α4 was the α subunit with the lowest abundancy of under 40 %. In

comparison, most of the β subunits had a much lower abundancy of only 10-15 %, with β7 being the most abundant one of about 28 %. The β2 and β6 subunits, however, were a little bit more abundant than the other β subunits with an expression level similar to the lowest α subunit (between 50-60 %). As the C-terminal HA tag on these subunits was observed before to cause growth phenotypes, this result should be taken with caution. Nevertheless, in general it can be said that the protein expression level of 20S proteasome α subunits is higher than for β subunits. This observation is consistent with the data obtained in earlier studies (Schwab, 2017).

2.2.2 Production of prototrophic yeast strains

Previous findings in our group had suggested that the proteasome subunits are affected by Rpn4 to a different extent in that β subunits were regulated stronger than α subunits (Schwab, 2017). As these findings were generated using C-terminally HA tagged proteins, which may possibly influence the expression or growth phenotype of cells, the aim was to repeat these experiments using the newly generated specific antibodies (see chapter 2.1) for detection of the endogenous proteasome subunit proteins. To do so, the idea was to generate yeast strains with comparable markers, and to detect different subunits in the same cell extract. The *RPN4*-induced gene expression between different proteasome subunits was compared using an *RPN4* deletion strain (*rpn4Δ*) and a strain expressing a stabilized version of Rpn4 (Rpn4*), additionally to the wild-type background.

As it was shown that the use of auxotrophic markers may have an impact on physiology and gene expression, such as cell growth and fatty acid production in *S. cerevisiae* (Pronk, 2002; Canelas *et al.*, 2010; Grüning *et al.*, 2010; Yan *et al.*, 2023), prototrophic yeast strains were produced. In the first step, strains with two marker sets and complementary mating types were generated. Therefore, the desired marker was cut from a *E. coli* plasmid using the required restriction enzymes and used to transform the respective yeast strain (see Table 2.2). In the next step, yeast strains with complementary mating types were crossed (JZ3xJZ5 and JZ4xJZ5), tetrad dissection was performed and spore clones were verified testing the markers and the mating types. All yeast strains that were produced including different marker combinations and the corresponding mating types are listed in Table 2.3.

Table 2.2 – Yeast strains generated by transformation.

Name	Mating-type	Genotype	Marker	Construction details		Stock number
				Yeast strain	Plasmid	
JZ3	*MAT*α	"WT"	*HIS3*, *LYS2*	JD337 JD53 + *HIS3* Sc. 1463	pFP5 KpnI_*LYS2*_BshTI Ec. 4695	Sc. 4714
JZ4	*MAT*α	*rpn4*Δ	*HIS3*, *LYS2*	JD330-3A *rpn4*Δ::*HIS3* Sc. 1250	pFP5 KpnI_*LYS2*_BshTI Ec. 4695	Sc. 4715
JZ5	*MAT*a	"WT"	*TRP1*, *LEU2*	MB1 JD47-13C + *TRP1* Sc. 4274	pJD278 BglII_*LEU2*_BglII Ec. 1367	Sc. 4716
JZ9	*MAT*α	*RPN4**	*HIS3*, *LYS2*, *LEU2*, *TRP1*	JZ6 JZ3xJZ5 Sc. 4717	pJZ28 NotI_P_{RPN4}RPN4$_{\Delta 1\text{-}10/\Delta 211\text{-}229}$::*LEU2*_NotI Ec. 4783	Sc. 4720

Table 2.3 – Prototrophic yeast strains generated by crossing and tetrad dissection.

Name	No	Mating-type	*RPN4*	Marker	Name	No	Mating-type	*RPN4*	Marker
JZ16	1	*MAT*α	WT	*HIS3*	JZ36	22	*MAT*a	WT	*HIS3*, *LYS2*, *LEU2*
JZ17	2	*MAT*a	WT	*HIS3*	JZ6	23	*MAT*α	WT	*HIS3*, *LYS2*, *TRP1*
JZ18	3	*MAT*α	WT	*LYS2*	JZ37	24	*MAT*a	WT	*HIS3*, *LYS2*, *TRP1*
JZ19	4	*MAT*a	WT	*LYS2*	JZ38	26	*MAT*a	WT	*HIS3*, *LEU2*, *TRP1*
JZ20	6	*MAT*a	WT	*LEU2*	JZ39	27	*MAT*α	WT	*LYS2*, *LEU2*, *TRP1*
JZ21	7	*MAT*α	WT	*TRP1*	JZ40	28	*MAT*a	WT	*LYS2*, *LEU2*, *TRP1*
JZ22	8	*MAT*a	WT	*TRP1*	JZ7	29	*MAT*α	WT	*HIS3*, *LYS2*, *LEU2*, *TRP1*
JZ23	9	*MAT*α	WT	*HIS3*, *LYS2*	JZ41	30	*MAT*a	WT	*HIS3*, *LYS2*, *LEU2*, *TRP1*
JZ24	10	*MAT*a	WT	*HIS3*, *LYS2*	JZ42	31	*MAT*α	*rpn4*Δ	*HIS3*
JZ25	11	*MAT*α	WT	*HIS3*, *LEU2*	JZ43	32	*MAT*a	*rpn4*Δ	*HIS3*
JZ26	12	*MAT*a	WT	*HIS3*, *LEU2*	JZ44	33	*MAT*α	*rpn4*Δ	*HIS3*, *LYS2*
JZ27	13	*MAT*α	WT	*HIS3*, *TRP1*	JZ45	34	*MAT*a	*rpn4*Δ	*HIS3*, *LYS2*
JZ28	14	*MAT*a	WT	*HIS3*, *TRP1*	JZ46	35	*MAT*α	*rpn4*Δ	*HIS3*, *LEU2*
JZ29	15	*MAT*α	WT	*LYS2*, *LEU2*	JZ47	36	*MAT*a	*rpn4*Δ	*HIS3*, *LEU2*
JZ30	16	*MAT*a	WT	*LYS2*, *LEU2*	JZ48	37	*MAT*α	*rpn4*Δ	*HIS3*, *TRP1*
JZ31	17	*MAT*α	WT	*LYS2*, *TRP1*	JZ49	39	*MAT*α	*rpn4*Δ	*HIS3*, *LYS2*, *LEU2*
JZ32	18	*MAT*a	WT	*LYS2*, *TRP1*	JZ50	40	*MAT*a	*rpn4*Δ	*HIS3*, *LYS2*, *LEU2*
JZ33	19	*MAT*α	WT	*LEU2*, *TRP1*	JZ51	41	*MAT*α	*rpn4*Δ	*HIS3*, *LYS2*, *TRP1*
JZ34	20	*MAT*a	WT	*LEU2*, *TRP1*	JZ52	44	*MAT*a	*rpn4*Δ	*HIS3*, *LEU2*, *TRP1*
JZ35	21	*MAT*α	WT	*HIS3*, *LYS2*, *LEU2*	JZ8	45	*MAT*α	*rpn4*Δ	*HIS3*, *LYS2*, *LEU2*, *TRP1*

Rpn4 is extremely short-lived *in vivo* and degraded in a ubiquitin-dependent and a ubiquitin-independent manner by the 26S proteasome. While the N-terminal ten amino acid residues of Rpn4 constitute the ubiquitin-independent degradation signal, residues 211-229 are required for ubiquitin-dependent degradation (Ju and Xie, 2006). To examine the differential response of proteasome subunit expression to elevated Rpn4 levels, a stabilized and transcriptionally active version of Rpn4 could be used. Therefore, an Rpn4 mutant was used, which is simultaneously deleted of residues 1-10 and 211-229 (Rpn4*) (Wang *et al.*, 2010). To produce a yeast strain that expresses *RPN4** from its native promoter integrated at the *LEU2* locus, the newly generated strain JZ6 was used and transformed with the NotI digested *RPN4* LEU2* cassette from plasmid pJZ28 (see Table 2.2).

As described above, the use of auxotrophic markers impacts the physiology and gene expression in yeast. Moreover, it was shown by flux balance analyses using a genome-wide metabolic model, that the activity status of some 200-300 reactions changes between different auxotrophic strains and the wild-type (Mülleder *et al.*, 2012). To reduce bias in physiological and metabolic studies, the removal of unnecessary auxotrophic markers and the construction of a prototrophic derivative is required (Canelas *et al.*, 2010). Therefore, the generated yeast strains restoring prototrophy in the genetic background will prevent any influence of auxotrophy on the phenotype and facilitates the exploitation of prototrophic yeast in both functional genomic and quantitative systems biology. For downstream applications, yeast strains JZ7 (WT, *RPN4 HIS3, LYS2, LEU2, TRP1 MAT*α), JZ8 (*rpn4*Δ *HIS3, LYS2, LEU2, TRP1 MAT*α) and JZ9 (*RPN4* HIS3, LYS2, LEU2, TRP1 MAT*α) were used.

2.5.3 *RPN4* induced gene expression for α subunits is stronger than expected

To analyze the *RPN4* induced gene expression for different proteasome subunits, the prototrophic yeast strains JZ7 (WT), JZ8 (*rpn4*Δ) and JZ9 (*RPN4**) were used. The advantage of these strains was that no tag or auxotrophic marker was present to possibly influence the physiology or gene expression of the cells. Furthermore, distinct amounts of the *E. coli* purified subunits (purification done as described in chapter 2.1.1) were loaded as a reference, and the distinct proteins were detected with the specific polyclonal antibodies

generated in this study (besides β7). Using this strategy, the exact amounts of different 20S CP subunits could be determined and compared (Figures 2.7-2.10).

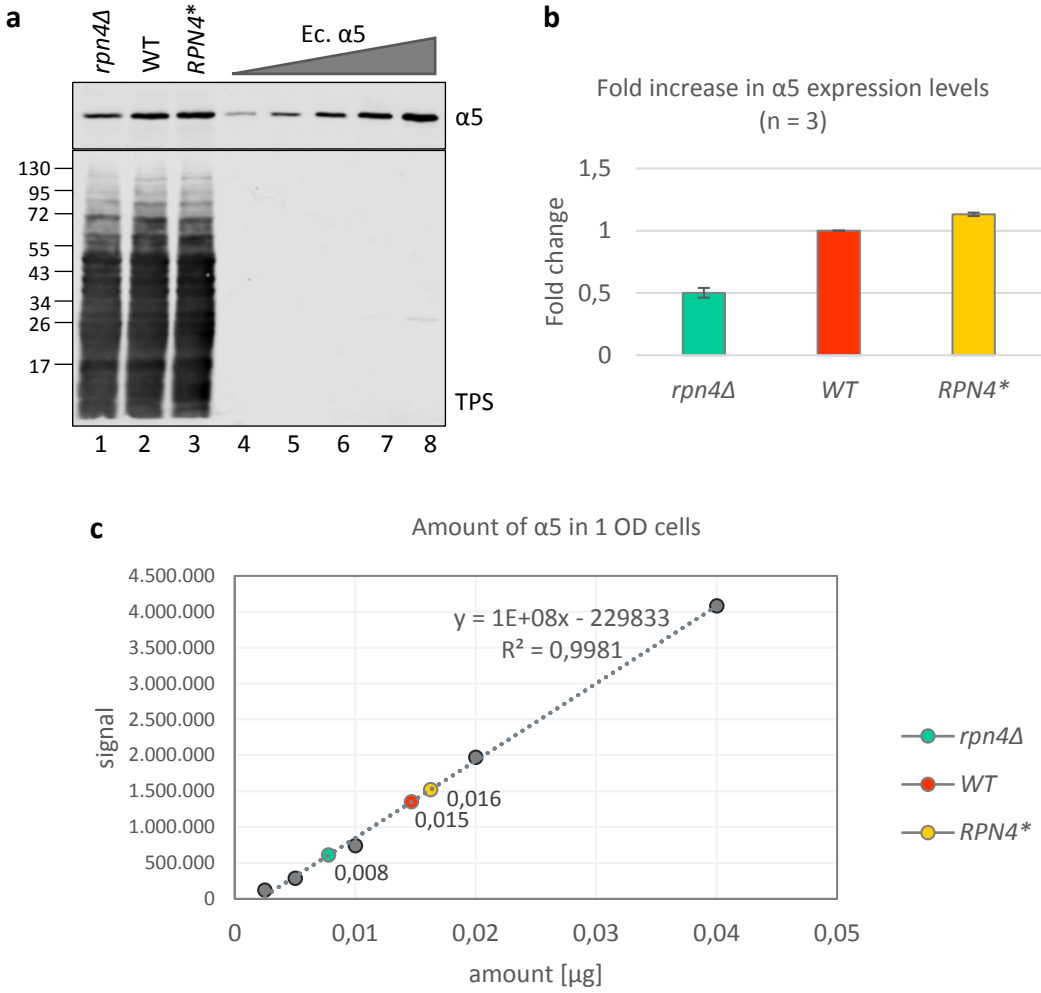

Figure 2.7 – Steady state levels of the yeast 20S proteasome subunit α5. (a) SDS-PAGE and western blotting of α5 expression levels. *S. cerevisiae* strains were grown at 30 °C in SD medium to an OD_{600} of about 0.8-1. Cells were harvested and proteins were extracted by boiling in Laemmli buffer. 1 OD of WT (JZ7), *rpn4*Δ (JZ8) and *RPN4** (JZ9) was analyzed by SDS-PAGE and anti-α5 western blotting. Distinct amounts of the subunit purified from *E. coli* were loaded as a reference (0.0025 µg, 0.005 µg, 0,01 µg, 0.02 µg, 0.04 µg). Total protein staining (TPS) was performed to control for loading differences. **(b)** Fold change in α5 expression levels. Bar graphs represent means ± SD (n=3) of proteasome subunit levels normalized to the corresponding total protein level. Relative proteasome subunit levels were calculated by setting the wild-type α5 protein levels as 100 %. **(c)** Amount of α5 in 1 OD cells. Reference values of the α5 subunit purified from *E. coli* were used to calculate a regression line. α5-signals in the different yeast background strains (WT, *rpn4*Δ, *RPN4**) were correlated to the amount in µg using the trend line, revealing the exact amount of the protein present in 1 OD cells.

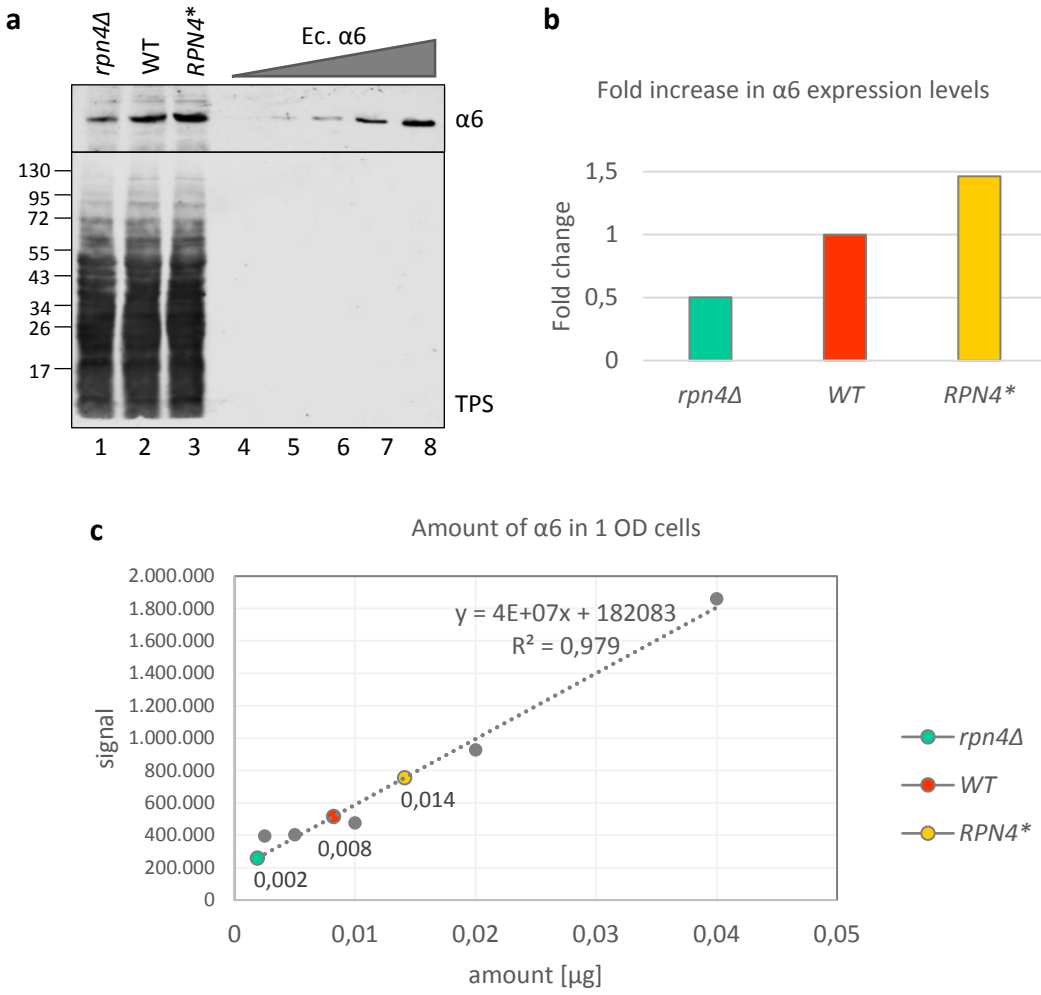

Figure 2.8 – Steady state levels of the yeast 20S proteasome subunit α6. (a) SDS-PAGE and western blotting of α6 expression levels. *S. cerevisiae* strains were grown at 30 °C in SD medium to an OD_{600} of about 0.8-1. Cells were harvested and proteins were extracted by boiling in Laemmli buffer. 1 OD of WT (JZ7), *rpn4*Δ (JZ8) and *RPN4** (JZ9) was analyzed by SDS-PAGE and anti-α6 western blotting. Distinct amounts of the subunit purified from *E. coli* were loaded as a reference (0.0025 µg, 0.005 µg, 0,01 µg, 0.02 µg, 0.04 µg). Total protein staining (TPS) was performed to control for loading differences. **(b)** Fold change in α6 expression levels. Bar graphs represent fold change of proteasome subunit levels normalized to the corresponding total protein level. Relative proteasome subunit levels were calculated by setting the wild-type α6 protein levels as 100 %. **(c)** Amount of α6 in 1 OD cells. Reference values of the α6 subunit purified from *E. coli* were used to calculate a regression line. α6-signals in the different yeast background strains (WT, *rpn4*Δ, *RPN4**) were correlated to the amount in µg using the trend line, revealing the exact amount of the protein present in 1 OD cells.

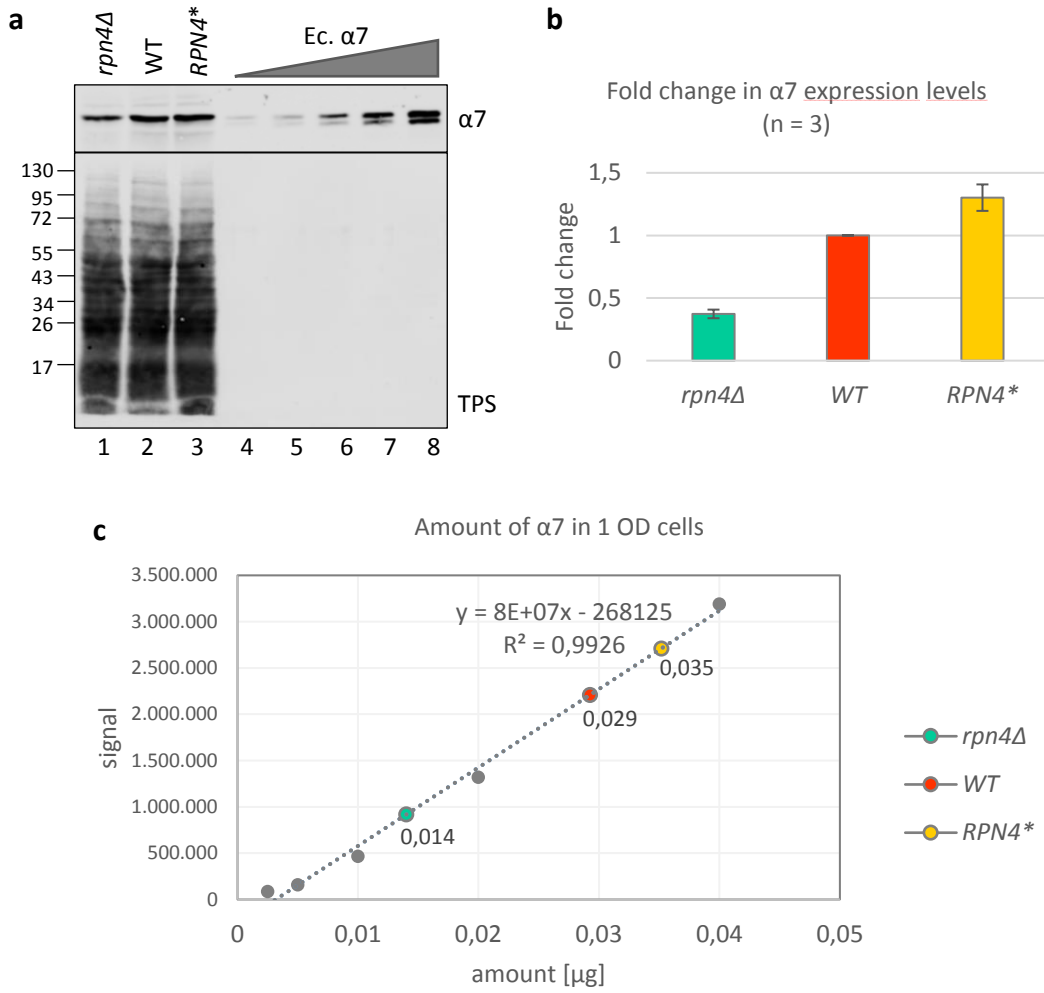

Figure 2.9 – Steady state levels of the yeast 20S proteasome subunit α7. (a) SDS-PAGE and western blotting of α7 expression levels. *S. cerevisiae* strains were grown at 30 °C in SD medium to an OD_{600} of about 0.8-1. Cells were harvested and proteins were extracted by boiling in Laemmli buffer. 1 OD of WT (JZ7), *rpn4*Δ (JZ8) and *RPN4** (JZ9) was analyzed by SDS-PAGE and anti-α7 western blotting. Distinct amounts of the subunit purified from *E. coli* were loaded as a reference (0.0025 µg, 0.005 µg, 0,01 µg, 0.02 µg, 0.04 µg). Total protein staining (TPS) was performed to control for loading differences. **(b)** Fold change in α7 expression levels. Bar graphs represent means ± SD (n=3) of proteasome subunit levels normalized to the corresponding total protein level. Relative proteasome subunit levels were calculated by setting the wild-type α7 protein levels as 100 %. **(c)** Amount of α7 in 1 OD cells. Reference values of the α7 subunit purified from *E. coli* were used to calculate a regression line. α7-signals in the different yeast background strains (WT, *rpn4*Δ, *RPN4**) were correlated to the amount in µg using the trend line, revealing the exact amount of the protein present in 1 OD cells.

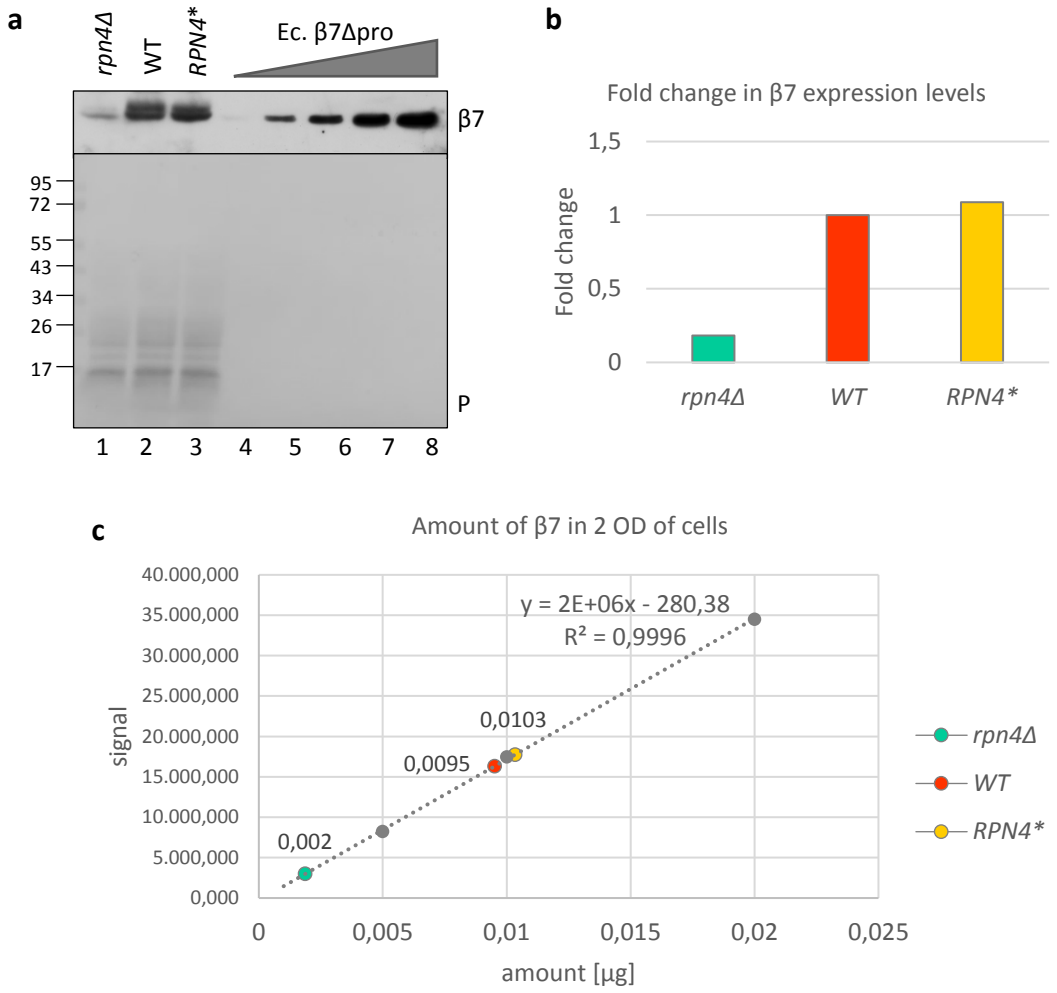

Figure 2.10 – Steady state levels of the yeast 20S proteasome subunit β7. (a) SDS-PAGE and western blotting of β7 expression levels. *S. cerevisiae* strains were grown at 30 °C in SD medium to an OD_{600} of about 0.8-1. Cells were harvested and proteins were extracted by boiling in Laemmli buffer. 2 OD of WT (JZ7), *rpn4*Δ (JZ8) and *RPN4** (JZ9) was analyzed by SDS-PAGE and anti-β7 western blotting (β7 antibody was not the one generated in this study but from Jäger *et al*., 1999). Distinct amounts of the subunit (β7Δpro) purified from *E. coli* were loaded as a reference (0.0025 µg, 0.005 µg, 0,01 µg, 0.02 µg, 0.04 µg). Ponceau staining (P) was performed to control for loading differences. **(b)** Fold change in β7 expression levels. Bar graphs represent fold change of proteasome subunit levels normalized to the corresponding total protein level. Relative proteasome subunit levels were calculated by setting the wild-type β7 protein levels as 100 %. **(c)** Amount of β7 in 2 OD cells. Reference values of the β7 subunit purified from *E. coli* were used to calculate a regression line. β7-signals in the different yeast background strains (WT, *rpn4*Δ, *RPN4**) were correlated to the amount in µg using the trend line, revealing the exact amount of the protein present in 2 OD cells.

Earlier results had indicated, that most 2xHA tagged α subunits levels do not show any remarkable difference when Rpn4 was deleted or stabilized in comparison to the wild-type (± 25 %) (Schwab, 2017). However, when endogenous α subunits were detected with specific antibodies, a clear difference between wild-type and *rpn4*Δ background strains was

observed. For both, α5 and α6, the protein level was decreased by 50 % and even by more than 60 % for α7, when Rpn4 was deleted (Figures 2.7-2.9). When Rpn4 was stabilized, the effect on the α subunits was quite different in comparison to the wild-type background. While the induction of α6 and α7 was ranging between ~145 % and 130 %, respectively, the expression rate of α5 was increased by only 15 %.

β subunits were shown to be much stronger regulated by Rpn4 than α subunits (Schwab, 2017). Among the different β subunits, the variation on protein expression in response to Rpn4 levels was ranging from 46 % to 171 %. For β7, the expression range was even between 22 % in *rpn4*Δ and 198 % in *RPN4** (Schwab, 2017), which supports the notion that β7 is the rate-limiting subunit in the 20S proteasome assembly pathway (Marques *et al.*, 2007). In agreement with these findings, β7 was even stronger regulated by Rpn4 than the tested α subunits. Whereas the expression of α5, α6 and α7 changed two- to three-fold comparing wild-type and *rpn4Δ*, the induction of β7 was changing about five-fold in these strains when endogenous subunits were detected using a specific antibody.

In total, the protein amount of α5 seems to be higher with about 0.015 µg in 1 OD of wild-type yeast cells in comparison to the amount of α6, lying at 0.008 µg. With ~0.029 µg, α7 is the most abundant of these three subunits. This results also fit approximately to the proportions observed in figure 2.6, showing that 2xHA tagged subunits differ from 85 % for α6 to 190 % for α5 to 260 % for α7 in comparison to α1-2xHA protein amounts. According to figure 2.10, the total protein amount of β7 in 1 OD yeast cells comprises about 0.005 µg. If one takes earlier findings into consideration, this result is not surprising, as the HA tagged variants of β subunits were shown to be much less abundant than identically tagged α subunits (Figure 2.6, Schwab, 2017). When 2xHA tagged subunits were analyzed, the amount of α5 was 6-7 times higher and α6 was at least 3 times more abundant than β7 (Figure 2.6). 0.005 µg for β7 is between two to six times less than the amount observed for the analyzed α subunits, which supports the idea that the rate-limiting subunit β7 is expressed less, but is more strongly up-regulated in an Rpn4-dependent manner than the other subunits. These results are considered as preliminary data and need to be proven by further investigations and repeating the experiments multiple times to obtain reliable statistics.

2.3 *In vitro* assembly of yeast proteasome precursor complexes

The step-wise process of 20S proteasome assembly in eukaryotes is still not fully understood. In contrast to the α-ring as an early assembly intermediate (see Introduction), we identified a preliminary complex containing distinct subsets of α and β subunits (α1-α4 and β2-β4) as well as the maturation factor Ump1 in our studies in *Saccharomyces cerevisiae*. This complex was termed Complex I and was found to accumulate in cells lacking functional Pba1-Pba2 assembly chaperones (Matias *et al*., in preparation). *In vitro* experiments demonstrated an α5-dependent interaction between Pba3-Pba4 and the subunits α5, α6 and α7, as well as preferential binding of human PAC1-PAC2 to α5 and α7 (Hirano *et al.*, 2005; Kusmierczyk *et al.*, 2008). In line with these findings, our model suggests that a complementary complex, namely Complex II, exists that contains the subunits α5, α6 and α7, as well as the chaperones Pba1-Pba2 and Pba3-Pba4. To recapitulate the step-wise assembly process and to determine whether Complex II is a functional intermediate, the aim was to assemble this complex *in vitro* from purified components.

2.3.1 Expression and purification of Complex II components from *E. coli*

For the *in vitro* assembly of complex II, yeast proteasome components were produced in *E. coli*. In addition to α5, α6 and Pba3-Pba4 (see 2.1.1), plasmids expressing the α7 subunit and the chaperone pair Pba1-Pba2 were generated. Similar to Pba3-Pba4, Pba1-Pba2 were expressed from the same vector under control of the same promoter but containing individual translation initiation sites. Furthermore, these proteins were again fused to 8His-SUMO1 to enhance the solubility and allow for selective affinity purification (Figure 2.11 a). Pba2 was additionally tagged with a FLAG epitope on the C-terminus. Boiled protein extracts and native protein extracts were analyzed by SDS-PAGE and Coomassie staining. All proteins were efficiently expressed in *E. coli* and yielded adequate soluble amounts (Figure 2.11 b, compare total (T) and soluble (SL) protein amounts). No corresponding protein was present in the empty vector (EV) control sample, confirming the specificity of the detected bands. Native protein extracts of *E. coli* cells were used to purify these subunits by Ni^{2+}-NTA affinity chromatography. In contrast to the protein purification for the antibody production, the 8His-SUMO1 tag was not cleaved during the purification to keep the proteins as soluble as possible. Samples of the input (IN), the unbound material (UB) and the elution (E) were

analyzed by SDS-PAGE, followed by Coomassie staining to verify the efficiency of the purification (Figure 2.11 c). All of the Complex II components were obtained in high amounts (approximately 5-15 mg) and purity. Due to the remaining 8His-SUMO1 tag, proteins stayed in a very soluble form. While Pba1-Pba2 were purified roughly in a 1:1 stoichiometry, the amount of 8His-SUMO1-Pba3 was clearly higher than for Pba4-HA. Sufficient amounts of soluble, pure proteins of all necessary proteasome components were obtained for *in vitro* assembly assays.

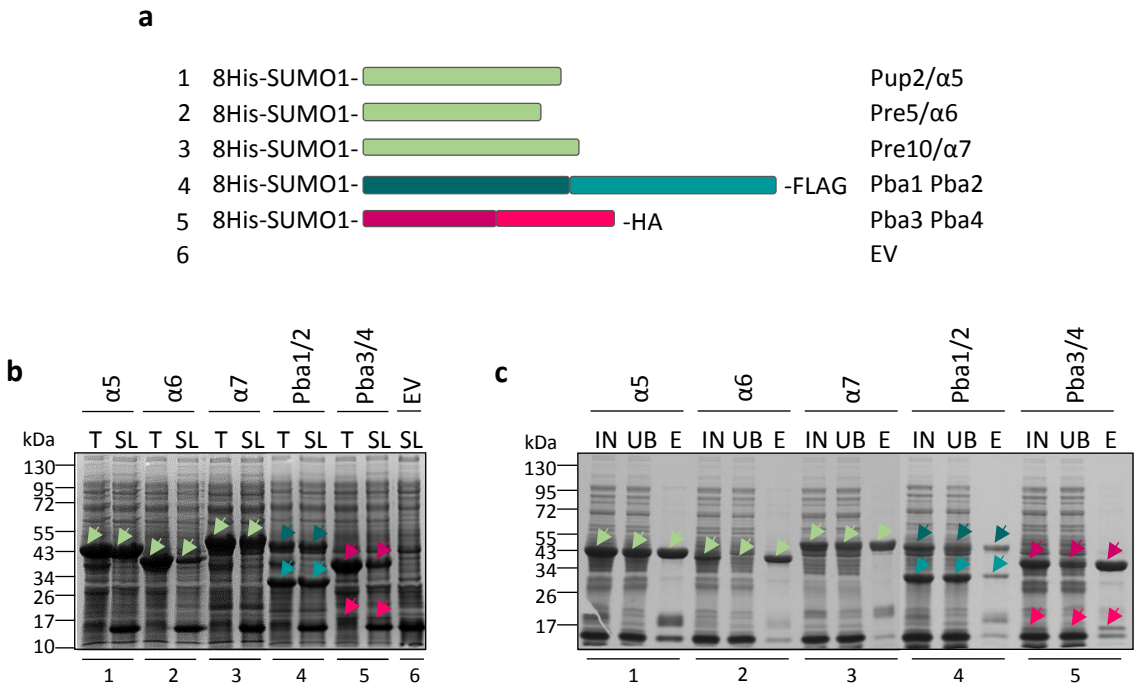

Figure 2.11 – Expression and purification of Complex II components. (a) Schematic representation of produced proteasome subunits Pup2/α5 (plasmid pJZ20), Pre5/α6 (plasmid pJZ21), Pre10/α7 (plasmid pJZ22) and the chaperone pairs Pba1-Pba2 (plasmid pJZ24) and Pba3-Pba4 (plasmid pJZ23) fused to SUMO1 and 8His. Pba2 contains additionally a FLAG epitope and Pba4 an HA tag on the C-terminus. **(b)** Comparison of total (T) and soluble (SL) protein amounts (0.2 OD) of 8His-SUMO1 tagged proteins in *E. coli* analyzed by 12 % SDS-PAGE followed by Coomassie staining. The empty vector (EV) serves as control. Specific proteins are indicated by arrows. **(c)** Proteins were purified using Ni^{2+}-NTA affinity chromatography. Samples of the input (IN), the unbound (UB) and the elution (E) were analyzed by 12 % SDS-PAGE and Coomassie staining. Loaded material corresponds to 0.2 OD of cells. Purified proteins were yielded in concentrations between ~10-30 mg/ml.

2.3.2 Complex II components except Pba1-Pba2 were co-eluted from HA resin

To investigate whether a complex containing the subunits α5, α6 and α7 and the chaperone pairs Pba1-Pba2 as well as Pba3-Pba4 can be assembled *in vitro*, a co-immunoprecipitation

(co-IP) experiment was performed. Therefore, Pba3-Pba4 was immobilized on HA resin using its C-terminal HA tag. Afterwards, α5, α6, α7 and Pba1-Pba2-FLAG were added. The 8His-SUMO1 tag was cleaved only during the binding step by Senp1. Using this method, the proteins were kept in a soluble state as long as possible. After washing, proteins were eluted and analyzed by 12 % SDS-PAGE and western blotting (Figure 2.12). For detection of α5 and α6, the antibodies generated in this study were used. 10 % of the 8His-SUMO1 tagged input were loaded in comparison to the binding reaction.

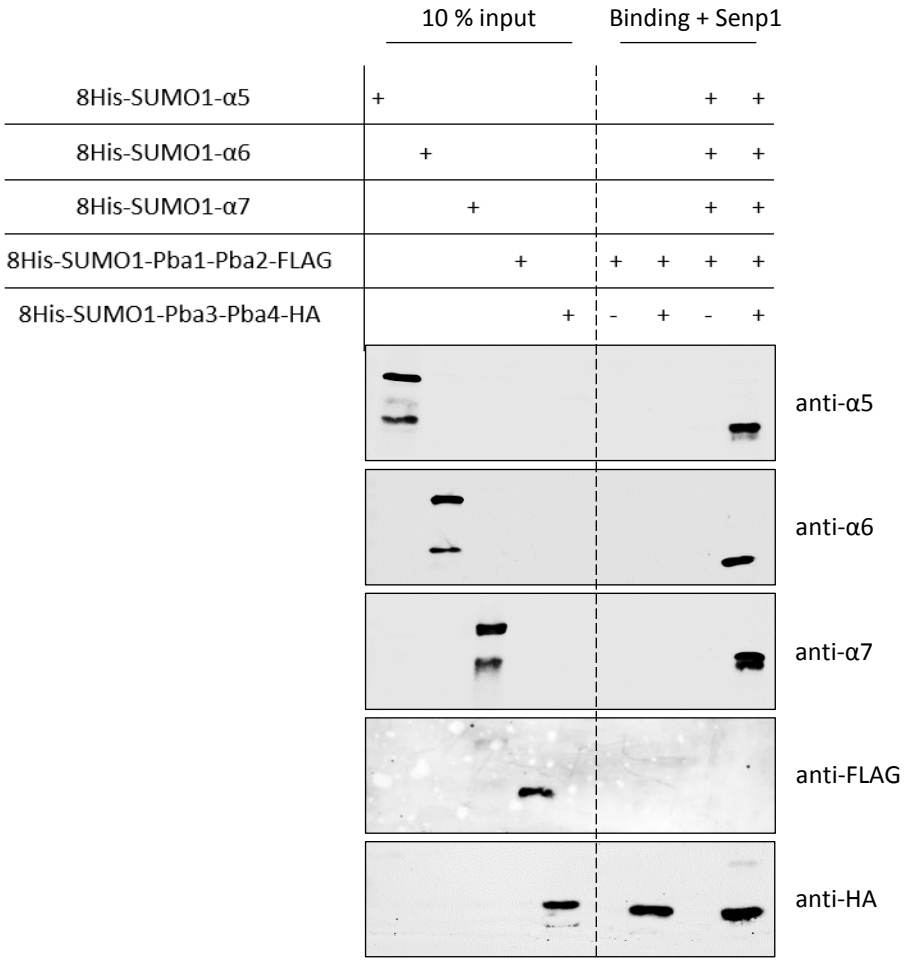

Figure 2.12 – Co-IP of Pba3-Pba4 with proteasome subunits α5, α6 and α7 and the chaperone pair Pba1-Pba2. Pba3-Pba4-HA was immobilized to HA resin and tested for binding to α5, α6, α7 and Pba1-Pba2-FLAG. All components were purified from *E. coli* as 8His-SUMO1 fusions, a solubility tag which was cleaved during the binding step. Bound proteins were eluted with imidazole and analyzed by SDS-PAGE and western blotting using specific antibodies (anti-α5, -α6, -α7, -FLAG and -HA). As a control, proteins were incubated without Pba3-Pba4-HA to exclude unspecific affinity to the resin. The two chaperone pairs Pba1-Pba2 and Pba3-Pba4 alone were tested for binding as well. For all utilized 8His-SUMO1 tagged proteins, 10 % input were loaded.

All three proteasome subunits α5, α6 and α7 were efficiently co-eluted with Pba3-Pba4 from the resin. When the test proteins were incubated without Pba3-Pba4, no signal was detected, excluding unspecific affinity of the proteins to the beads. Pba1-Pba2, however, was not present in the elution fraction. The reason for this could be either that the affinity of Pba1-Pba2 to the other proteins is too low to overcome the washing or that this chaperone is just not part of the complex. The two chaperone pairs Pba1-Pba2 and Pba3-Pba4 alone were tested for binding as well, but similar to the binding reaction with α5, α6 and α7, Pba1-Pba2 was not eluted from the resin.

2.3.3 Pba1-Pba2 leads to a shift from Complex I to 15S PC

In wild-type yeast cells, almost all of the Ump1 protein is present in 15S precursor complexes (Ump1-HA). In contrast, in cells lacking the *PBA1* gene (*pba1Δ* Ump1-HA), Ump1 is mainly detected in Complex I, when analyzed by native-PAGE (Nunes, 2015). This and the previous experiment (see figure 2.12) led to the question whether the amount of Pba1-Pba2 available in the cell could become rate limiting for 15S PC formation and if this chaperone pair is able to convert Complex I to 15S PC. To address this idea experimentally, a mutant strain was used in which the promoters of the *PBA1* and *PBA2* genes were substituted by the carbon source-controlled *GAL1* promoter (P_{GAL1}). P_{GAL1} is induced in the presence of galactose and repressed in the presence of glucose. When these cells were grown in galactose, both Pba1 and Pba2 were overexpressed. Mixing the crude extract of *pba1Δ* cells with the crude extract of a P_{GAL1}*PBA1*, P_{GAL1}*PBA2* ("P_{GAL1}*PBA1-PBA2*") strain grown in galactose media led to a shift from Complex I to 15S PC (Figure 2.13 a). It did not make a difference whether the samples were incubated at room temperature or at 4 °C. However, when the cells were grown in glucose, where *PBA1* and *PBA2* expression was repressed, no 15S PC was formed upon combination of the two crude extracts.

In another experiment, the crude extract of *pba1Δ* cells was mixed with increasing amounts of Pba1-Pba2 expressed and purified from *E. coli* (Figure 2.13 b). Again, a significant amount of Complex I was shifted to 15S PC, when Pba1-Pba2 was added. However, it did make a difference if the proteins were N-terminally or C-terminally tagged. Whereas a FLAG tag at the C-terminus of Pba2 did not interfere with the interaction of Complex I, an 8His-SUMO1 tag at the N-terminus of Pba1 did completely abolish the

interaction. The observation that accumulated Complex I was converted into 15S PC upon overexpression of Pba1-Pba2 indicates that this complex is not an off-pathway product, but instead an intermediate competent for subsequent assembly with Complex II. What still remained to be clarified was, if Pba1-Pba2 is an inherent part of Complex II or mainly has the task to bring complexes I and II together to form a 13S intermediate on the way to 15S PC.

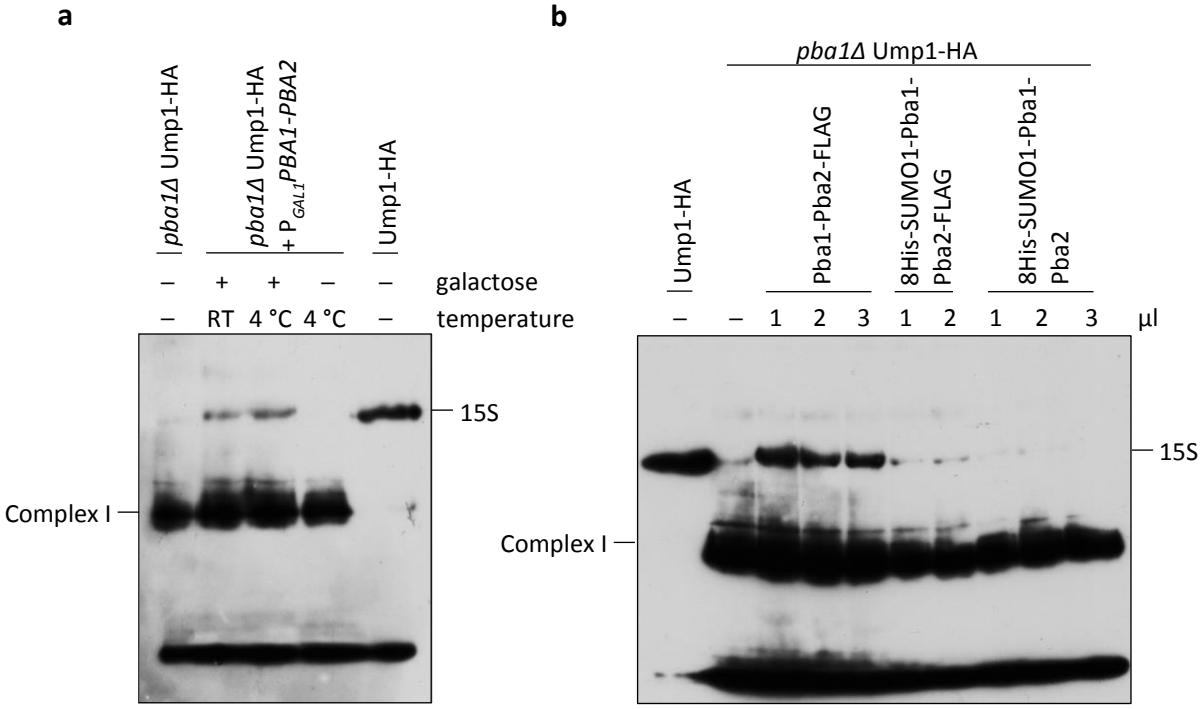

Figure 2.13 – Complex I is converted into 15S PC in yeast extracts upon addition of Pba1-Pba2. (a) Yeast cells were grown in media containing glucose (or galactose in case of P_{GAL1}*PBA1-PBA2*). Crude extracts of *pba1Δ* Ump1-HA (CM184) and P_{GAL1}*PBA1* P_{GAL1}*PBA2* (MO26) cells were mixed and incubated for 12 minutes at room temperature or 4 °C. Afterwards, samples were analyzed by native-PAGE and detected with anti-HA. Extracts from *pba1Δ* Ump1-HA and Ump1-HA (JD129) were loaded as controls. **(b)** Yeast cells were grown in media containing glucose. Crude extracts of *pba1Δ* Ump1-HA were mixed with increasing amounts of Pba1-Pba2 expressed and purified from *E. coli*. Pba1-Pba2 contained either a N-terminal 8His-SUMO1 tag or a C-terminal FLAG tag or both. Samples were analyzed by native-PAGE and detected with anti-HA. Extracts from *pba1Δ* Ump1-HA and Ump1-HA were loaded as controls.

2.3.4 Pba1-Pba2 is not part of Complex II

To further analyze whether Pba1-Pba2 is part of Complex II, an *in vitro* binding experiment was performed. The advantage compared to the co-IP on HA-resin was the simplicity of the experiment and that no washing steps were necessary that may abolish weak protein-protein

interactions. Proteins (α5, α6, α7, Pba1-Pba2-FLAG and Pba3-Pba4-HA) expressed and purified from *E. coli* were mixed and incubated for 90 min at 4 °C. The N-terminal 8His-SUMO1 tag was cleaved during the assay by Senp1, ensuring proteins to stay soluble as long as possible. Samples were analyzed on native- and SDS gels and detected using specific antibodies (Figure 2.14).

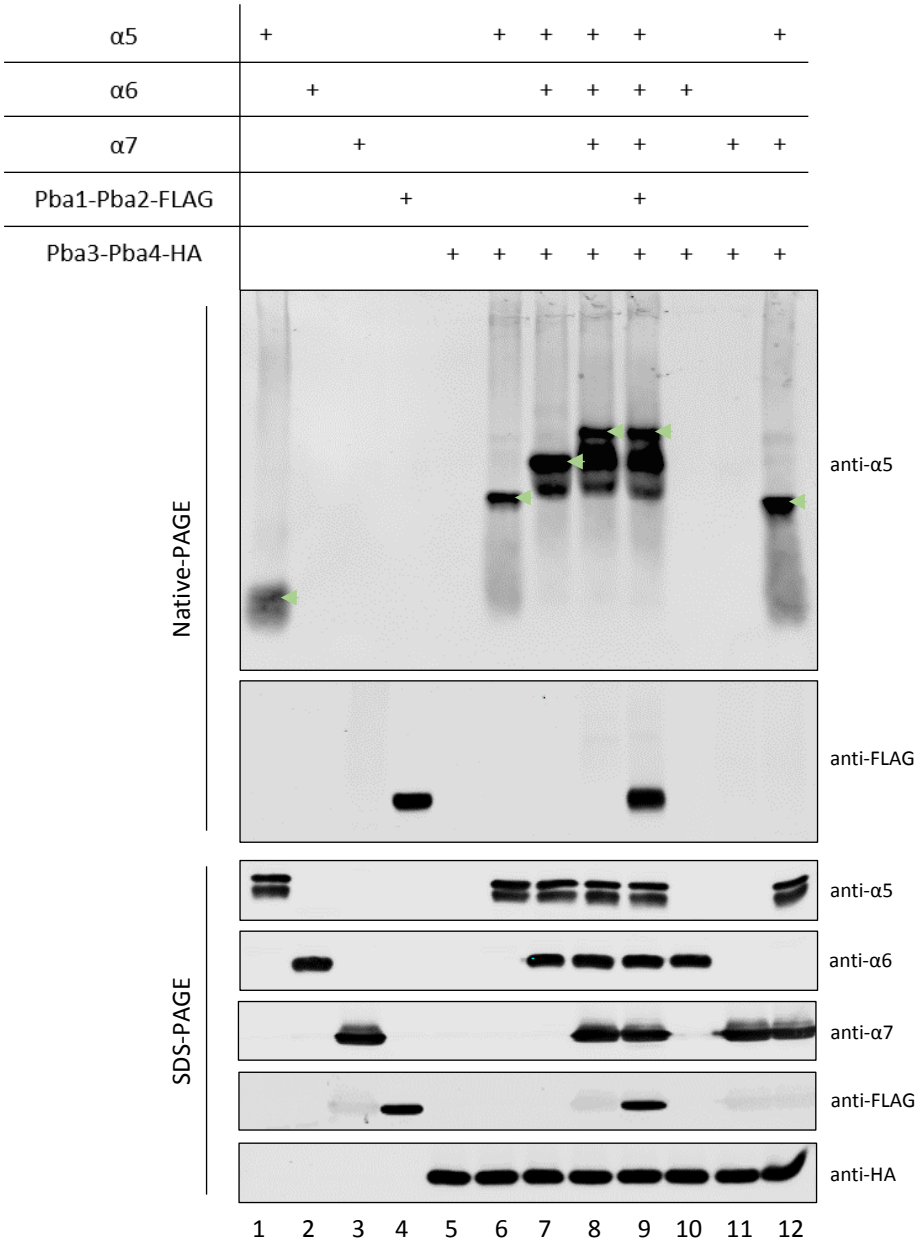

Figure 2.14 – *In vitro* assembly of Pba3-Pba4, α5, α6 and α7. Proteins were expressed in *E. coli* and purified using their N-terminal His tag. 20 µg α5, α6, α7, Pba1-Pba2-FLAG and Pba3-Pba4-HA were mixed in different combinations and incubated at 4 °C for 90 minutes. The N-terminal 8His-SUMO1 tag was cleaved by Senp1 during the binding process to keep the proteins soluble as long as possible. Afterwards, 5 µl of the samples were directly analyzed using native- and SDS-PAGE followed by western blotting, and proteins were detected with specific antibodies.

After addition of each protein (Pba3-Pba4 + α5, + α6 + α7), a shift to a higher molecular weight complex was visible, confirming that these proteins indeed form a complex (lanes 6-9). Only upon addition of Pba1-Pba2, the mobility of this band did not change (lane 9) in comparison to the input (lane 4) or the lane without Pba1-Pba2 (lane 8), indicating that Pba1-Pba2 is not part of Complex II. Furthermore, this experiment revealed the order of events taking place. After binding of Pba3-Pba4 and α5, α6 has to join the complex prior to α7. Without α6, α7 is not able to bind to Pba3-Pba4 or α5 (lane 12). The input of each protein was loaded as control. Samples were additionally analyzed by SDS-PAGE to prove the presence of the distinct proteins in the particular sample. Taken together, the results hint to the fact that Pba1-Pba2 is not part of Complex II itself, but may act as the glue with the task to bring the two intermediates, Complex I and Complex II, together.

2.4 *In vitro* binding studies between Ump1 and β7

Although deletion of *UMP1* is not lethal in *S. cerevisiae*, Ump1 is important for efficient 20S proteasome assembly and correct maturation of the active sites (Ramos *et al.*, 1998). Especially the flexible Ump1 N-terminus seems to fulfill a signifincant task in this process, for instance by making contact to several subunits (Li *et al.*, 2007; Sá-Moura *et al.*, 2013; Kock *et al.*, 2015). One aim of this study was to identify functional domains of the Ump1 proteasome assembly chaperone and the interactions they engage in. Specifically, the role of the Ump1 N-terminal domain was intended to be analyzed. Cross-linking experiments had suggested that the N-terminus of Ump1 is located near the interface of the incoming β7 subunit, and Ump1 inhibits the dimerization of half-proteasomes until β7 is incorporated, whose C-terminal extension helps to overcome Ump1 inhibition (Ramos *et al.*, 2004; Li *et al.*, 2007; Kock *et al.*, 2015). As described below, it was observed in the present work that an intact N-terminal part of Ump1 is required for normal incorporation of β7 during the assembly process, indicating that the two proteins might directly interact in the process (Zimmermann *et al*., 2022).

2.4.1 Expression and purification of β7 variants from *E. coli*

To investigate a possible physical interaction between Ump1 and the proteasome β7 subunit, plasmids for *E. coli* expression of different β7 variants were used: full-length β7 (β7) or truncated versions lacking either the N-terminal leader sequence (ΔLS-β7) or the C-terminal extension (β7-ΔCTE). As described before, proteins were fused to 8His-SUMO1 (Figure 2.15 a). Total (T) and soluble (SL) protein amounts were analyzed by SDS-PAGE and Coomassie-staining. All proteins were efficiently expressed in *E. coli* and obtained in soluble form and adequate amounts (Figure 2.15 b). No corresponding protein was present in the empty vector (EV) control sample, confirming the specificity of the detected bands. Crude extracts were used to purify these proteins by consecutive Ni^{2+}-NTA and TALON affinity chromatographies. The 8His-SUMO1 tag was cleaved using Senp1 (Sentrin-specific protease 1). Samples of the input (IN), the elution after Ni-NTA chromatography (E) and the concentrated material after cleavage of the 8His-SUMO1 tag (C) were analyzed by SDS-PAGE, followed by Coomassie staining to verify the efficiency of the purification (Figure 2.15 c). All β7 variants were obtained in a very pure form and good amounts (~ 2-6 mg). During the purification, a majority of the proteins lost their solubility, probably after cleavage of the SUMO1-tag. This is why 20x amount (4 OD) was loaded for the final material (C) in comparison to the input (IN, 0.2 OD) and the eluates (E, 0.2 OD). Nevertheless, sufficient amounts of soluble, pure proteins for *in vitro* binding experiments were obtained.

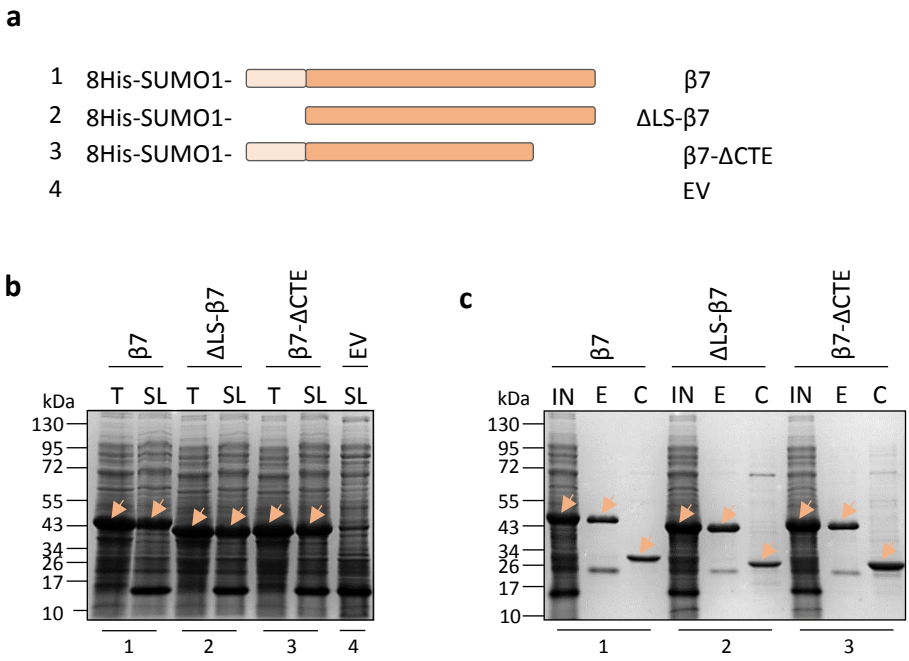

Figure 2.15 – Expression and purification of β7 variants. (a) Schematic representation of produced β7 variants. Full length β7 (plasmid pJZ17), a truncated version lacking the N-terminal leader sequence ΔLS-β7 (plasmid pJZ18), and a truncated version lacking the C-terminal extension β7-ΔCTE (plasmid pJZ19) fused to 8His-SUMO1. **(b)** Comparison of total (T) and soluble (SL) protein amounts (0.2 OD) of 8His-SUMO1 tagged proteins in *E. coli* analyzed by 12 % SDS-PAGE followed by Coomassie staining. The empty vector (EV) served as a control. Specific proteins are indicated by arrows. **(c)** β7 variants were purified using consecutive Ni^{2+}-NTA and TALON affinity chromatographies. The 8His-SUMO1 tag was cleaved during the procedure using Senp1. Samples of the input (IN), the elution after Ni-NTA chromatography (E) and the concentrated material after cleaving off SUMO1 (C) were analyzed by 12 % SDS-PAGE and Coomassie staining. Loaded material of the input and the eluates corresponds to 0.2 OD of cells, for the final material (C) amounts corresponding to 4 OD were loaded. Purified proteins were yielded in concentrations between ~2-8 mg/ml.

2.4.2 β7 binds to Ump1 *in vitro*

To investigate whether Ump1 and β7 bind to each other in isolation *in vitro*, binding assays were performed. Therefore, both proteins were produced in *E. coli* and β7 was purified as described above (see 2.4.1). Either full-length Ump1, or an N-terminal (1-81) or a C-terminal part (82-148) of it (Figure 2.16 a) were immobilized via C-terminal 6His tags on Ni-NTA resin, and incubated with recombinant full-length β7 subunit. All three versions of resin-bound Ump1 specifically retained β7, whereas resin treated with a mock (empty vector, EV) extract displayed only low background levels of β7 binding (Figure 2.16 b). A lack of binding between β1 and Ump1 further supports the specificity of this interaction (Figure 2.16 c). The N-terminal part of Ump1 (residues 1-81) yielded a stronger binding of β7 than the C-terminal part (residues 81-148) (Figure 2.16 b). Binding of the Ump1 N-terminal half

was abrogated by two point mutations (I3T or S11P) very close to the N-terminus that together were shown before to interfere with 15S PC dimerization (data not shown). All in all, it can be concluded that the binding between β7 and the Ump1 N-terminus is relatively strong, but the C-terminal part of Ump1 also plays a role in the interaction with β7 *in vitro*.

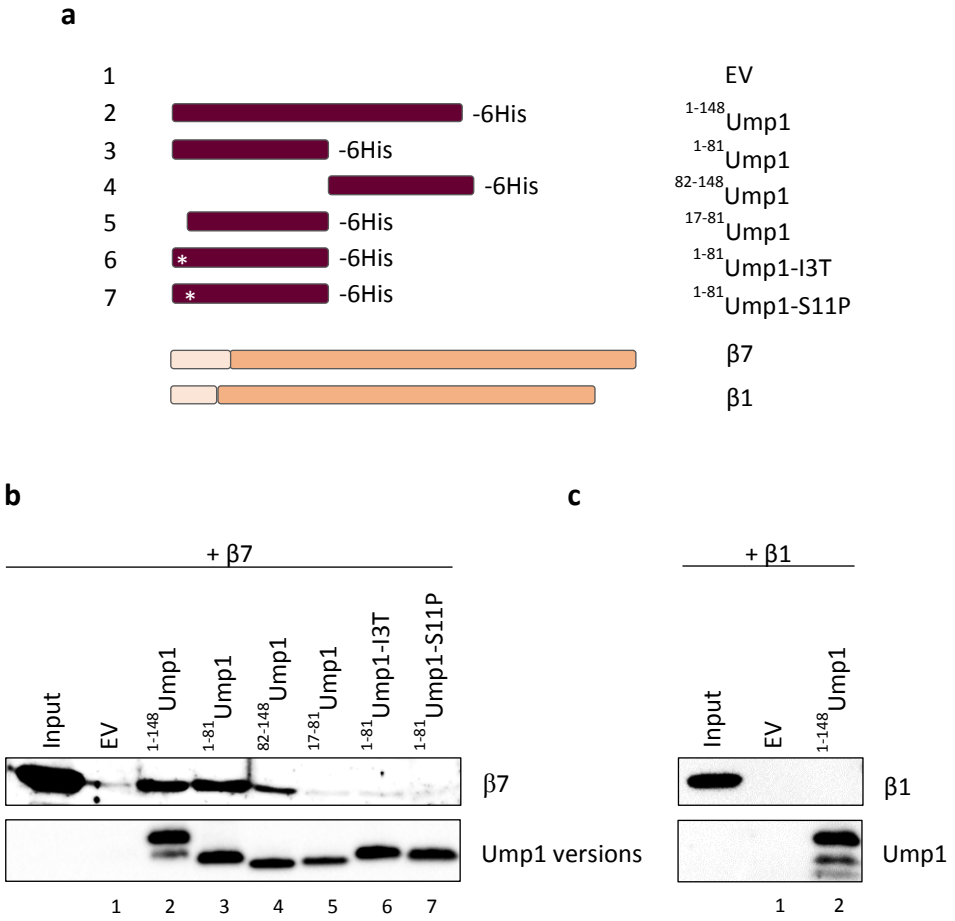

Figure 2.16 – Ump1 N-terminal domain interacts with β7 subunit *in vitro*. (a) Schematic representation of Ump1 variants as well as the subunits β7 and β1 expressed in *E. coli*. Ump1 polypeptides were C-terminally tagged with 6His. Positions of the point mutations I3T and S11P are indicated by stars. β7 and β1 were initially expressed as fusions to 8His-SUMO1 and later after cleaving off SUMO1, obtained in an untagged form (see 2.3.1). **(b)** Interaction of the different Ump1 polypeptides with recombinant full-length β7. Ni-NTA resin was first loaded with Ump1 variants or empty vector (EV) purified from *E. coli* extracts and then incubated with full-length β7. After washing, bound proteins were eluted with imidazole and analyzed by SDS-PAGE and anti-β7 and anti-6His western blotting. The numbers at the bottom refer to the constructs represented in (a). **(c)** Interaction assay as described in (b) but between full-length Ump1 and recombinant full-length β1. Figure adapted from Zimmermann *et al*., 2022.

2.4.3 β7 propeptide promotes binding to Ump1 *in vitro*

To further dissect the observed interaction between Ump1 and β7, the propeptide and the CTE of β7 were tested for the relevance of the binding. Different β7 variants were produced in *E. coli* either lacking the N-terminal propeptide (ΔLS-β7) or the C-terminal extension (β7-ΔCTE) (Figure 2.17 a, see 2.4.1). After immobilizing full-length Ump1-6His to Ni-NTA resin, full-length β7 and the different truncated β7 variants were assayed for binding. In comparison to full-length β7, deletion of the β7 propeptide (ΔLS-β7) led to a strong reduction in binding to Ump1 (Figure 2.17 b, c). Deletion of the CTE (β7-ΔCTE), however, had no significant effect.

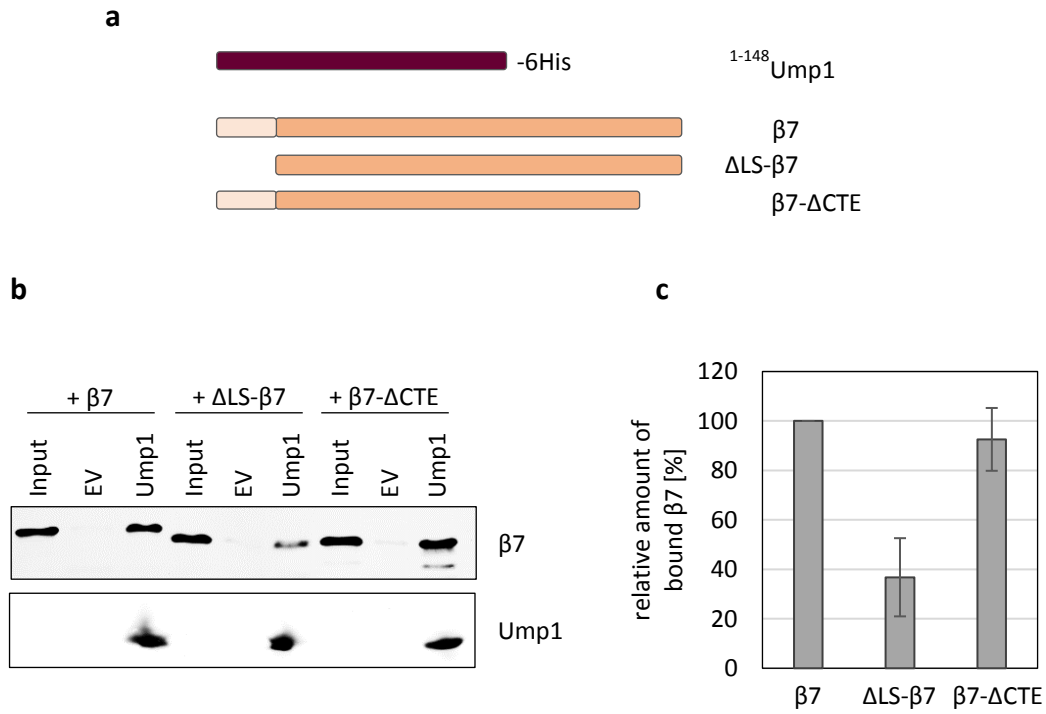

Figure 2.17 – The propeptide of the β7 precursor polypeptide promotes binding to Ump1. (a) Schematic representation of Ump1 and β7 versions used in this experiment: Ump1 fused to 6His, and three distinct untagged β7 versions (full-length, without leader sequence (ΔLS) and without C-terminal extension (ΔCTE). **(b)** Native extracts from *E. coli* cells transformed either with a plasmid expressing Ump1-6His or with an empty vector control (EV) were incubated with Ni-NTA resin, which was then washed and assayed for binding with purified β7 variants. Bound proteins were eluted with imidazole and analyzed by SDS-PAGE and anti-β7 and anti-Ump1 western blotting. **(c)** Comparison of the binding efficiencies between full-length Ump1 and the different β7 versions. Quantitative evaluation was performed with the Li-COR infrared scanner. Signals of the β7 variants eluted from Ump1-loaded resin were first set in relation to the input, of which 10 % was loaded on the gel. Background β7-EV signals were subtracted. The mean value for recovery of full-length β7 was set to 100 %, and the signals for the truncated variants were related to it. Error bars represent standard deviation of the mean (n = 3). Figure adapted from Zimmermann *et al.*, 2022).

This observation was consistent with results from an assay in which it was tested whether the β7-CTE itself would bind to Ump1 (Figure 2.18). Therefore, the β7-CTE fused to the C-terminus of maltose binding protein (MBP) or a MBP control (Figure 2.18 a) were immobilized to amylose resin and assayed for binding to full-length Ump1 or a version lacking the first 16 amino acid residues of Ump1 (Figure 2.18 a). No specific signal was detected for the tested interactions between β7-CTE and the Ump1 variants, indicating that the C-terminal extension of β7 itself does not promote binding to Ump1 (Figure 2.18 b). The results point to an important role of the β7 propeptide in the interaction with Ump1, whereas the CTE is not important for the interaction of these two polypeptides, at least *in vitro*.

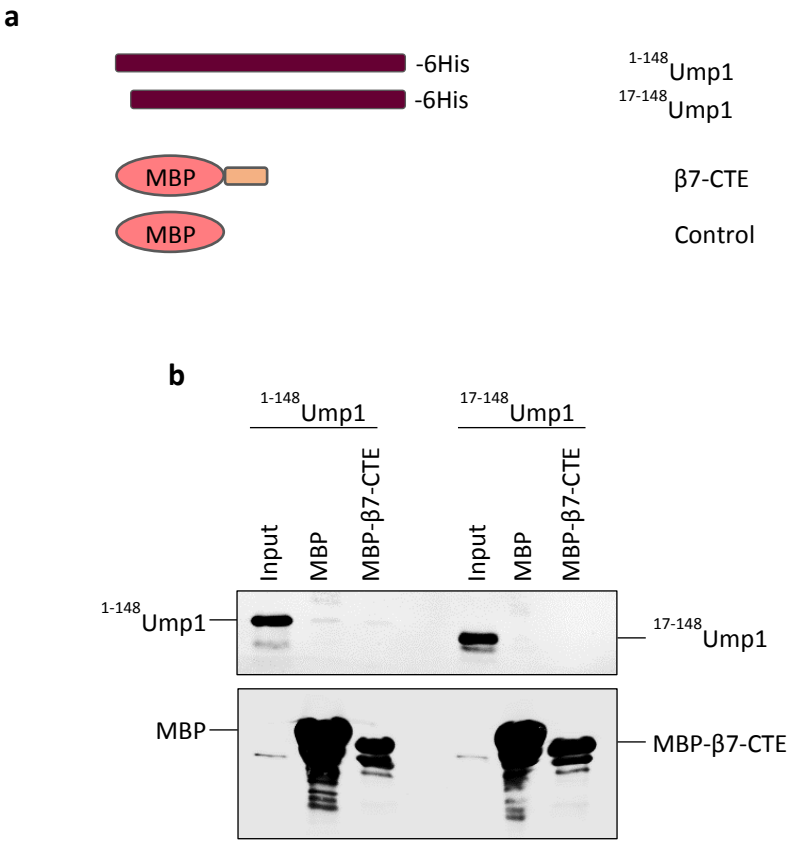

Figure 2.18 – The C-terminal extension of β7 by itself does not promote binding to Ump1. (a) Schematic representation of 6His tagged full-length Ump1, Ump1 with an N-terminal deletion of 16 amino acid residues ($^{17\text{-}148}$Ump1) and β7-Cterminus (β7-CTE) fused to maltose binding protein (MBP). MBP alone was used as control. **(b)** Western Blot analysis of interactions between Ump1 variants and the β7 C-terminus. Native protein extract of 50 OD cells expressing MBP β7-CTE or MBP control was incubated with amylose resin. After washing, resin-bound material was assayed for binding to the same amount of the Ump1 variants. Samples were washed and eluted in 40 µl Sample buffer. Samples of 10 µl were loaded on a SDS-gel next to 1 % Input of the Ump1 variants and analyzed by western blotting using anti-β7 and anti-Ump1 antibodies. Figure adapted from Zimmermann *et al*., 2022.

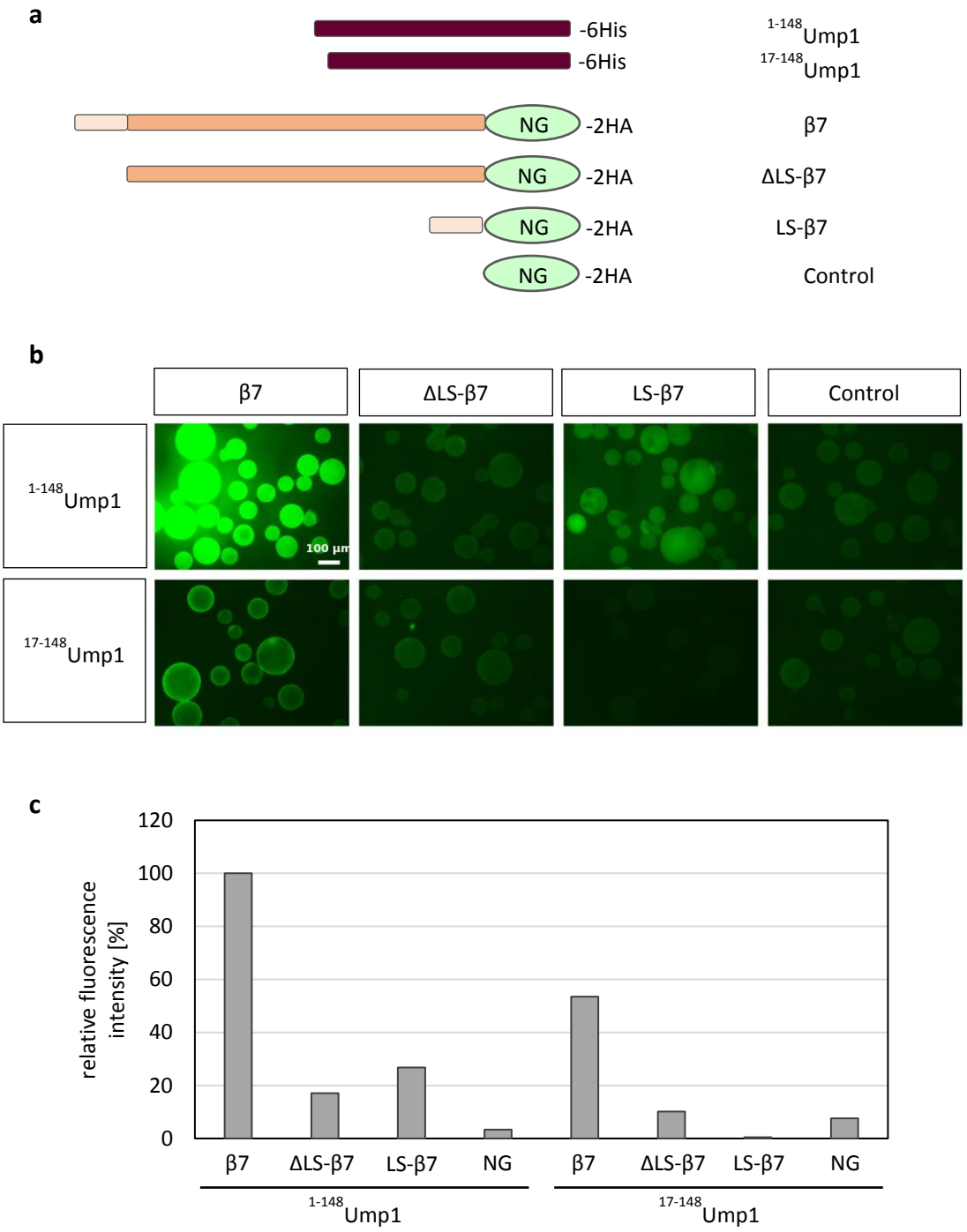

Figure 2.19 – Interaction between Ump1 and β7 is mainly between the Ump1 N-terminus and the β7 propeptide. (a) Schematic illustration of Ump1-6His and β7-NG-2HA variants produced in *E. coli*. NG-2HA alone was used as control. **(b)** Fluorescence-microscopy-based on-bead binding assay. Ump1 variants were immobilized on Ni-NTA beads, assayed for binding with β7 variants and imaged under the fluorescence microscope with identical exposure times. The scale bar indicates 100 µm. Images were prepared using OMEGA and PowerPoint (Microsoft). **(c)** Quantitative analysis of the results shown in (b). Image quantification of signals detectable on beads of the same diameter was performed with Fiji (ImageJ) (*n*=5). Background β7-NG signals obtained with Ni-NTA beads incubated with extract from an empty vector were subtracted (not shown). Signals obtained for full-length β7-NG bound to full-length Ump1 were set to 100 % and the signals for the other NG variants were calculated relative to them. Image quantification was performed with Fiji (ImageJ). Figure adapted from Zimmermann *et al*., 2022.

To analyze whether the propeptide-dependent interaction of β7 involves the above-mentioned N-terminal domain of Ump1, a modified version of the binding assay was performed. Either full-length Ump1-6His or Ump1 lacking the first 16 amino acid residues ($^{17\text{-}148}$Ump1-6His) was immobilized to Ni-NTA beads and tested for binding with full-length β7, β7 without leader-sequence (ΔLS-β7), or just the β7 propeptide (LS-β7) (Figure 2.19 a). Each of the β7 variants was fused to the fluorescent protein mNeongreen (NG) to enable for evaluation of the on-bead binding by fluorescence microscopy (Figure 2.19 b). Neongreen alone was used as control. Consistent with the earlier findings (Figure 2.16), a strong reduction in binding efficiency (~50 %) was observed when the N-terminal 16 residues of Ump1 were deleted (Figure 2.19 b, c). Similarly, the importance of the β7 propeptide for the interaction with Ump1 was confirmed by the strong reduction in binding to ~20 % upon deletion of the β7 propeptide compared with full-length β7. Furthermore, this assay revealed that the propeptide itself is able to promote binding of the fluorescent reporter protein to full-length Ump1. Strikingly, this interaction was completely abrogated when the first 16 amino acid residues of Ump1 were deleted. Together, these findings reveal critical functions of the Ump1 N-terminal domain and the β7 propeptide in the recruitment of β7 precursor during proteasome assembly, a step that drives dimerization of 15S PCs and formation of 20S CPs.

2.5 *In vitro* dimerization of 15S precursor complexes

The 15S proteasome precursor complex (PC) containing all α and β subunits, except for β7, as well as the chaperones Ump1 and Pba1-Pba2, is a critical intermediate in 20S CP assembly. The β7 subunit is thought to be the last subunit to be incorporated into the complex, thereby triggering the dimerization of two such complexes (Li *et al.*, 2007). The aim of this study was to prove this process *in vitro* and to follow the subsequent events such as the maturation of the active sites (β1, β2 and β5), the degradation of Ump1, becoming the first substrate of the mature 20S core particle, and the release of Pba1-Pba2.

2.5.1 Affinity purification of 15S complexes

In wild-type cells, the abundance of the 15S precursor complex (PC) is quite low. In order to have a sufficient amount to purify the 15S PC intermediate and to enable a functional analysis regarding its dimerization, a specific yeast strain MO27 was established in a previous study (Kock *et al.*, 2015). This strain carries a C-terminal truncation of β7, more precisely a deletion of the last 19 amino acid residues (*Pre4-*Δ*C19*) that, together with an N-terminally FLAG-6His tagged version of Ump1 (*FH-Ump1*), enriches the cellular 15S PC population by preventing its dimerization and enables selective affinity purification.

As mentioned above, the critical step that drives dimerization of 15S PCs, is the incorporation of the β7 subunit. The truncated β7 is inefficient in this function thus leading to an unusual accumulation of 15S PC (Ramos *et al.*, 2004). The *Pre4-*Δ*C19* mutation thereby does not affect the structure of the 15S PC because this subunit is absent from the complex (Marques *et al.*, 2007). In wild-type cells, almost all of the Ump1 protein is detected in the 15S PC (Ramos *et al.*, 1998). Previous experiments revealed that, in cells lacking the *PBA1* gene (*pba1*Δ), in contrast to the wild-type, Ump1 is also detected in complexes with a faster electrophoretic mobility, Complex I (Nunes, 2015). Relative high amounts of Complex I were also detected in the *Pre4-*Δ*C19 FH-UMP1* background, where precursor complexes are massively accumulated and only poor 20S formation is observed, suggesting that the amount of Pba1-Pba2 available in the cell becomes rate-limiting for 15S PC formation in these conditions. Therefore, the yeast strain MO27 carried the carbon source-controlled *GAL1* promoter (P_{GAL1}) instead of the native promotors of the *PBA1* and *PBA2* genes. P_{GAL1} is induced in the presence of galactose, leading to a stable overexpression of Pba1 and Pba2, and repressed in the presence of glucose. When *Pre4-*Δ*C19 FH-UMP1* P_{GAL1}*PBA1* P_{GAL1}*PBA2* cells are grown in the presence of galactose, the overexpression of Pba1 and Pba2 leads to a significant reduction of Complex I as well as to an increase of the amount of 15S PC. Furthermore, the MO27 strain contained a deletion of the *BLM10* gene (*blm10*Δ) to further increase 15S PC homogeneity by preventing precursor complexes to associate with Blm10 instead of the Pba1-Pba2 chaperone.

Since Ump1 is absent from mature proteasomes, a FH-tagged version of Ump1 enables the direct and selective purification of the 15S PC. The tag is present at the N-terminus because it is exposed in the 15S PC, while the C-terminus is buried inside the complex

(Ramos *et al.*, 1998). Crude extracts from MO27 cells were used to purify 15S PCs by consecutive Ni^{2+}-NTA and FLAG affinity chromatographies. Elution was done using FLAG peptide and the eluted material was analyzed by native-PAGE and silver staining to verify the efficiency of the purification (Figure 2.20 a left). Additionally, the 20S core particle was purified as it was done for the 15S PC using the yeast strain MO24 carrying a FLAG-6His tagged version of Pre1/β4 (*PRE1-FH*). 20S samples were later used as a reference for the size of eventually dimerizing 15S particles (Figure 2.20 a right). Both 15S PCs and 20S CPs were successfully purified by consecutive Ni^{2+}-NTA and FLAG affinity chromatographies via their FLAG-6His tag. However, for the 15S PC, three different bands of comparable intensity were detected instead of one distinct signal, suggesting that the complex is either not stable and some components fall off, or other precursor complexes are purified along with the 15S PC (e.g. 13S PC). A mass spectrometry (MS) analysis revealed that, indeed, β1 was missing in the bottom band, lower abundance of β5 was observed in the middle and bottom bands and the highest β6 amount was detected in the top band, indicating that these three subunits, which make the difference between 13S PC and 15S PC, are somehow missing in some of the complexes. All other subunits α1-α7 and β2-β4 as well as the chaperones Ump1 and Pba-Pba2 were found in all three bands (Data from Paula C. Ramos, not shown). Nevertheless, purified materials were used to analyze the dimerization events of 15S precursor complexes triggered by addition of the β7 subunit *in vitro*.

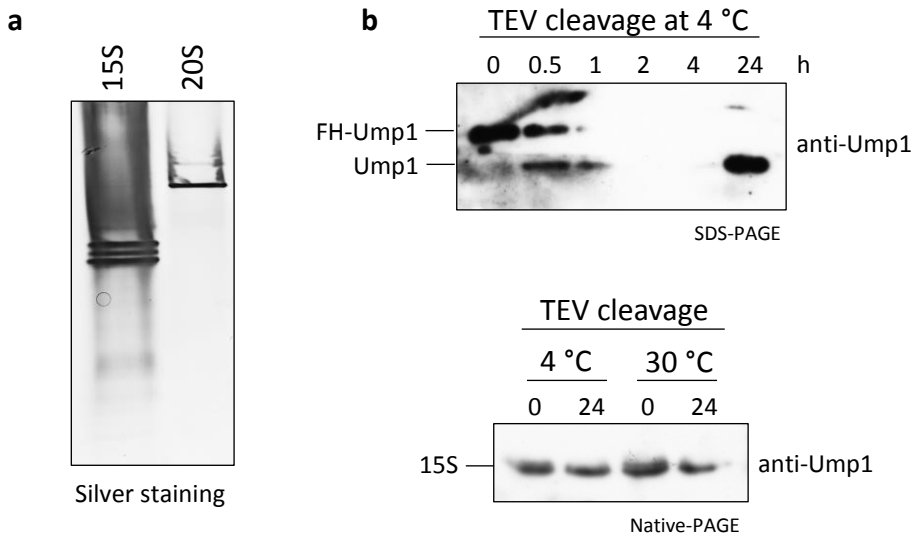

Figure 2.20 – Purification of 15S complexes. (a) 15S and 20S particles were purified using the yeast strains MO27 (*PRE4*Δ*C19 FH-UMP1 P*$_{GAL1}$*PBA1 P*$_{GAL1}$*PBA2 BLM10*Δ) and MO24 (*PRE1-FH*), respectively. After consecutive Ni^{2+}-NTA and FLAG chromatographies, complexes were eluted using FLAG peptide and analyzed by native-PAGE and silver staining. Purification of the 15S and 20S complexes as well as Figure 2.20 a were prepared by Paula C. Ramos. **(b**, top panel**)** Test TEV cleavage assay. 50 µg FH-15S were mixed with 1 µl AcTEV protease (Thermo Fisher), incubated at 4 °C and samples were taken after different time points (0, 0.5, 1, 2, 4 and 24 hours). FH-Ump1 and Ump1 amounts over time were compared using SDS-PAGE and anti-Ump1 western blotting. **(b**, bottom panel**)** Comparison of 15S complexes at time point 0 and after incubation with AcTEV protease at 4 °C or 30 °C for 24 hours. Samples were analyzed using native-PAGE and anti-Ump1 western blotting.

To do so, the FLAG-6his tag at the N-terminus of Ump1 had to be cleaved off as this domain was suggested to be critical for the formation of functional 20S particles (Burri *et al.*, 2000; Li *et al.*, 2007; Sá-Moura *et al.*, 2013). Therefore, a test cleavage assay was performed incubating the purified FH-15S with TEV protease at 4 °C and the amount of cleaved Ump1 was checked at different time points (0, 0.5, 1, 2, 4 and 24 hours). Analyzing FH-Ump1 and Ump1 by SDS-PAGE revealed that approximately half of the tagged proteins were already cleaved after 0.5 hours at 4 °C (Figure 2.20 b top panel). 100 % of cleavage was apparently reached after an incubation at 4 °C for 24 hours. However, due to blotting problems, the time points 2 and 4 hours could not be evaluated and were not taken into consideration. As no obvious difference for the 15S PC was visible between 0 and 24 hours of incubation at 4 °C, for subsequent experiments, TEV cleavage of FH-15S was done for 24 hours overnight at 4 °C (Figure 2.20 b bottom panel). Notably, in contrast to the silver staining after the purification, by detection with Ump1 antibody only one or maximal two bands were detected for the 15S. This raises the question if the 15S is unstable and converted into 13S over time.

2.5.2 β7 is sufficient to trigger dimerization of 15S complexes *in vitro*

The dimerization of two 15S precursor complexes is suggested to be triggered by the incorporation of the β7 subunit, whose C-terminal extension reaches out into the other half stabilizing the newly formed 20S complex. β7 is viewed as the rate-limiting factor in this process (Ramos *et al.*, 2004; Li *et al.*, 2007; Marques *et al.*, 2007). To prove this notion *in vitro*, purified materials of the 15S precursor complex (see 2.5.1) and the β7 subunit (see 2.4.1) were mixed and samples were tested for formation and maturation of 20S core particles. As it was shown before that the 15S PC in the purified material seems not to be stable, probably losing one or more of the subunits β1, β5 and β6 (see 2.5.1), these subunits were added to the mixture as well. The purified 20S proteasome served as a control.

After dimerization of two 15S PCs, proteolytic subunits β1, β2 and β5 peptides are auto-catalytically cleaved to become active (Chen and Hochstrasser, 1996). The catalytic subunit β5 was shown to preferentially cleave peptide bonds after hydrophobic residues (Groll *et al.*, 2005). This chymotrypsin-like activity of β5 was most suitable to check for dimerization of 15S PCs triggered by the addition of β7, and resulting proteasomal activity *in vitro*. This was done measuring the release of fluorescent 7-amino-4-methylcoumarin (AMC) after cleavage from specific substrates. Specifically, the chymotryptic activity assay was based on the enzymatic processing of the substrate Suc-LLVY-AMC (N-succinyl-leucine-leucine-valine-tyrosine-AMC) (Kisselev and Goldberg, 2005) (Figure 2.21).

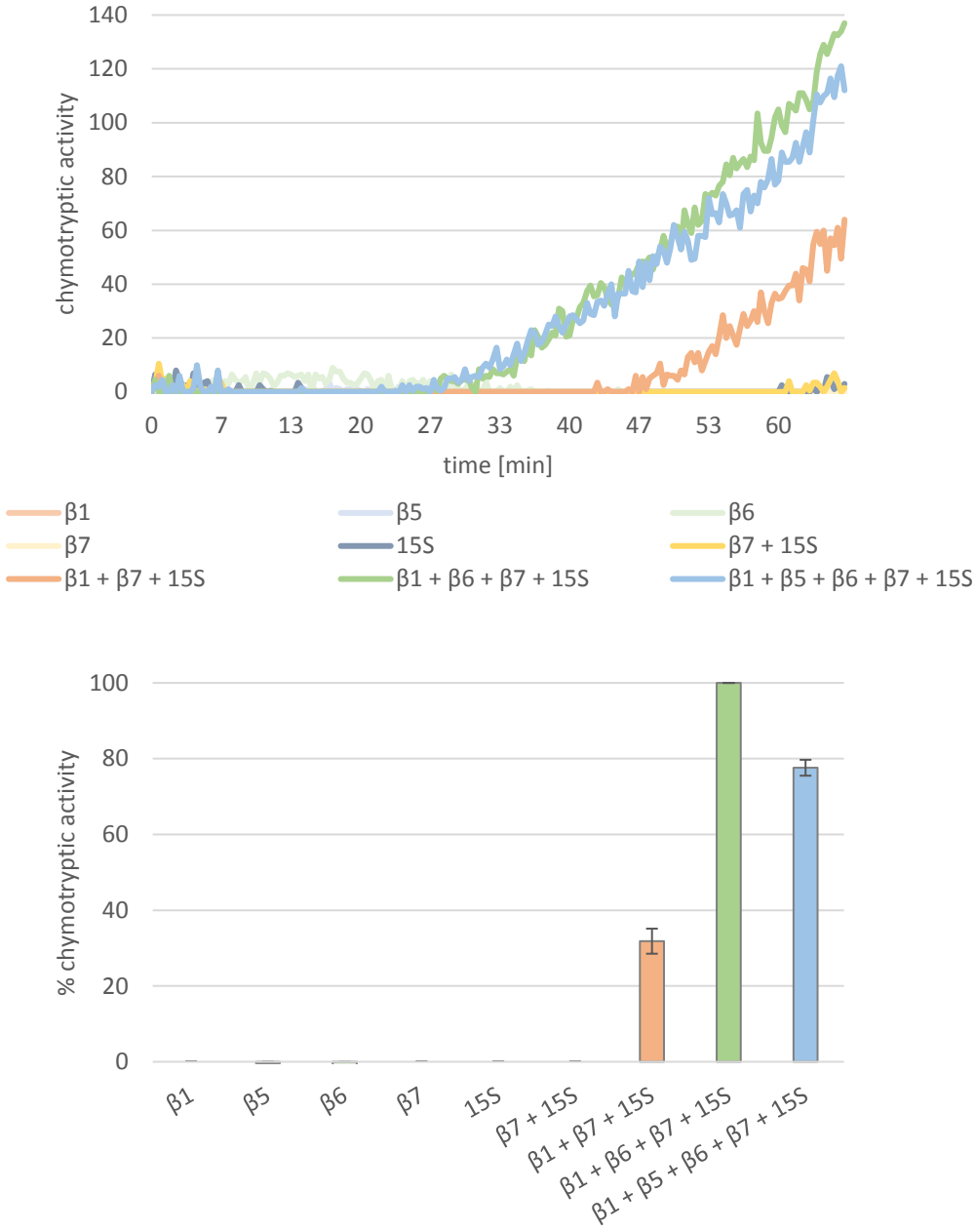

Figure 2.21 – Proteasomal chymotryptic activity. Chymotryptic activity measured in samples containing 10 µg purified 15S PC and 25 µg of β7, β1, β5 and β6 subunits in different combinations over the time. 15S PC and each subunit alone were used as control (upper panel). Quantitative analysis of the results shown in the upper panel. Signals obtained for 15S + β1, β6 and β7 were set to 100 % and the signals for the other samples were calculated relative to them. Values are means of two independent measurements (n =2) (lower panel).

The highest chymotrypsin-like proteasome activity was measured in samples containing purified 15S PC together with subunits β1, β6 and β7 (green). For the samples containing only β7 and 15S PC, no activity was measured at all (yellow). To achieve a minimum of activity (~ 30 %), at least β1 had to be present additionally to β7 (orange). The addition of

β5 to samples containing 15S PC, β1, β6 and β7 did not further increase the chymotryptic activity (blue). For the individual subunits, as well as for the 15S precursor complex alone, no activity was detected, indicating that the measured activities were indeed proteasome-specific. This is supported by the fact that the activities in the samples were not present from time point 0. The first activity was detected after about 30 minutes, which makes sense, as the 15S PC and β7 (as well as the other subunits) have to find each other before the dimerization of two complexes is triggered. Furthermore, the assembly process needs to be finalized and the maturation of the active sites has to occur, before the proteasome is active. The results obtained in this experiment support the observation that the 15S PC was not stably purified and some subunits besides β7 were missing. As indicated by the MS of the purified 15S PC (see 2.5.1), these subunits seemed to be β1 and β6, at least.

To follow the formation of 20S proteasomes and subsequent events such as the maturation of other active subunits besides β5 and the degradation of Ump1, samples from the activity measurement were analyzed by native-PAGE as well as SDS-PAGE followed by western blotting (Figure 2.22). Interestingly, when the purified 15S PC alone was analyzed after the assay by native-PAGE using Pup1-antibody, only the bottom one of the three bands previously observed after silver staining was detected (Figure 2.22 a, b). After addition of β7 and other subunits (β1, β5 and β6), again a second band was visible, indicating that one or more of these subunits are binding to the complexes present in the 15S PC preparation. Additionally, another band appeared at the height of the 20S proteasome. However, the amounts of this complex, likely representing the 20S CP, were relatively low and were only present if a high amount of 25 µg of β subunits was used. Surprisingly, a faint 20S CP band was also visible for samples containing exclusively 15S PC and β7 (Figure 2.22 b). This result seems to be in contrast to the activity assay, which was expected to be more sensitive than western blotting, where no activity was detected for this sample. These results may indicate that dimerization of intermediates lacking β1 may be promoted by β7 without leading to a functional active proteasome. Therefore, further assays were performed to monitor functionality of the detected 20S complexes. To follow the active site maturation of β2 and the degradation of Ump1, samples were analyzed by SDS-PAGE. Ump1 was nicely detected before and after cleavage of its N-terminal FLAG-6His tag, showing a small difference in size (Figure 2.22 c). In samples containing 15S PC together with β7 or together with β1, β5, β6 and β7, the signal visible for Ump1 was much weaker, indicating that Ump1

was degraded in this samples. When the maturation of β2 was examined using a Pup1/β2 antibody, in samples containing the 15S complex alone, only the unprocessed (propeptide-containing) form of β2 was detected. Removal of the propeptide was only observed in the sample containing 15S PC together with β1, β5, β6 and β7. For 15S PC and β7 alone, no β2 maturation could be seen at all (Figure 2.22 d). The 20S CP sample served as a control, comprising only mature β2.

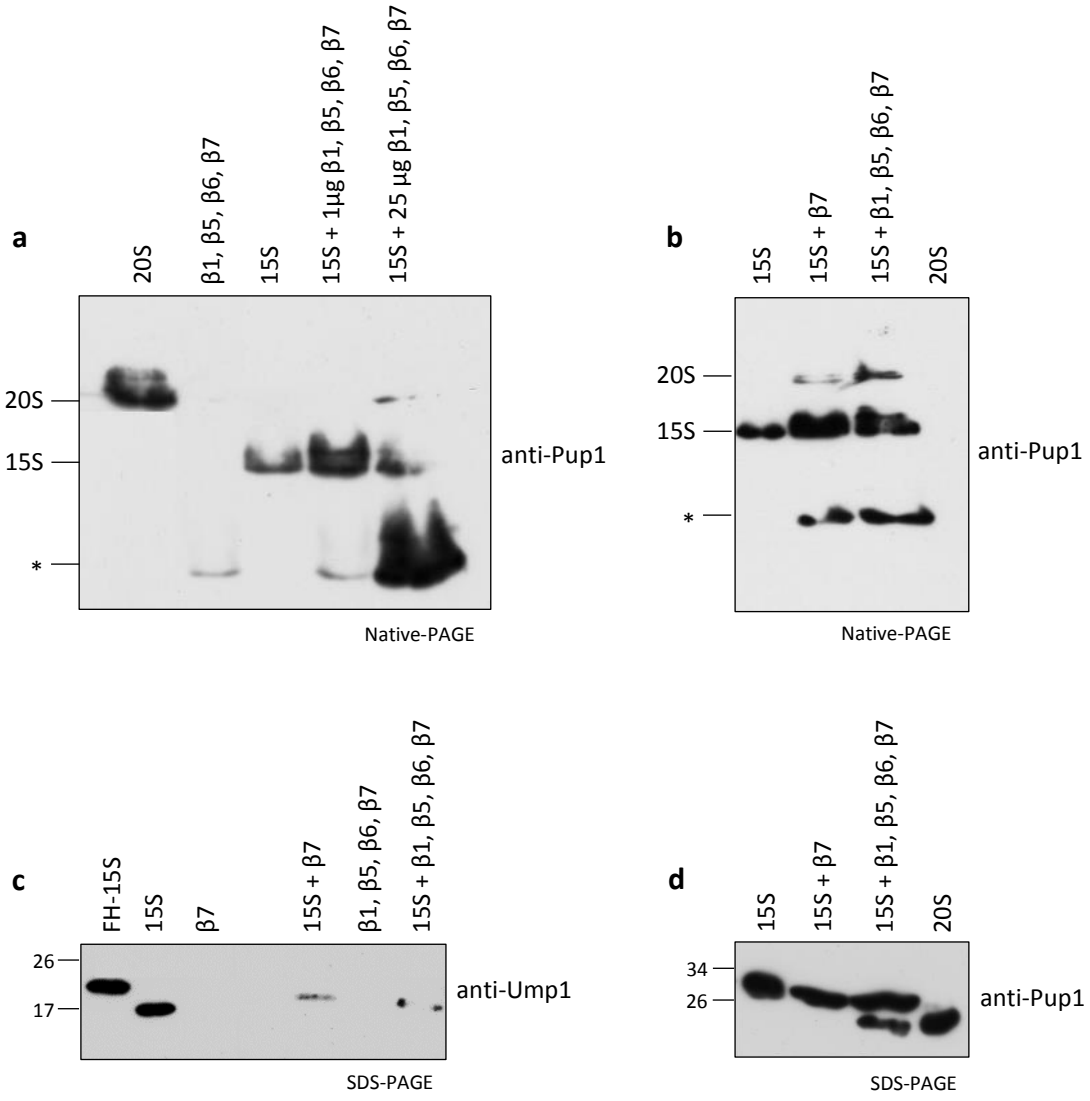

Figure 2.22 – Dimerization of 15S complexes. After measuring the chymotryptic activity, samples were analyzed by native-PAGE and SDS-PAGE. **(a, b)** Dimerization of 15S complexes was analyzed by native-PAGE and anti-Pup1 western blotting. **(c)** Degradation of Ump1 was analyzed by SDS-PAGE and anti-Ump1 western blotting. **(d)** Maturation of β2 was analyzed by SDS-PAGE and anti-Pup1 western blotting.

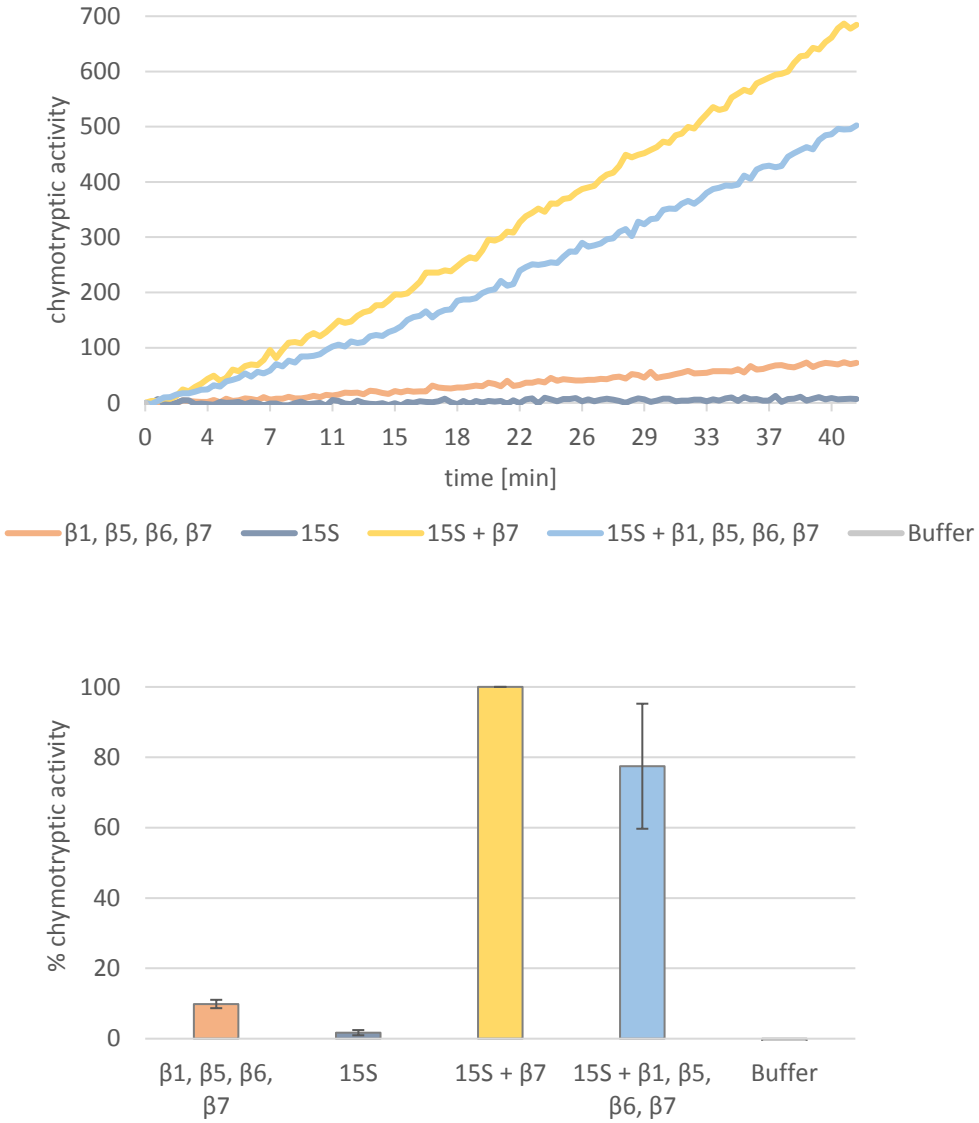

Figure 2.23 – Reconstitution of proteasomal chymotryptic activity using rapidly and freshly purified 15S PC and β7. Chymotryptic activity measured in samples containing 20 µg freshly purified 15S PC and 25 µg of β7, β1, β5 and β6 subunits in different combinations over the time. 15S PC and the subunits alone were used as control (upper panel). Quantitative analysis of the results shown in the upper panel. Signals obtained for 15S + β7 were set to 100 % and the signals for the other samples were calculated relative to them. Values are means of three independent measurements (n = 3) (lower panel).

As the 15S precursor complex was observed to be not completely stable under the employed conditions, being present in three different bands directly after the purification procedure, most likely lacking subunits β1 and β6, a modified much shorter protocol was applied. Instead of a consecutive Ni^{2+}-NTA and FLAG chromatographies, a simple Ni^{2+}-NTA purification was done. Elution was directly performed using TEV protease to remove the

FLAG-6His tag from the Ump1 N-terminus and release the 15S complexes from the beads. As the elution was done before using FLAG peptide and the FH tag was proteolytically cleaved overnight, this was a huge saving of time. Directly after the purification, 20 µg of fresh 15S PC were mixed with 25 µg of subunits. After an incubation of 90 minutes at 37 °C, formation of 20S proteasomes was analyzed by measuring the chymotryptic activity as described before (Figure 2.23).

In contrast to the activity measurement that was done before after a long purification procedure and a freeze-thaw cycle of the 15S PC, a clear activity could be detected for samples containing fresh 15S PC and the β7 subunit exclusively (yellow). For samples comprising additionally the subunits β1, β5 and β6, the activity did not increase further (blue). For 15S PC (dark blue) or β subunits alone (orange), only a low background activity was detectable.

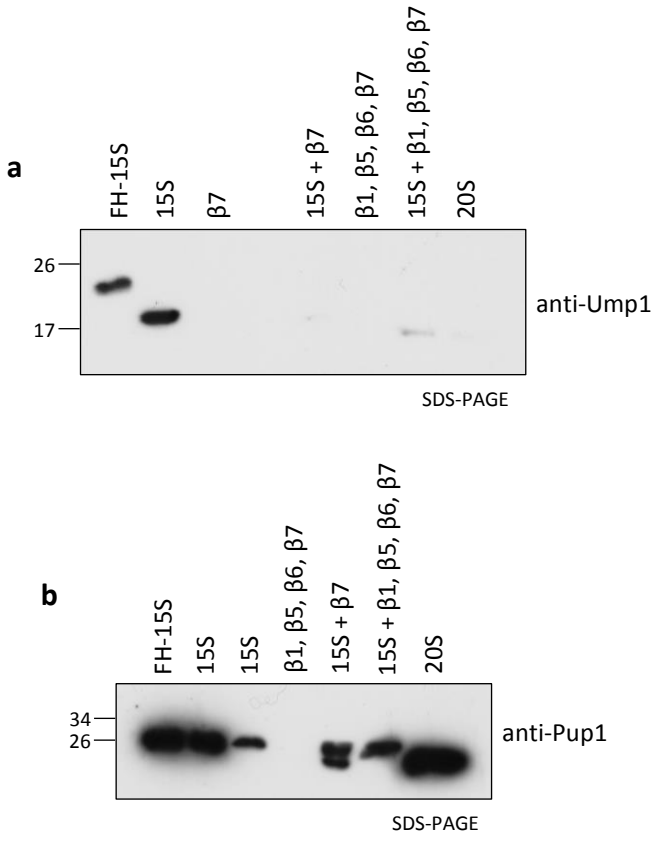

Figure 2.24 – Maturation of 20S complexes after dimerization of 15S PCs by addition of β7. After measuring the chymotryptic activity, samples were analyzed by SDS-PAGE. (a) Degradation of Ump1 was analyzed by anti-Ump1 western blotting. (b) Maturation of β2 was analyzed by anti-Pup1 western blotting.

To follow the fate of Ump1 upon dimerization of 15S PCs, samples from the chymotryptic activity measurement were analyzed by SDS-PAGE and anti-Ump1 western blotting (Figure 2.24 a). Again, Ump1 was nicely detected before and after cleavage of its N-terminal FH tag. As Ump1 is degraded after maturation of the active sites, becoming the first substrate of the mature 20S proteasome, no signal for Ump1 is expected for the 20S control sample. Interestingly, also for samples containing 15S PC together with β7, no Ump1 signal was detected at all. This would mean, that all of the 15S complexes were dimerized to 20S proteasomes and all Ump1 molecules were degraded. For samples that contained 15S PCs as well as β1, β5 and β6 subunits in addition to β7, still a faint band was detected for Ump1, which corresponds to the slightly lower activity of this samples in comparison to 15S PC and β7 alone. However, when the maturation of β2 was analyzed by anti-Pup1 western blotting, only about 50 % of β2 was cleaved (Figure 2.24 b). Samples containing the 15S complex alone comprised only the unprocessed (propeptide-containing) form of β2. As expected, the 20S control sample contained exclusively mature β2. Surprisingly, for the mixture of 15S, β1, β5, β6 and β7, no maturation of β2 was observed at all.

Together these findings obtained on the basis of the chymotryptic activity assay and the analysis of the dimerization events, demonstrate that the addition of the β7 subunit to 15S precursor complexes is sufficient to trigger the dimerization of two such complexes *in vitro*, leading to the formation of 20S proteasomes. Furthermore, the assembly process is followed by the autocatalytic cleavage of the proteolytic subunits β2 and β5 propeptides, resulting in active 20S core particles. Furthermore, degradation of Ump1 upon *in vitro* formation of 20S complexes could be observed.

The detection of the maturation of the last of three active subunits β1 as well as the release of the chaperone Pba1-Pba2 would complete the analysis of events taking place after dimerization of two 15S precursor complexes triggered by addition of β7. Unfortunately, the available antibodies were insufficient to detect a specific signal for this chaperone in the material purified from yeast. The production of highly specific antibodies against β1 as well as Pba1-Pba2 would be one aim for future experiments. To verify these results and to prove that indeed 20S proteasomes are formed upon addition of the β7 subunit to the 15S precursor complexes, it would be necessary to determine the components of the occurring band at the size of the 20S by mass spectrometry, for instance.

3 Discussion

3.1 Produced antibodies specifically detect yeast proteasome components

The specific detection of unmodified proteins is a useful tool to analyze their particular functions and engagement in protein-protein interactions for instance. Therefore, it was necessary to obtain adequate quantities of the soluble, functional antigen, which often already displays a major challenge. Using an integrated approach comprising codon adaptation and gene fusion technologies as well as a particular purification procedure, it was possible to generate the yeast proteasome subunits α5 and α6 as well as the assembly chaperone pair Pba3-Pba4 in high, soluble amounts (Figure 2.1).

Yeast proteasome genes were adapted for *E. coli* by codon-optimization using JCat and manual editing, to increase the yield of heterologous protein expression. To further improve expression levels in *E. coli* and to enhance the solubility of the protein, human SUMO1 was attached to the N-terminus (Wang *et al.*, 2010). An octa-histidine (8His) tag enabled highly selective purification of the gene fusion product, involving Ni-sepharose and TALON chromatographies as well as cleavage of the solubility tag by Sentrin-specific protease 1 (Senp1, Figure 2.2). Indeed, proteasome components α5, α6, and Pba3-Pba4 were selectively purified in large quantities of about 20-40 mg protein. Using the method of expressing the proteins together with a solubility fusion tag and cleaving the tag after purification, all proteasome components were obtained in soluble form. Even though most proteins were observed to lose some of their solubility during the purification, most likely due to cleavage of the solubility tag, this was not a major problem because of the enormous amounts of protein that could still be purified.

After testing the pre-immune blood sera concerning unspecific background cross-reactivity to yeast proteins and choosing one rabbit for each antigen, proteins were sent for

antibody production to an external company (Figure 2.3). The quality of the antibodies was then improved by incubation with membranes loaded with yeast proteins lacking the desired antigen. The goal of this approach was to remove antibodies from the polyclonal serum that bind non-specifically to any yeast protein other than the desired antigen. In contrast to *PBA3*, which is not essential for viability in yeast, *PUP2*/α5 and *PRE5*/α6 are essential and could not be deleted. Therefore, yeast strains were used expressing these proteasome subunits under control of the galactose-inducible promoter P_{GALS}. After cells were grown in galactose, they were shifted to glucose medium overnight to repress production of these proteins. Using this method, specific antibodies for all three proteasome components, α5, α6 and Pba3(-Pba4-HA) were generated (Figure 2.4). Especially for purified *E. coli* proteins these antibodies are highly efficient and specific, but also in yeast boiled extracts the distinct protein can be specifically detected. Furthermore, antibodies for the β subunits β1, β5, β6 and β7 were obtained. At least for the specific detection of purified *E. coli* proteins these antibodies are efficient. Together with the antibodies against other proteasome components, which were already present in the laboratory, they will be useful tools for the analysis of distinct proteasome assembly steps and to study particular protein-protein interactions. In this study, the newly generated antibodies could be used for investigations *in vitro* and *in vivo*.

3.2 Expression regulation of the yeast 20S proteasome

Rpn4 was shown to be required for mediating the regulation of proteasome gene expression (Xie and Varshavsky, 2001b). Especially when proteasome activity is impaired, or under stress conditions, Rpn4 is indispensable for cell viability (Ju *et al.*, 2004). The discovery of the different PACE and PACE-like sequences was an indication that the regulation of proteasome gene expression is not uniform and that the 20S CP subunits might not be synthesized in nearly stoichiometric amounts. To directly compare the steady state levels of the subunits α1-α7 and β1-β7, a set of strains was used that contained modified proteasome genes encoding 2xHA tagged versions of them expressed from the native promoters at authentic genomic locations (Ramos *et al.*, 1998; Matias *et al.*, 2022). To determine the relative protein amounts, cell extracts from these strains were analyzed by western blotting. Interestingly, the detected protein amounts of the proteasome subunits were not

stoichiometric, instead α subunits were shown to be present in strikingly higher levels than β subunits (Figure 2.6). In average, the relative protein amounts of α subunits were four to five-fold higher than the amounts for β subunits consistent with earlier findings (Schwab, 2017). In general, as the C-terminal 2xHA tag on some of these subunits was observed before to cause growth phenotypes, these results should be taken with caution. Furthermore, minor blotting differences between the subunits cannot be excluded. However, as the size of the different subunits is very similar (22.5 - 31.6 kDa), and both electrophoresis and transfer were performed under denaturing conditions, blotting differences are expected to be negligible.

One explanation for different expression levels could be that early precursor complexes of the highly abundant subunits are formed, which allows a rapid mobilization to form mature 20S CPs under stress-conditions. According to this hypothesis, possibly all seven α subunits and β2, β3 and β4 would be expected to be part of these early precursors. At least HA tagged β2 was shown to be present at similar levels as HA tagged α4 subunit. In contrast, for β3 and β4, lower expression rates were observed, comparable to those of the later assembling β subunits (Figure 2.6). Another possibility for α subunits to be present in higher amounts would be that the single subunits are stored at a specific location in the cell and, upon stress, they get quickly mobilized to start with the formation of early precursor complexes. If this were true, the question arises, where these subunits are stored in the cell. To get further information about the location of the subunits, different extraction methods could be compared yielding different subcellular fractions, or microscopy could be performed using a fluorescent protein tag. Whether the unequal abundance of α and β subunits on protein level is a result of differential transcription or protein stability remains to be clarified. A systematic analysis of proteasome subunit mRNA levels by qPCR would give insight in transcription levels, while protein stability could be analyzed by cycloheximide or pulse-chase assays. Although a differential transcription of proteasome subunit genes seems unlikely at first glance, as all 20S CP subunits, except for α6 and β2, contain an authentic PACE sequence in their promoters, several studies have suggested the presence of additional transcription factors, downstream or independent of Rpn4, which might regulate the transcription of proteasome subunit genes by other mechanisms (Fleming *et al.*, 2002; Shirozu *et al.*, 2015). The identification of these putative transcription factors would add another layer of complexity in the regulation control of proteasome genes.

Discussion

To systematically compare the *RPN4*-mediated induction of α and β subunits, the protein abundance in wild-type, *rpn4*Δ and *RPN4** background yeast strains was analyzed (Figures 2.7-2.10). Rpn4 overexpression (Rpn4*) was achieved by expressing a stabilized and transcriptionally active variant of Rpn4 in addition to the endogenous *RPN4* gene copy (Wang *et al.*, 2010). The experiments were performed using authentic yeast strains containing no protein tags or auxotrophic markers (besides URA3) to prevent any influence of amino acid levels on gene expression or physiology (Pronk, 2002; Canelas *et al.*, 2010; Grüning *et al*., 2010; Yan *et al.*, 2023). Distinct amounts of various subunits purified from *E. coli* were loaded as a reference, and proteins were detected with specific antibodies. Using this strategy, the exact amount of different 20S CP subunits could be determined and compared. In contrast to previous findings from our group, which have shown that the maximum protein regulation spectrum of α subunits was about ± 25 % (Schwab, 2017), the protein abundance in this study ranged from - 60 % to + 45 % for α5, α6 and α7. However, these findings are in line with a previous study that exemplarily analyzed the expression of a small subset of subunits genes on mRNA level. When wild-type and Rpn4-overexpressing yeast cells were compared, mRNA levels of α4, α6 and α7 were shown to be increased more than three-fold (Shirozu *et al*., 2015).

In contrast to α subunits, the variation in protein expression of β subunits was shown to be much more extreme and differing (Schwab, 2017). Especially β7, which is the last subunit to be incorporated into dimerizing 15S complexes (Marques *et al.*, 2007), was found to have the strongest expression difference between wild-type, *rpn4*Δ and *RPN4**-expressing cells (Schwab, 2017). These results, however were obtained using HA tagged variants of the different proteasome subunits, which may affect the function of the proteasome and, as a consequence, possibly also the regulation of proteasome gene expression (London *et al.*, 2004). In the present study, therefore, an otherwise similar analysis was performed using prototrophic yeast strains to exclude any possible effects of tags or auxotrophic mutations on the regulation (Figures 2.7-2.10). Comparing *rpn4*Δ and wild-type in this setup, the expression level of β7 was strikingly higher (~5-fold) in wild-type when the endogenous protein was detected with a specific antibody (Figure 2.10). This observation further supports the hypothesis that β7 as the rate-limiting β subunit, incorporation of which completes the assembly of the 20S CP (Marques *et al.*, 2007) is most strongly regulated by Rpn4.

Regarding mRNA levels, for β4 an increase of about 2-fold in wild-type compared to *rpn4*Δ cells was shown (Karpov *et al.*, 2016). The results of this study and of Karpov *et al*. point more in the direction, that the Rpn4-mediated regulation of α and β subunits, with the exception of β7, is rather similar, with differences between *rpn4*Δ and wild-type being in the range of 2-fold. By contrast, β7 is present in 5-fold higher amounts in the wild-type compared to *rpn4*Δ. These observations lead to the hypothesis that β7 is up-regulated by Rpn4 more strongly than other CP subunits to promote rapid formation of mature 20S proteasomes from pre-formed precursors. This hypothesis is in line with the observation that overexpression of β7 caused lower levels of 15S PC and higher proteasomal activity (Marques *et al.*, 2007). This mechanism may enable a rapid production of 20S CP by mobilizing pre-assembled precursor complexes without the requirement for a *de novo* synthesis of all subunits and chaperones. Such a response may represent a first line of defense that could help cells to deal with acute proteotoxic stress (London *et al.*, 2004). However, as the available β subunit antibodies (anti-β1, anti-β5 and anti-β6) were not sufficient to detect specific proteins in yeast extracts, it was not possible to compare the results for β7 with the Rpn4-mediated induction of other β subunits. Therefore, these results have to be considered as preliminary data and need to be proven by further investigations and repeating the experiments multiple times to obtain reliable statistics. For example, to compare transcription and protein stability, a systematic analysis of proteasome subunit mRNA levels by qPCR and a cycloheximide or pulse-chase assay could be performed, respectively. Another objective would be the identification of putative additional relevant transcription factors.

3.3 20S proteasome assembly – Complex I-Complex II model

In contrast to the α-ring as an early assembly intermediate, we identified a preliminary complex containing distinct subsets of α and β subunits (α1-α4 and β2-β4) as well as the maturation factor Ump1 in our studies in *Saccharomyces cerevisiae* (Figure 3.1). This complex was termed Complex I and was found to accumulate in cells lacking functional Pba1-Pba2 assembly chaperones (Kock *et al.*, 2015; Matias, 2010). Experiments showing that Complex I, that had accumulated in yeast cells in the absence of Pba1-Pba2, is converted *in vitro* in yeast extracts into 15S PC upon addition of Pba1-Pba2 indicated that Complex I

is not an off-way product, but instead a natively occurring short-lived assembly intermediate (Figure 2.13).

The subset of α and β subunits present in Complex I is located in the same half of the 20S CP, with the β2-β3-β4 subunits sitting on top of the α1-α2-α3-α4 subunits, and were shown in CX-MS analysis of the 15S PC to have the most inter-subunit cross-links, indicating a higher structural order in exactly this side of the half proteasome (Groll *et al.*, 1997; Kock *et al.*, 2015). Consistent with our model, which suggests that Ump1 enters the 20S CP assembly at a very early stage and is part of an intermediate that contains only a subset of the seven α subunits, previous studies identified Ump1, β2, β3, and β4 in early precursor complexes (Nunes, 2015). A strong interaction between the α1 subunit and Ump1 was demonstrated in several binding assays and may point to important contacts between these proteins during Complex I assembly (Cagney *et al.*, 2001; Krogan *et al.*, 2006). Our data are further supported by recent findings that identify a protein complex *in vivo* containing a subgroup of α and β subunits (α1-α4 and β2-β4) instead of a complete α-ring, indicating that α-rings are not obligate precursors for the formation of the 13S intermediates in eukaryotes (Hammack *et al.*, 2020).

In vitro experiments by others demonstrated an α5-dependent interaction between Pba3-Pba4 and the subunits α5, α6, and α7 (Kusmierczyk *et al.*, 2008; Yashiroda *et al.*, 2008). Similarly, it was show that human PAC1-PAC2, the ortholog of Pba1-Pba2 (see Table 1.2) preferentially bind α5 and α7 (Hirano *et al.*, 2005). In line with these findings, we could identify an early precursor complex, namely Complex II, that contains the subunits α5, α6, and α7 as well as the chaperones Pba3-Pba4 (Figure 2.12 and 2.14). Furthermore, it was shown that after Pba3-Pba4 and α5, α6 has to join the complex before α7 is able to bind (Figure 2.14). Pba1-Pba2 does not seem to be part of Complex II itself, but may rather aid the task to bring complexes I and II together (Figures 2.12-2.14). According to our model, these complementary complexes Complex I and Complex II together form the 13S complex, likely facilitated by Pba1-Pba2. During this step, Pba3-Pba4 is thought to be released. The following steps of 20S assembly, starting by the incorporation of the subunits β5, β6, and β1 are conducted as previously described for the α-ring model.

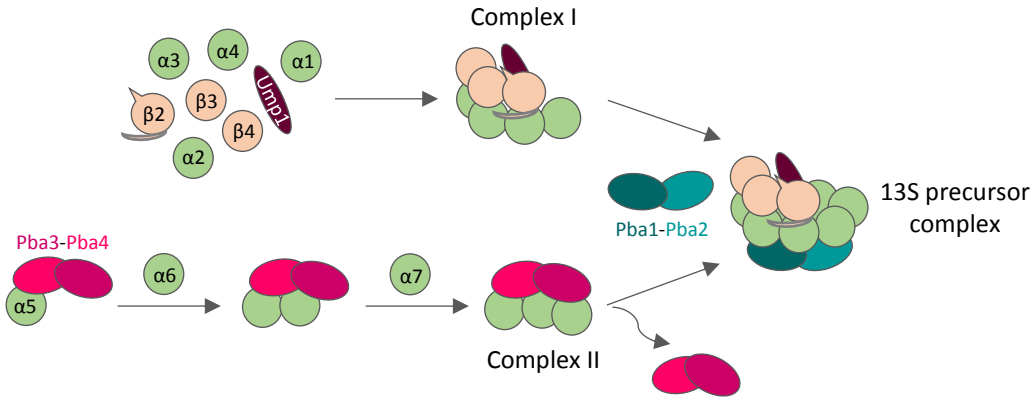

Figure 3.1 – Complex I-Complex II model. Schematic representation showing the different α (light green) and β subunits (light orange). Complex I, comprising the subunits α1-α4 as well as β2-β4 and the maturation factor Ump1, and Complex II, consisting of α5-α7 and the assembly chaperones Pba3-Pba4, merge to form the 13S precursor complex. This task appears to be aided by the assembly chaperone Pba1-Pba2. During this step, Pba3-Pba4 is thought to dissociate from the complex. The following steps of 20S assembly, starting by the incorporation of the subunits β5, β6, and β1, are as described for the α-ring model.

3.4 Ump1 N-terminal domain interacts with Pro-β7 to promote 15S PC dimerization

Ump1 has been implicated in the proper assembly of proteasome precursor complexes (15S PCs), their dimerization, and subsequent execution of active site maturation by processing of β subunit propeptides (Ramos *et al.*, 1998; Ramos and Dohmen, 2008). Biochemical, biophysical and structural analyses suggested recombinant yeast Ump1 to be a natively disordered protein, whose structure only becomes stabilized during interaction with proteasome subunits, looping around the inner chamber of the 15S PC (Sá-Moura *et al.*, 2013; Kock *et al.*, 2015). β7 is absent from 15S PCs, being the last subunit that is incorporated into the complex. Thereby, it helps to overcome Ump1 inhibition and drives the dimerization of 15S PCs to form 20S CPs (Li *et al.*, 2007; Marques *et al.*, 2007). In this study, the Ump1 N-terminal domain was shown with the help of *in vitro* binding experiments to physically interact with Pro-β7, a process likely involved in promoting 15S PC dimerization.

To analyze possible direct interactions between the two proteins, Ump1 was immobilized on a resin and was assayed for binding to β7. In contrast to a control experiment using β1,

which did not show a detectable binding to Ump1 under the same experimental conditions, β7 was specifically co-eluted with Ump1 (Figure 2.16). A sample without Ump1 excluded unspecific binding of β7 to the resin. In more detail, different domains of Ump1 were tested for the importance of these interaction. Therefore, a binding between β7 and Ump1 lacking different parts of its N- or C-terminus was tested. The N-terminal part of Ump1 yielded a stronger binding of β7 than the C-terminal fragment. Binding of the Ump1 N-terminus to β7 was abrogated by two point mutations (I3T or S11P) very close to the N-terminus that together were shown before to interfere with 15S PC dimerization. Together these findings highlight the importance of the Ump1 N-terminus interaction with β7 for this assembly step (Figure 2.17). To further dissect whether the propeptide or the C-terminal extension (CTE) of β7 would be relevant, different β7 variants were assayed for binding to Ump1. The CTE of β7, which intercalates between the Pre3/β1 and Pup1/β2 subunits of the opposing half during dimerization of 15S PCs, was shown to be important for this process to occur efficiently (Ramos *et al.*, 2004). However, the *in vitro* binding experiments indicated that the CTE is not engaging in an interaction with Ump1 (Figure 2.18). Instead, the propeptide of the β7 precursor subunit promoted binding to Ump1 *in vitro,* and this interaction depended on the presence of the N-terminal 16 residues of Ump1 (Figure 2.19). Consistent with this biochemical data, crosslinking of Ump1 residue ^{19}Lys to residue ^{91}Lys of β6 suggested that the N-terminal domain of Ump1 is likely not too far away from the position where Pro-β7 will insert (Kock *et al.*, 2015). In the structure of the mature 20S CP, the distance of ^{91}Lys of β6 to the N-terminal Thr of processed β7 is only ~15 Å, indicating that the N-terminal domain of Ump1 is probably well-positioned to interact with the propeptide of the incoming Pro-β7 subunit (Groll *et al.*, 1997).

The data obtained by *in vitro* binding studies clearly demonstrated the capacity of the β7 propeptide to bind to Ump1, but only if the N-terminal 16 residues of Ump1 were present (Figure 2.19). Together with *in vivo* experiments using yeast mutants (data not shown, see Zimmermann *et al.*, 2022), these results identified a novel function of the Ump1 N-terminus, the recruitment of Pro-β7 to the 15S PC complexes to drive their dimerization. Although the β7 propeptide and the N-terminal part of Ump1 appear to be mainly responsible for their interaction, other parts may additionally contribute, at least according to the *in vitro* binding experiments. The high sensitivity of the *in vitro* binding assays was critical to track down this interaction, because Pro-β7 cannot be detected in 15S PC isolated from yeast even when

a truncation of the CTE reduces efficiency of 15S PC dimerization (Marques *et al.*, 2007). The latter observation further suggested that stable incorporation of the β7 subunit requires multiple interactions and events. Based upon the new results, it can be proposed that an interaction between the N-terminal part of Ump1, which likely protrudes from the β-ring (Kock *et al.*, 2015), and the propeptide of β7 initially provide one such interaction. Another interaction is the above-mentioned intercalation of the β7 CTE between the β1 and β2 subunits of the juxtaposed 15S PC upon their dimerization. An efficient and complete stabilization of a nascent 20S CP pre-holo enzyme is probably only achieved when a 15S PC dimer is clamped together by two β7 subunits.

3.5 *In vitro* dimerization of 15S precursor complexes

The 15S precursor complex (PC) is a critical intermediate in 20S proteasome assembly, containing a complete α-ring as well as all β subunits except for β7, the maturation factor Ump1, and the dimeric chaperone Pba1-Pba2 (Marques *et al.*, 2007; Kock *et al.*, 2015). *In vivo* data suggested that incorporation of the β7 subunit drives and is the rate-limiting step for 15S PC dimerization (Marques *et al.*, 2007). In the present study, it was shown that β7 is sufficient to drive *in vitro* dimerization of purified 15S PC to form functional 20S CPs. Furthermore, the assembly process was demonstrated to be followed by autocatalytic cleavage of the proteolytic subunits β2 and β5 propeptides, and the degradation of Ump1.

In wild-type yeast cells, the abundance of the 15S precursor complex is quite low. In order to have a sufficient amount to purify the 15S PC intermediate and to enable a functional analysis regarding its dimerization, the yeast strain MO27 was used (Kock *et al.*, 2015). A C-terminal truncation of β7, more precisely a deletion of the last 19 amino acid residues, together with an N-terminally FLAG-6His tagged version of Ump1, enables for the enrichment of the cellular 15S PC population and a selective affinity purification. Incorporation of the β7 subunit is the critical step that drives dimerization of 15S PCs, and the truncated β7 is inefficient in this function thus leading to an unusual accumulation of 15S (Ramos *et al.*, 2004). Therefore, the *Pre4-ΔC19* mutation does not affect the structure of the 15S PC because this subunit is absent from this complex. Furthermore, the endogenous promoter of the *PBA1* and *PBA2* genes is substituted by the carbon source-controlled *GAL1*

promoter (P_{GAL1}). This promoter is induced in the presence of galactose, leading to a stable overexpression of Pba1 and Pba2, and repressed in the presence of glucose. In the *Pre4-ΔC19 FH-UMP1* background, cells grown in glucose behave like *pba1*Δ cells accumulating a faster electrophoretic migrating complex than the 15S complex, which is termed Complex I. However, when the same cells were grown in the presence of galactose, both Pba1 and Pba2 were overexpressed and a significant reduction of Complex I as well as an increase of the 15S PC amount was achieved. Additionally, the strain contains a deletion of *BLM10* gene (*blm10*Δ) to further increase 15S homogeneity by preventing precursor complexes to associate with Blm10 instead of Pba1-Pba2. The 15S complex was efficiently purified using consecutive Ni^{2+}-NTA and FLAG affinity chromatographies (Figure 2.20). Final elution was done using FLAG peptide and the FLAG-6His tag at the N-terminus of Ump1 was cleaved by incubation with TEV protease for 24 hours at 4 °C. Silver staining of the purified material, however, revealed that the 15S complex was not completely stable, apparently often missing the subunits β1 and β6. Thus, for later experiments the purification protocol was adapted to a much shorter version. Instead of using a consecutive two-step purification, a simple Ni^{2+}-NTA chromatography was performed and the elution was done enzymatically using TEV protease to cleave off the FLAG-6His tag, releasing the 15S complex from the beads. The material was directly used for downstream applications preventing any freeze-thaw cycles.

As the β7 subunit was never detected in 15S precursor complexes containing all other α and β subunits, β7 is assumed to be the last subunit that is incorporated into the complex. Dimerization of two 15S PCs is thought to be promoted by β7's C-terminal extension reaching out into the other half and stabilizing the newly formed 20S proteasome (Ramos *et al.*, 2004; Li *et al.*, 2007; Marques *et al.*, 2009). This study could confirm that the addition of the β7 subunit to 15S precursors is sufficient to trigger the dimerization of such complexes *in vitro* (Figures 2.23 and 2.24). To check for the dimerization of 15S complexes, the chymotrypsin-like activity of β5 was used. Therefore, 15S and β7 were mixed and the release of fluorescent 7-amino-4-methylcoumarin (AMC) after cleavage from a specific substrate (Suc-LLVY-AMC) was measured. For samples containing purified β7 from *E. coli* and 15S PC freshly purified from yeast, a clear chymotryptic activity was measured. This not only confirmed that the dimerization of 15S complexes into 20S proteasomes is dependent on the β7 subunit, but that this process is followed by active site maturation of the proteolytic β5

subunit propeptide leading to active 20S PCs *in vitro*. As the measured activity was absent from samples containing β7 or 15S PC alone, it appears to represent specific 20S proteasome activities.

To follow the events taking place after completion of 20S proteasome assembly, samples were analyzed by SDS-PAGE and western blotting. As expected, in samples containing the 15S complex alone, only the unprocessed (propeptide-containing) form of β2 was detected. When samples containing 15S PC and β7 were probed with anti-Pup1/β2, a band with a slightly smaller molecular weight than the precursor β2 was detected, most likely the mature form of the β2 subunit. Analyzing samples using anti-Ump1 antibody revealed that the amount of Ump1 was reduced in samples containing β7 and 15S PC in comparison to samples containing 15S PC alone.

Together these findings show the sufficiency of β7 to drive *in vitro* dimerization of purified 15S PC indicating that no additional factors such as general chaperones are essential for this process. That β7-driven *in vitro* dimerization of 15S PCs recapitulated authentic formation of functional 20S CPs could be demonstrated by following the maturation of the catalytic subunit β2 by western blotting and of β5 propeptides by following appearance of chymotryptic activity of proteolytically active 20S CPs. Finally, Ump1 was degraded also *in vitro*, as indicated by its absence from the newly formed 20S CP, confirming that it becomes the first substrate of the mature proteasome.

Though it was shown that β7 is sufficient to drive *in vitro* dimerization of purified 15S PCs without any additional factors, the involvement of general chaperones for example cannot be excluded. Possibly, such components might further promote or increase the efficiency of individual assembly steps at it was shown for Hsp70 and Hsp110 (Matias *et al.*, 2022).

An additional detection of the maturation of β1, the last of three active subunits, as well as of the release of the chaperone Pba1-Pba2 would complete the analysis of events taking place after dimerization of two 15S precursor complexes triggered by addition of β7. Unfortunately, the antibodies available were not able to detect specific signals for these polypeptides in the material purified from yeast. The production of highly specific antibodies against β1 as well as Pba1-Pba2 would therefore be one aim for future experiments. Another approach to verify the results and to prove that indeed authentic 20S proteasomes are formed

upon addition of the β7 subunit to the 15S precursor complexes, it would be necessary to determine the components of the occurring band at the size of the 20S CP by mass spectrometry, for instance. Using this method, it would be possible to verify if all components expected for the 15S (α1-7, β1-6, Ump1 and Pba1-Pba2) and for the 20S (α1-7, β1-7) are present. Furthermore, the functionality of the *in vitro* assembled 20S CP could be probed by measuring all three catalytic activities (tryptic and past-acidic in addition to chymotryptic) (Mizuno *et al.*, 1987; Kisselev *et al.*, 2003), and/or by using it to reconstitute 26S proteasomes by adding purified 19S activator complexes and test their performance in the degradation of ubiquitylated protein.

Another interesting question would be, if the dimerization of two 15S precursor complexes into 20S proteasomes is dependent on the amount of β7 present in the proximity of the 15S PC, or requires certain sites of the β7 subunit or the 15S complex to enable efficient 20S assembly. To test this, different amounts of β7 could be mixed with 15S and analyzed for the dimerization rate. Cross-linking experiments suggested that the N-terminus of Ump1 is located near the interface of β6 and the incoming β7 subunit, possibly able to sense the arrival of β7 in the complex (Figure 3.2) (Kock *et al.*, 2015). Furthermore, our data obtained by *in vitro* binding studies, clearly demonstrated the capacity of the β7 propeptide to bind to Ump1, but only if the N-terminal 16 residues of Ump1 were present, identifying a novel function of the Ump1 N-terminus in the recruitment of Pro-β7 to the 15S PC complexes to drive their dimerization (see 3.4). Additionally, the long C-terminal extension of the β7 subunit might be significant for this process, as a C-terminal deletion of the last 19 amino acid residues leads to the accumulation of 15S complexes and less 20S proteasomes in the cell (Ramos *et al.*, 2004). To investigate these hypotheses experimentally, one could now rely on the established *in vitro* reconstitution assay to test how truncations of different domains of the β7 subunit or the Ump1 protein effect *in vitro* dimerization and CP maturation afterwards.

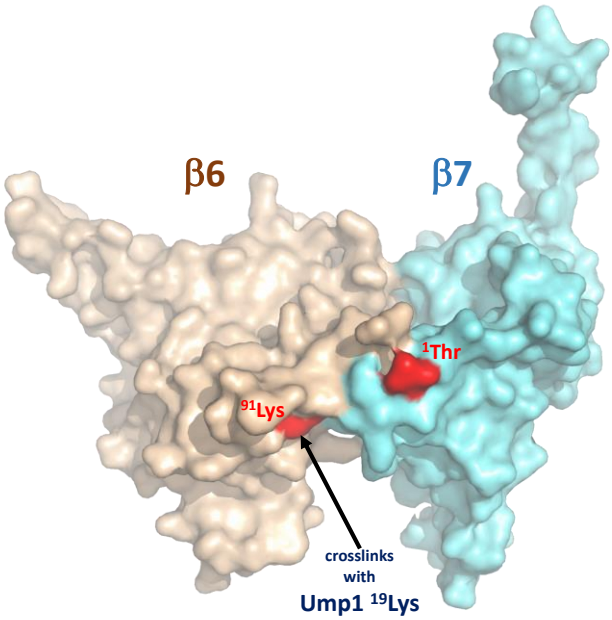

Figure 3.2 – Proximity of Ump1 crosslinking site and the N-terminus of β7. Surface representation of subunits β6 and β7 as found in the structure of the mature *S. cerevisiae* 20S CP (PDB code 1RYP) (Groll *et al*., 1997). Highlighted in red are the N-terminal ^{1}Thr of mature β7 and ^{91}Lys of β6. The latter crosslinked with residue ^{19}Lys of Ump1 in the 15S PC (Kock *et al*., 2015). The figure was generated using PyMOL.

Interestingly, examining the new model of 20S proteasome assembly, some similarities of early and late assembly steps can be noticed. In both cases, two complexes are brought together by a third component, and one of the assembly chaperones is released. Pba1-Pba2 brings Complex I and Complex II together to form the 13S precursor complex and Pba3-Pba4 is expelled. Similarly, 15S PC dimerization is driven by β7 leading to 20S proteasomes and resulting in the release of Pba1-Pba2.

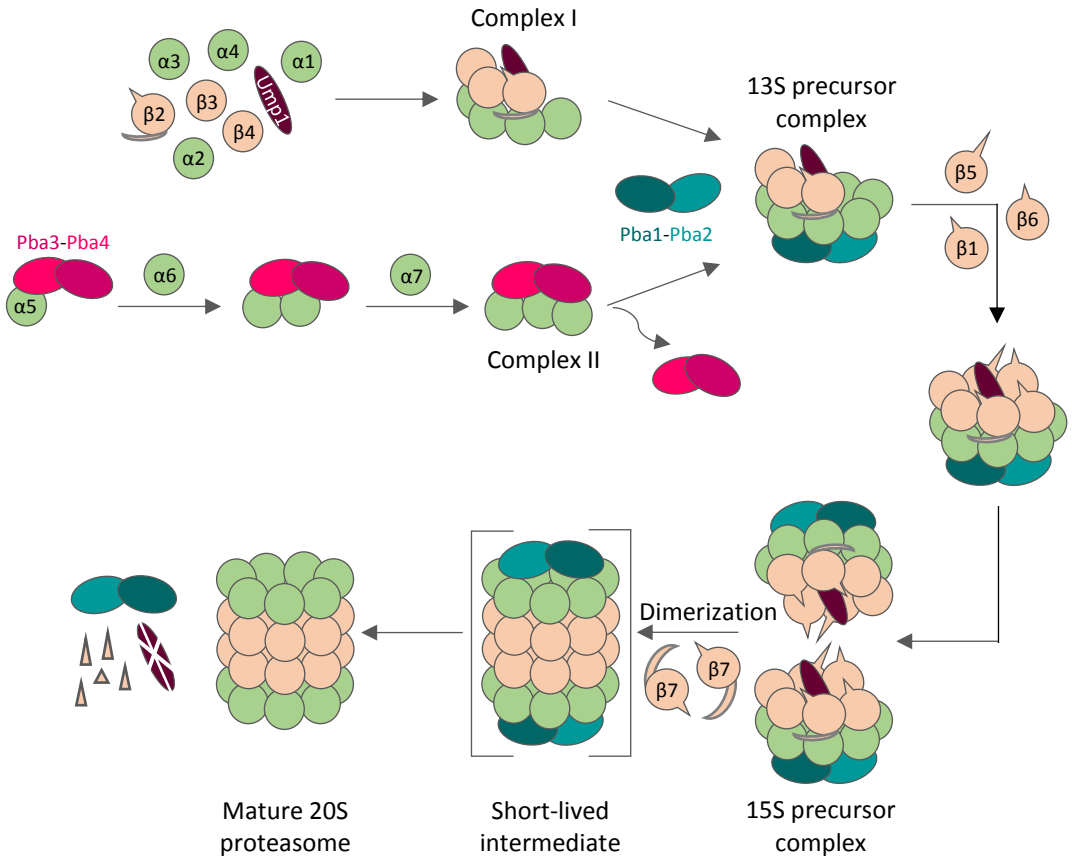

Figure 3.3 – Final model of 20S proteasome assembly. Schematic representation showing the different α (light green) and β subunits (light orange). Complex I, comprising the subunits α1-α4 as well as β2-β4 and the maturation factor Ump1, and Complex II, consisting of α5-α7 and the assembly chaperones Pba3-Pba4, merge to form the 13S precursor complex. This task appears to be aided by the assembly chaperone Pba1-Pba2. During this step, Pba3-Pba4 is thought to dissociate from the complex. After incorporation of β5, β6 and β1, the complex is called 15S PC or half-proteasome. The last subunit entering the complex is β7. The C-terminal extension of β7 reaches into the other half of the 20S CP to stabilize the nascent proteasome which is short-lived (shown in brackets) and drives dimerization of two 15S PCs. Likely, this process is promoted by a physical interaction of the Ump1 N-terminus and Pro-β7. The nascent proteasome is activated by autocatalytic maturation of the β subunits (propeptides are drawn as little extensions), Ump1 is degraded, and Pba1-Pba2 is released.

4 Material and Methods

4.1 Material

The materials, chemicals and laboratory instruments used for the experiments described are listed in the following section.

4.1.1 Oligonucleotides

Table 4.1 – Oligonucleotides used for PCR and sequencing.

Name	Sequence	Details
JZ5367	5'-CGCACCGGTGGCATGACCCAGCAGCCGATC-3'	FW AgeI_*PRE4*Δ*PRO*
JZ5368	5'-CGCGGATCCTTAGATTTTCT-3'	RV *PRE4*_BamHI
JZ5369	5'-CGCAACAGACCGGTGGCATG-3'	FW *SUMOI*_(AgeI)_ATG
JZ5370	5'-CGCGGATCCTTAAACCTGCAGGTTTTT-3'	RV *PRE4*Δ*CTE*_BamHI
JZ5483	5'-CGCACCGGTGGCATGCTTTTTAAACAATGG-3'	FW Age1_*PBA1*
JZ5484	5'-CGCGGATCCTCACTTGTAATC-3'	RV *FLAG*_BamHI
JZ5707	5'-CGCGAATTCATGGTTTCTAAGGGTGAAGAAGAC-3'	FW EcoRI_*mNG*
JZ5710	5'-CGCGGTACCCCTTGTACAATTCGTCCATACCCA-3'	RV *mNG*_KpnI
JZ5716	5'-CGCATGCATCGTGGAACTCAAAGAAAGG-3'	FW NsiI_P_{RPN4}
JZ5717	5'-CGCCTGCAGCTAACCCATGACATAACCA-3'	RV *RPN4**_PstI
JZ5731	5'-CGCGAATTCATGAACCACCCGTTCTCTTGGG-3'	FW EcoRI_*PRE4*
JZ5732	5'-CGCGCGGCCGCGATTTTCTGGGTACCGTAGCCTTTG-3'	RV *PRE4*_NotI
JZ5746	5'-CGCGGATCCTCACAGGTACCCATTGTATAAATC-3'	RV *PBA2*_KpnI_BamHI
JZ5764	5'-CGCGGATCCTCAATTGTATAAATCTACAAATTTAT-3'	RV *PBA2*_BamHI

JZ5786	5’-CGCGAATTCATGACCCAGCAGCCGATCGTTAC-3’	FW EcoRI_*PRE4ΔPro*
JZ5970	5’-CCTTCTTAAAGTTAAACAAAATTATTTTTATTTAGCG TACATGTCTTTGATGCATTTCAG-3’	RV *PBA3-RBS*
JZ5971	5’-TTTGTTTAACTTTAAGAAGGAGATATACATATGCTG GTTAAAACCATCTCTCGTACCATC-3’	FW *RBS-PBA4*
FW NotI_mNG	5’-CGCGCGGCCGCGATGGTTTCTAAGGGTGAAGAAGA C-3’	FW NotI_*mNG*
proPRE4 short RV	5’-CGCGGATCCCGCGCGGCCGCGTTAACCATCGGAGA TGCACC-3’	*proPRE4short_* NotI_BamHI RV
SS5049	5' CGCGGATCCTCTAGACTGCATAGTCAGG 3'	RV *HA*_BamHI
T7	5’-TAATACGACTCACTATAGGG-3’	FW T7 promoter
pRSET-RP	5’-ATGCTAGTTATTGCTCAGC-3’	RV T7 terminator

4.1.2 gBlocks® Gene Fragments

Table 4.2 – gBlocks Gene Fragments used for In-Fusion HD cloning.

Name	Sequence	Details
77573834	TCTACCAGGAACAG**ACCGGT**GGCATGTTCCTGACCCGTTCTG AATACGACCGTGGTGTTTCTACCTTCTCTCCGGAAGGTCGTCT GTTCCAGGTTGAATACTCTCTGGAAGCTATCAAACTGGGTTC TACCGCTATCGGTATCGCTACCAAAGAAGGTGTTGTACTGGG TGTTGAAAAGCGTGCTACCTCTCCGCTGCTGGAATCTGACTC CATCGAAAAAATCGTTGAAATCGACCGTCACATCGGTTGCGC TATGTCTGGTCTGACCGCTGATGCACGTTCTATGATCGAACA CGCTCGTACCGCAGCTGTTACCCACAACCTGTACTACGACGA AGACATCAACGTTGAATCTCTCACCCAGTCTGTGTGCGACCT CGCGCTGAGGTTCGGCGAAGGTGCGTCTGGTGAAGAACGTCT GATGTCTCGTCCGTTCGGTGTTGCTCTGCTGATCGCTGGTCAC GACGCTGATGACGGTTACCAGCTGTTCCACGCTGAACCGTCT GGTACCTTCTACCGTTACAACGCTAAAGCAATCGGTTCTGGC TCCGAAGGTGCACAGGCTGAACTGCTGAACGAATGGCACTCT TCCCTGACCCTGAAAGAGGCTGAACTGCTAGTTCTGAAAATC CTGAAACAGGTTATGGAAGAGAAACTGGACGAAAACAACGC TCAGCTGTCTTGCATCACCAAACAGGACGGTTTCAAAATCTA CGACAACGAAAAGACCGCTGAACTGATCAAAGAACTGAAAG AGAAGGAAGCTGCAGAATCTCCGGAGGAAGCTGACGTTGAA ATGTCTTAA**GGATCC**GGCTGCTAAC	AgeI_*PUP2*_BamHI
77573835	TCTACCAGGAACAG**ACCGGT**GGCATGTTCCGTAACAACTAC GACGGTGACACCGTTACCTTCTCTCCGACCGGTCGTCTGTTCC AGGTTGAATACGCTCTGGAAGCTATCAAACAGGGTTCTGTTA CCGTAGGTCTGCGTTCTAACACCCACGCTGTTCTGGTAGCTCT GAAACGTAACGCTGACGAACTGTCTTCCTACCAGAAAAAGAT CATCAAATGCGACGAACACATGGGTCTGTCTCTGGCTGGTCT GGCTCCGGACGCTCGTGTTCTGTCTAACTACCTGCGTCAGCA GTGCAACTACTCTTCCCTGGTTTTCAACCGTAAACTGGCTGTT GAACGTGCTGGTCACCTGCTGTGCGACAAAGCTCAGAAAAAC ACCCAGTCTTACGGTGGACGTCCGTACGGTGTTGGACTGCTG ATCATCGGTTACGACAAATCTGGTGCTCACCTGCTGGAATTC CAGCCGTCTGGTAACGTTACCGAACTGTACGGTACCGCTATC GGTGCTCGTTCTCAGGGTGCTAAAACCTACCTGGAACGTACC CTGGACACCTTCATCAAAATCGACGGTAACCCGGACGAACTG	AgeI_*PRE5*_BamHI

	ATCAAAGCTGGTGTTGAAGCTATCTCTCAGTCCCTGCGTGAC GAATCTCTGACCGTTGACAACCTGTCTATCGCTATCGTTGGTA AAGACACCCCGTTCACCATCTACGACGGTGAAGCTGTTGCAA AATACATCTAA**GGATCC**GGCTGCTAAC	
77573836	TCTACCAGGAACAG**ACCGGT**GGCATGACCTCTATCGGTACC GGATACGACCTGTCTAACTCCGTTTTCTCTCCGGACGGTCGTA ACTTCCAGGTTGAATACGCTGTTAAAGCTGTTGAAAACGGTA CCACCTCTATCGGTATCAAATGCAACGATGGCGTTGTATTCG CCGTTGAAAAACTGATCACCTCTAAACTGCTGGTTCCGCAGA AGAACGTTAAAATCCAGGTTGTAGACCGTCACATCGGTTGCG TTTACTCTGGTCTGATCCCGGACGGTCGTCACCTGGTTAACCG AGGTCGTGAAGAAGCGGCGAGCTTCAAAAAGCTGTACAAAA CCCCGATCCCAATACCGGCGTTCGCTGACCGTCTCGGTCAGT ACGTTCAGGCTCACACCCTGTACAACTCTGTTCGTCCGTTCGG TGTTTCTACCATCTTCGGTGGAGTTGACAAAAACGGTGCTCA CCTGTACATGCTGGAACCGTCTGGTTCTTACTGGGGTTACAA AGGTGCAGCTACCGGTAAAGGACGTCAGTCTGCGAAAGCTG AACTGGAGAAACTGGTTGACCACCACCCGGAAGGTCTGTCTG CTCGTGAAGCTGTTAAACAGGCTGCAAAAATCATCTACCTGG CTCACGAAGACAACAAAGAAAAAGACTTCGAACTGGAAATC TCTTGGTGCTCACTGTCTGAAACCAACGGTCTGCACAAATTC GTTAAAGGTGACCTGCTGCAGGAAGCTATCGACTTCGCTCAG AAAGAAATCAACGGTGACGATGACGAAGACGAAGATGACTC TGACAACGTTATGTCTTCAGACGACGAAAACGCTCCGGTTGC AACCAACGCTAACGCTACCACCGACCAGGAAGGTGACATCC ACCTGGAATAA**GGATCC**GGCTGCTAAC	AgeI_*PRE10*_BamHI
77594828	TCTACCAGGAACAG**ACCGGT**GGCATGATCTCTTACGAATTTC AGACCCACCTGCCGAAAGGTAAAGACTCTTCCCTGAACGCTT CTTCCGAGAACAAAGAACTGTACGTTCAGGCTACCCACTTCA ACAACACCATCCTGCTGCAGATCCGTCTGAACGGTGAAATGG ACTCTACCTACGAAGTTTCCTCTAAAGGTCTGAACCCGATCCT GGACATCAACGTTCCGCTGGCTGGTAACCTGGGTAACACTGG TGGCGACTACGATGACGAAGAGGAAGAGTTTGTACGTGACC ACCTGTCTGACTACCAGGTTGTAACCAAACTGGGTGACTCTG CTGACCCGAAAGTTCCAGTCGTATGCGTCCAGATCGCTGAAC TGTACCGTCGAGTTATCCTGCCGGAAGTTTCAGGTACCATGG CTCAGGACAACATGCAGTTCTCTCTGCTGATCTCTATGTCCTC TAAAATCTGGCGTGCTACCAAAGAACAGAGCGCTGACGATA ACGACTTCGGCAAACTGGTGTTCGTACTGAAATGCATCAAAG ACATGTACGCTAAATAATGACGCAAGCTTGCAAACCCGAAG GAGGTGTGAGATGCTGGTTAAAACCATCTCTCGTACCATCGA ATCTGAATCAGGTTTCCTGCAGCCGACCCTGGACGTTATCGC TACCCTGCCGGCTGACGACCGTTCTAAGAAAATCCCGATCTC TCTGGTTGTAGGTTTCAAACAGGAAGCTTCTCTGAACTCTTCA TCTTCACTGTCTTGCTACTATTACGCTATCCCGCTGATGCGTG ACCGACACATCAACCTGAAATCTGGAGGTTCAAACGTTGTCG GTATCCCGCTGCTGGACACCAAAGACGACCGTATCCGAGACA TGGCTCGTCACATGGCTACCATCATCTCTGAACGTTTCAACCG TCCGTGCTACGTTACCTGGTCTTCACTGCCGTCTGAAGACCCG TCTATGCTGGTTGCTAACCACCTGTACATCCTGAAGAAATGC CTGGACCTACTGAAAACCGAACTGGGTGAATACCCATACGAT GTTCCAGATTACGCTTGA**GGATCC**GGCTGCTAAC	AgeI_*PBA3-SD-PBA4-HA*_BamHI

4.1.3 Plasmids

Table 4.3 – Plasmids used in this study.

Name	Relevant genotype	Derived from	Source	Stock no.
pET11a	*PT7-EcoRI-Insert-KpnI-6His-BamHI; Amp resistance gene*	pET11a	Novagen	504
pJZ14	*8His-SUMO1-PRE3/β1*	pET11a	Master thesis	4472
pJZ15	*8His-SUMO1-PRE2/β5*	pET11a	Master thesis	4473
pJZ16	*8His-SUMO1-PRE7/β6*	pET11a	Master thesis	4474
pJZ17	*8His-SUMO1-PRE4/β7*	pET11a	Master thesis	4475
pJZ18	*8His-SUMO1-ΔLS-PRE4/β7*	pET11a	This study	4613
pJZ19	*8His-SUMO1-PRE4/β7-ΔCTE*	pET11a	This study	4615
pJZ20	*8His-SUMO1-PUP2/α5*	pET11a	This study	4617
pJZ21	*8His-SUMO1-PRE5/α6*	pET11a	This study	4619
pJZ22	*8His-SUMO1-PRE10/α7*	pET11a	This study	4621
pJZ24	*8His-SUMO1-PBA1-PBA2-FLAG*	pET11a	This study	4630
pJZ27	*mNG-2HA*	pET11a	This study	4782
pJZ28	P_{RPN4}*-RPN4*(*Δ_{1-10}/$\Delta_{211-229}$*)::LEU2*	pUC21	This study	4783
pJZ29	*PRE4/β7-mNG-2HA*	pET11a	This study	4785
pJZ30	*LS-PRE4/β7-mNG-2HA*	pET11a	This study	4787
pJZ32	*8His-SUMO1-PBA1-PBA2*	pET11a	This study	4791
pJZ33	*ΔLS-PRE4/β7-mNG-2HA*	pET11a	This study	4793
pJZ34	$^{17-148}$*UMP1-6His*	pET11a	This study	4795
pJZ39	*8His-SUMO1-PBA3-PBA4-HA*	pET11a	This study	4873
pCR32	$^{1-81}$*UMP1-6His*	pET11a	Paula C. Ramos	3418
pCR33	$^{82-148}$*UMP1-6His*	pET11a	Paula C. Ramos	3419
pCR61	$^{17-81}$*UMP1-6His*	pET11a	Paula C. Ramos	-
pCR62	$^{1-81}$*UMP1-I3T-6His*	pET11a	Paula C. Ramos	-
pCR64	$^{1-81}$*UMP1-S11P-6His*	pET11a	Paula C. Ramos	-
pJD492	$^{1-148}$*UMP1-6His*	pET11a	Jürgen Dohmen	848
pMALc-2x	*MBP*	pMALc-2x	NEB	2206
pMO6	*MBP-PRE4/β7-CTE*	pMALc-2x	Maria Nunes	3357

4.1.4 *Escherichia coli* strains

Table 4.4 – *E. coli* strains used for cloning, plasmid amplification and expression.

Strain	Relevant genotype	Source
XL1-Blue	*recA1 endA1 gyrA96 thi-1 hsdR17 supE44 relA1 lac [F´proAB lacI^{q}ZΔM15 Tn10 (Tetr)*	Lab collection
BL21 (DE3)	*F- ompT dcm hsdS(r_{B-} m_{B-}) gal λ(DE3)*	Lab collection
BL21 codon plus	*F- ompT gal dcm Ion hsdS(rB- mB-) λ(DE3 [lacI lacUV5-T7 gene 1 ind1 sam7*	Lab collection

4.1.5 *Saccharomyces cerevisiae* strains

Table 4.5 – *S. cerevisiae* strains used in this study.

Name	Relevant genotype	Derived from	Source	Stock
JD47-13C	*MATa leu2-3, 112 lys2-801 his3-Δ200 trp1-Δ63 ura3-52*	"WT"	Dohmen et al., 1995	188
JZ3	*WT +HIS3, +LYS2*	JD330-3A + pFP5_KpnI_BshTI	This study	4714
JZ4	*rpn4Δ::HIS3 +LYS2*	JD330-3A + pFP5_KpnI_BshTI	This study	4715
JZ5	*WT +LEU2, +TRP1*	MB1 + pJD278_BglII	This study	4716
JZ6	*WT +HIS3, +LYS2,+TRP1*	JZ3xJZ5	This study	4717
JZ7	*WT +HIS3, +LYS2, +LEU2, +TRP1*	JZ3xJZ5	This study	4718
JZ8	*rpn4Δ::HIS3, +LYS, +LEU2, +TRP1*	JZ4xJZ5	This study	4719
JZ9	*RPN4*::LEU2, + HIS3, + LYS2, + TRP1*	JZ6 + pJZ28_NotI	This study	4720
CM184	*pba1Δ::HIS3 UMP1-HA::LEU2*	PR118	Paula C. Ramos	3299
CM257	*PRE9/α3-2HA::YIplac211*	JD47-13C	Ana Matias	3258
CM273	*PRE5/α6-2HA::YIplac211*	JD47-13C	Ana Matias	3654
CM61	*PUP3/β3-2HA::YIplac211*	JD47-13C	Ana Matias	2383
FP16	*PBA4-HA::URA3*	JD47-13C	Filipa Pardelha	2407
FP6	*PRE3/β1-2HA::YIplac211*	JD47-13C	Filipa Pardelha	595
JD129	*UMP1-HA::LEU2*	JD47-13C	Jürgen Dohmen	540
JD138	*PRE2/β5-2HA::YIplac211*	JD47-13C	Jürgen Dohmen	569
JD139	*PUP1/β2-2HA::YIplac211*	JD47-13C	Jürgen Dohmen	570
JD2701	*SCL1/α1-2HA::YIplac211*	JD47-13C	Jürgen Dohmen	2701

JD2702	*PRE8/α2-2HA::YIplac128*	JD47-13C	Jürgen Dohmen	2702
JD2704	*PRE6/α4-2HA::YIplac211*	JD47-13C	Jürgen Dohmen	2704
JD2705	*PUP2/α5-2HA::YIplac211*	JD47-13C	Jürgen Dohmen	2705
JD2707	*PRE10/α7-2HA::YIplac211*	JD47-13C	Jürgen Dohmen	2707
JD330-3A	*rpn4::HIS3*	ML4xJD300-3D	Jürgen Dohmen	1250
JD337	*WT +HIS3*	JD53	Jürgen Dohmen	1463
JD71	*PRE1/β4-2HA::YIplac211*	JD47-13C	Jürgen Dohmen	282
JM10	*PRE5/α6-HA::LEU2*	JD47-13C	Joao Matos	1349
JM9	*PUP2/α5-HA::URA3*	JD47-13C	Joao Matos	1348
MB1	*WT +TRP1*	JD47-13C	Kerstin Nürrenberg	4274
MN36	*PRE7/β6-2HA::YIplac211*	JD47-13C	Margarida Neto	3382
MO24	*PRE1-FLAG-6His*	JD47-13C	Maria Nunes	3534
MO26	P_{GAL1}*PBA1* P_{GAL1}*PBA2*	JD47-13C	Maria Nunes	3536
MO27	*pre4-ΔC19 FLAG-6His-UMP1 blm10Δ::kanMX6* P_{GAL1}*PBA1::TRP1* P_{GAL1}*PBA2::HIS3*	AM31	Maria Nunes	3537
PG28	*POC3-HA::URA3*	JD47-13C	Paulo Gouveia	2406
PR123	*pba3*Δ*, α5-HA::URA3*	JD47-13C	Paula C. Ramos	3037
PR57	P_{GALS}*PUP2/α5, α7-HA::URA3*	JD47-13C	Paula C. Ramos	2783
PR65	P_{GALS}*PRE5/α6, α5-HA::URA3*	JD47-13C	Paula C. Ramos	2735
SS4	*PRE4/β7-2HA::YIplac211*	JD47-13C	Stefanie Schwab	3995

4.1.6 Antibodies

Table 4.6 – Antibodies used in this study.

Antibody	Host, class	Dilution	Source
Anti-6His	mouse	1:2000	Invitrogen
Anti-FLAG M2	mouse	1:1000	Sigma
Anti-HA 3F10	rat	1:1000	Sigma
Anti-HA 3F10, HRP	rat	1:2500	Roche
Anti-MBP	mouse	1:10000	New England Biolabs
Anti-Pba3/Pba4-HA	rabbit	1:1000	This study/Pineda
Anti-Tpi1	rabbit	1:5000	Lab collection
Anti-Ump1-6His	rabbit	1:500	Lab collection
Anti-α5/Pup2	rabbit	1:1000	This study/Pineda

Anti-α6/Pre5	rabbit	1:1000	This study/Pineda
Anti-α7/Prs1	rabbit	1:1000	Lab collection/Pineda
Anti-β1/Pre3	rabbit	1:5000	This study/Pineda
Anti-GST-β2/Pup1	rabbit	1:1000	Lab collection/Pineda
Anti-β5/Pre2	rabbit	1:5000	This study/Pineda
Anti-β6/Pre7	rabbit	1:5000	This study/Pineda
Anti-β7/Pre4	rabbit	1:1000	This study/Pineda
Anti-β7/Pre4 (28.10.96)	rabbit	1:1000	(Jäger *et al.*, 1999)
Anti-mouse Alexa Fluor Plus 680	goat	1:5000	Thermo Fisher
Anti-mouse, HRP	goat	1:5000	Sigma
Anti-rabbit Alexa Fluor Plus 800	goat	1:5000	Thermo Fisher
Anti-rabbit, HRP	donkey	1:5000	GE Healthcare
Anti-rat Alexa Fluor 680	goat	1:5000	Thermo Fisher
Anti-rat, HRP	goat	1:5000	Abcam

4.1.7 Enzymes

Table 4.7 – Enzymes used in this study.

Enzyme	Company
AcTEV™ Protease	Thermo Fisher
DNaseI	Roche
DreamTaq DNA Polymerase	Thermo Fisher
FastAP Alkaline Phosphatase	Thermo Fisher
FastDigest AgeI/BshTI	Thermo Fisher
FastDigest BamHI	Thermo Fisher
FastDigest BglII	Thermo Fisher
FastDigest EcoRI	Thermo Fisher
FastDigest KpnI	Thermo Fisher
FastDigest NotI	Thermo Fisher
FastDigest Nsi1	Thermo Fisher
FastDigest PstI	Thermo Fisher
In-Fusion HD Enzyme Premix	Takara Bio
Lysozyme	Serva
RNase A	Omega Bio-Tek
S7 Fusion DNA Polymerase	Mobidiag
Sentrin-specific protease 1 (Senp1)	Thomas Hermanns
T4 DNA Ligase	New England Biolabs
Zymolyase	Carl Roth

4.1.8 Chemicals

Table 4.8 – Chemicals used in this study.

Chemical	Company
Acrylamide mix (30 % acrylamide/ 0.7 % bisacrylamide)	Carl Roth
Adenine	Carl Roth
Agar	Formedium
Agarose	Sigma-Aldrich
Ammonium persulfate (APS)	Sigma-Aldrich
Ampicillin	AppliChem
Amylose resin	New England Biolabs
Bacto peptone	Thermo Fisher
Bromophenol blue	Serva
Calcium dichloride	Acros Organics
Chloramphenicol	Sigma-Aldrich
cOmplete, EDTA-free Protease Inhibitor Cocktail Tablets	Sigma-Aldrich
Coomassie CBB G-250	Sigma-Aldrich
D(+)Glucose monohydrate	Carl Roth
Developer	Agfa
Disodium hydrogen phosphate	VWR
Deoxynucleotide triphosphates (dNTPs)	New England Biolabs
Dithiothreitol (DTT)	AppliChem
Ethylenediaminetetraacetic acid (EDTA)	Carl Roth
Ethanol	VWR
EZview Red Anti-HA Affinity Gel	Sigma-Aldrich
EZview Red Anti-FLAG Affinity Gel	Sigma-Aldrich
Fixer	Agfa
Galactose	VWR
Glacial acetic acid	VWR
Glass beads ≤ 106 µm	Merck
Glass beads 425-600 µm	Merck
Glycerol	AppliChem
Glycine	VWR
Hydrochloric acid	VWR
Hydrogen peroxide (30 %)	Sigma-Aldrich
Imidazole	Sigma-Aldrich
IPTG	VWR
Isopropanol	VWR
Kanamycin	Applichem

L-Arginine	Carl Roth
L-Histidine	Merck
Liquid nitrogen	Lab filling system
L-Isoleucine	Carl Roth
Lithium acetate	Sigma-Aldrich
L-Leucine	AppliChem
L-Lysine	Carl-Roth
L-Methionine	Merck
L-Phenylalanine	Carl Roth
L-Threonine	AppliChem
L-Tryptophan	VWR
Magnesium chloride	Carl Roth
Methanol	VWR
MG132	Sigma-Aldrich
Midori Green Xtra	Biozym
Milk powder	Carl Roth
Milli-Q water	Lab filling system
MOPS PUFFERAN®	Carl Roth
Ni-NTA Superflow	Qiagen
NucleoSpin Gel and PCR Clean-up	Macherey-Nagel
Omega Bio-Tek E.Z.N.A Plasmid DNA Mini Kit	Omega Bio-Tek
PageRuler Plus Prestained Protein Ladder	Thermo Fisher
Peptone	Formedium
Phenylmethylsulfonylfluorid (PMSF)	Sigma-Aldrich
Polyethylene glycol (PEG)	Sigma-Aldrich
Ponceau S	Sigma-Aldrich
Potassium chloride	AppliChem
Potassium dihydrogen phosphate	VWR
PureCube Co-NTA MagBeads	Cube Biotech
Raffinose	Serva
Revert™ 700 Total Protein Stain	LI-COR
Sodium dodecyl sulfate (SDS)	Serva
Serva Stain Clear G	Serva
Sodium acetate	VWR
Sodium azide	Sigma-Aldrich
Sodium chloride	VWR
Sodium dihydrogen phosphate	Merck
Sodium hydroxide	Merck
Suc-LLVY-AMC	Bachem

Sucrose	Merck
SuperSignal™ West Femto Maximum Sensitivity Substrate	Thermo Fisher
TALON dynabeads	Thermo Fisher
TALON® Metal Affinity Resin	Clontech/Takara
Tetracycline hydrochloride	Sigma-Aldrich
Tetramethylethylenediamine (TEMED)	AppliChem
Tris-(hydroxymethyl)-aminomethane (Tris)	Carl Roth
Triton X-100	Sigma-Aldrich
Tryptone	Formedium
Tween-20	Sigma-Aldrich
Uracil	Sigma-Aldrich
Urea	Carl Roth
Yeast extract	Formedium
Yeast nitrogen base	Formedium
β-mercaptoethanol	Sigma-Aldrich

4.1.9 Laboratory instruments

Table 4.9 – Instruments used in this study.

Instrument	Company
2D Multi-fluorescence scanner Typhoon 9400	GE Healthcare Life Sciences
Agarose gel electrophoresis chamber	Peqlab
BioSpectrometer Basic	Eppendorf
Blue light table, dark reader	Clare Chemical Research
ChemiDoc Imaging System	Bio-Rad
Centrifuge 5425	Eppendorf
Centrifuge 5430 R	Eppendorf
Centrifuge 5810 R	Eppendorf
Centrifuge Allegra X-22R	Beckman Coulter
Centrifuge Avanti J-20 XP	Beckman Coulter
Centrifuge Avanti J-26S XP	Beckman Coulter
Developer for X-ray films Curix 60	Agfa
DynaMag Magnetic particle concentrator	Invitrogen
Electric pipette controller	VWR
Electric stirrer	H + P
FastGene® PAGE Gel 4-12 % or 4-20 %	NIPPON Genetics
Fluorescence microscope Axioplan 2	Zeiss
Gel documentation system	Bio-Rad

Glass Econo-Column®, Chromatography columns	Bio-Rad
Incubators INFORS HT ECOTRON	INFORS HT
Incubators innova 4230	New Brunswick Scientific
Macro pipette controller	Brand
Micropipettes	Gilson
Microscope for titrate dissection	Zeiss
Mixer Mill MM400	Retsch
Nanodrop One	Eppendorf
NativePAGE™ 4-16 % Bis-Tris Gel	Invitrogen
Nitrocellulose membrane 0.2 µm	GE Healthcare
Odyssey Imager	LI-COR
pH meter	Mettler Toledo
Power supplies	Biometra, Amersham Biometra Biotec, VWR
Pump	KNF Lab
Rocking platform	Biometra, Edmund Bühler
Scanner for X-ray films, 4870 photo	Epson
SDS-PAGE Electrophoresis unit	Hoefer
SDS-PAGE Mini PROTEAN Tetra Cell	Bio-Rad
SDS-PAGE XCell SureLock™ Mini-Cell	Invitrogen
Sonopuls homogeniser	Bendelin
Spectrophotometer Ultrospec 3000	Pharmacia Biotech
T3 Thermocycler	Biometra
Plate reader Inifnite F200 pro	Tecan
PVDF membrane 0.45 µm	GE Healthcare
Trans-Blot SD Semi-dry transfer cell	Bio-Rad
Thermomixer compact	Eppendorf
Ultrasonic cleaner	VWR
Vibrax VXR Basic	IKA
Vivaspin® 6 50,000 MWCO	Sartorius
Vivaspin ® Turbo 4 10,000 MWCO	Sartorius
Vortex Mixer Uzusio VTX-3000L	LMS

4.2 Molecular biology techniques

4.2.1 Polymerase chain reaction

Polymerase chain reaction (PCR) was performed either for the amplification of DNA fragments in order to clone a new plasmid or for the verification of the relevant genotype of a *E. coli* or yeast strain. Whereas for cloning purpose a high-fidelity DNA polymerase was used, for an analytic PCR this was not necessary. Instead of plasmid DNA, a small amount of fresh cells was resuspended in 1 µl water and incubated for one minute in a microwave. The protocol of the PCR reaction mix, and the PCR program for both variants are listed below.

Table 4.10 – PCR reaction mix.

High-fidelity PCR		**Colony PCR**	
Ingredient	**Amount**	**Ingredient**	**Amount**
5 x HF buffer	20.0 µl	10x DreamTaq Buffer Green	2.0 µl
plasmid DNA	1.0 µl	cell suspension	1.0 µl
dNTPs (10 mM)	2.0 µl	dNTPs (10 mM)	0.4 µl
Primer 1 (100 µM)	0.5 µl	Primer 1 (100 µM)	0.1 µl
Primer 2 (100 µM)	0.5 µl	Primer 2 (100 µM)	0.1 µl
S7 Fusion Polymerase	1.0 µl	DreamTaq DNA polymerase	0.1 µl
Milli-Q water	75.0 µl	Milli-Q water	16.3 µl
Total volume	100.0 µl	Total volume	20.0 µl

Table 4.11 – PCR program.

	High-fidelity PCR			**Colony PCR**		
Step	**Temperature**	**Duration**	**Cycles**	**Temperature**	**Duration**	**Cycles**
1 Initial	98 °C	30 s	1	95 °C	1-3 min	1
2 Denaturation	98 °C	5-10 s	29	95 °C	30 s	34
3 Annealing	<Tm + 3 °C	10-30 s		Tm-5 °C	30 s	
4 Extension	72 °C	15-30		72 °C	1 min	
5 Final extension	72 °C	5-10 min	1	72 °C	5-15 min	1
6 Cooling	4 °C	hold	1	4 °C	hold	1

4.2.2 Agarose gel electrophoresis

In order to purify or analyze DNA such as PCR fragments and restriction digests, agarose gel electrophoresis was performed. The gel was usually prepared by dissolving 1 % (w/v) agarose in TAE buffer (40 mM Tris, 20 mM sodium acetate, 1 mM EDTA). For visualization of the DNA, 4 µl SERVA DNA Stain G or 2 µl Midori Green Xtra were added to ~50 ml of agarose gel solution. If necessary, samples were mixed with 10x DreamTaq buffer Green prior to application. DNA standard markers such as GeneRuler 50 bp or 1 kb DNA Ladder were loaded along with the samples for estimation of the molecular weight. The gel electrophoresis was typically carried out at 100 V for 30 minutes and the DNA was visualized under blue light using a gel documentation system. As required, the band of interest was cut from the agarose gel.

4.2.3 DNA purification

DNA extracted from an agarose gel and PCR reactions were purified using the NucleoSpin Gel and PCR Clean-up Kit from Macherey-Nagel according to the manufacturers' protocol. Usually, the elution was done in 20 µl.

4.2.4 Estimation of DNA concentration

The concentration of a DNA sample was determined measuring sample volumes of 2 µl with the help of a 1 mm µCuvette at 260 and 280 nm using an Eppendorf BioSpectrometer. The ratio of absorbance at 260 nm and 280 nm is used to estimate the purity of a DNA sample. Whereas a ratio of ~1.8 is generally accepted as pure for DNA, a ratio above 1.8 is indicating RNA contamination and a ratio below 1.8 points to the presence of protein, phenol or other contaminants that absorb strongly near 280 nm.

4.2.5 Restriction digestion of DNA

Restriction digestion was performed in order to produce a new plasmid, verify a genotype of a clone or prior to an integration of the DNA into the yeast genome. The protocol of the restriction digest is listed below. If necessary, additionally 1 µl FastAP alkaline phosphatase

was added to the vector digestion. The reaction mix was typically incubated at 37 °C for 30 minutes, and if desired, heat inactivation of the endonucleases was performed according to the required temperature and time.

Table 4.12 – Reaction mix for restriction digestion of DNA.

	Digestion of plasmid DNA	Digestion of PCR
Ingredient	**Amount**	
10x FD (Green) Buffer	2.0 µl	2.0 µl
DNA	5.0-15.0 µl	16.0 µl
Restriction endonuclease 1	1.0 µl	1.0 µl
Restriction endonuclease 2	1.0 µl	1.0 µl
Milli-Q water	11.0-1.0 µl	-
Total volume	20.0 µl	20.0 µl

4.2.6 Ligation of DNA fragments

In order to create a new plasmid, the previously digested and purified DNA fragments were ligated with the vector backbone. Therefore, the concentration of insert and vector was determined and a ratio of 3:1 was used for simple two-part ligations and a ratio of 5:1 was applied for three-part ligations, respectively. A ligation without insert served as negative control. The ligation mix was prepared according to the following instructions and usually incubated for 1 hour at room temperature.

Table 4.13 – Ligation reaction mix.

Ingredient	Amount
10x T4 DNA Ligase Buffer	2.0 µl
Vector backbone	3-5x less than insert
Insert	3-5x more than vector backbone
T4 DNA ligase	1.0 µl
Milli-Q water	fill up to 20.0 µl
Total volume	20.0 µl

4.2.7 In-Fusion HD Cloning

As an alternative to the conventional cloning method at restriction sites, a strategy called In-Fusion HD Cloning was used. By this technique, gBlocks® Gene Fragments or PCR products

can be assembled into the linearized vector by homologous ends. The mix for such an In-Fusion reaction was prepared as shown below and incubated at 50 °C for 15 minutes to 1 hour. As a control, the same mixture was done without insert.

Table 4.14 – In-Fusion HD Cloning mix.

Ingredient	Amount
5x In-Fusion HD Enzyme Premix	2.0 µl
Vector backbone	60 ng
Insert	100 ng
Milli-Q water	fill up to 10.0 µl
Total volume	10.0 µl

4.2.8 Preparation of chemically competent *E. coli* cells

For preparation of chemically competent *E. coli*, the desired cells were grown with 180 rpm agitation in 5 ml Luria-Bertani (LB) medium at 37 °C overnight. The next day, the culture was diluted with LB medium to an OD_{600} of 0.2 in a total volume of 50 ml. Cells were grown shaking at 37 °C until their exponential growth phase at ~0.6 OD_{600}. Afterwards, the culture was transferred to pre-cooled 50 ml falcon tubes on ice to ensure rapid cooling. Cells were harvested by centrifugation at 3,000 rpm and 4 °C for 10 minutes and the supernatant was discarded. The pellet was gently resuspended in 25 ml ice-cold, sterile 0.1 M $CaCl_2$ and the suspension was incubated for 20 minutes on ice. After another centrifugation, cells were resuspended in 2 ml ice-cold, sterile 0.1 M $CaCl_2$ containing 15 % glycerol and incubated for 1 hour on ice. Finally, aliquots of 100 µl competent *E. coli* cells were transferred to pre-cooled reaction tubes and stored at -80 °C.

4.2.9 Transformation of *E. coli* cells

For each transformation, a 50-100 µl sample of chemically competent *E. coli* cells was incubated with 0.5 µl plasmid DNA, 10 µl ligation- or 10 µl In-Fusion HD Cloning mix for 15 minutes on ice. After a heat-shock at 42 °C for 45 seconds, 1 ml LB medium was added, and cells were incubated at 37 °C and 300 rpm for 45 minutes. In the use of plasmid DNA, 50 µl of the suspension were directly plated on LB-agar plates containing the appropriate antibiotics. In case of ligation- or In-Fusion HD Cloning mix, samples were centrifuged at

13,200 rpm for 1 minute and the supernatant was discarded. The cell pellet was resuspended in 100 µl LB medium and the suspension was plated on plates with proper antibiotics. Plates were incubated at 37 °C overnight.

4.2.10 Transformation of *S. cerevisiae* cells

To introduce DNA into *S. cerevisiae*, yeast transformation was done as described below. 2 ml YPD medium were inoculated with a pipette tip of the desired yeast cells and incubated at 30 °C overnight. The next day, cultures were diluted to 0.25 OD_{600} in 5 ml YPD medium for each transformation and grown at 30 °C until an OD_{600} between 0.6 and 0.8 was reached. Afterwards, cells were harvested by centrifugation at 3,000 rpm for 3 minutes. The pellet was washed once in sterile Milli-Q water, transferred to a 1.5 ml reaction tube and centrifuged shortly for about 8 seconds. Cells were resuspended in the following transformation mix (Table 4.15) and incubated at 30 °C for 25 minutes before being transferred to 42 °C for 20 minutes. After another short centrifugation, the supernatant was discarded, the pellet was resuspended in 100 µl Milli-Q water and plated on appropriate selective medium. Plates were incubated at 30 °C for 3 days.

Table 4.15 – *S. cerevisiae* transformation mix.

Ingredient	Amount
50 % PEG	240.0 µl
1 M lithium acetate	36.0 µl
E. coli carrier DNA	5.0 µl
Restriction digest of plasmid DNA	10.0 µl
Milli-Q water	69.0 µl
Total volume	360.0 µl

4.2.11 Glycerol stocks

For long-term storage, *E. coli* or *S. cerevisiae* strains were grown in the appropriate selective medium and supplemented with 15 % (v/v) glycerol final concentration before being frozen and stored at -80 °C.

4.2.12 Isolation of plasmid DNA from *E. coli*

E. coli cells bearing the plasmid of interest were grown in LB medium containing the appropriate antibiotics at 37 °C with constant shaking overnight. Cells were collected by centrifugation and plasmid DNA was isolated using the E.Z.N.A. Plasmid DNA Mini Kit I according to the manufacturers' instructions. Elution was usually done in 50 µl.

4.2.13 DNA sequencing

Custom DNA Sanger Sequencing was done by the company Eurofins. Therefore, purified plasmid DNA with a concentration of 50-100 ng/µl or purified PCR products with a concentration of 1-10 ng/µl, depending on the size, were either sent together with 5 µM of the desired primer (LightRun, 10 µl total volume) or a standard primer from the company was used (SupremeRun, 15-20 µl total volume). Sequencing results were analyzed using Benchling.

4.3 Media and growth conditions

4.3.1 *Escherichia coli*

E. coli cells were grown in Luria-Bertani (LB) medium containing 0.5 % (w/v) yeast extract, 1 % (w/v) tryptone and 1 % (w/v) sodium chloride. For agar plates, additionally 2 % (w/v) bacto-agar was added. A preculture of *E. coli* was started by resuspending some cells from a plate or glycerol stock in liquid LB-medium and cells were grown overnight at 37 °C with agitation at 180 rpm. If necessary, the medium contained antibiotics such as 100 µg/ml ampicillin, 25 µg/ml chloramphenicol or 30 µl/ml kanamycin for selection.

4.3.2 IPTG induction

Protein expression was done in *E. coli* BL21 cells containing the IPTG inducible T7 RNA polymerase gene. Therefore, a preculture was diluted to an optical density at 600 nm (OD_{600}) of 0.2 in LB medium containing the appropriate antibiotics. Cells were grown at 37 °C until

their exponential growth phase at OD_{600} of ~0.6. To induce protein expression, 1 mM IPTG final concentration was added, and cells were grown at 18 °C and 180 rpm overnight.

4.3.3 *Saccharomyces cerevisiae*

S. cerevisiae strains were grown in complete (YP) medium containing 1 % (w/v) bacto-yeast extract and 2 % (w/v) bacto-peptone or synthetic (SD) medium, both including 2 % (w/v) glucose, 2 % (w/v) galactose or 2 % (w/v) raffinose. SD medium was composed of 0.67 % (w/v) bacto-yeast nitrogen base without amino acids further supplemented with 0.002 % (w/v) L-arginine, 0.001 % (w/v) L-histidine, 0.006 % (w/v) L-isoleucine, 0.006 % (w/v) L-leucine, 0.004 % (w/v) L-lysine, 0.001 % (w/v) L-methionine, 0.006 % (w/v) L-phenylalanine, 0.005 % (w/v) L-threonine, 0.004 % (w/v) L-tryptophan, 0.004 % (w/v) uracil, and 0.002 % (w/v) adenine, as appropriate. For solid plates, additionally 2 % (w/v) bacto-agar was added. Yeast cultures were started transferring some cells from a fresh plate or a glycerol stock to the desired liquid medium and cells were grown overnight at 30 °C with agitation at 180 rpm. The next day, the preculture was diluted in the desired medium to an OD_{600} of 0.25 and grown at 30 °C and 180 rpm agitation to OD_{600} ~0.8-1. If necessary, 10 µg/ml tetracycline was added to the medium to prevent bacterial growth.

4.3.4 Mating and sporulation

In order to cross haploid yeast cells, two strains with opposing mating types (*MATa* and *MATα*) were mixed on YPD. After incubation for 1 day at 30 °C, cells were replica-plated to a plate selecting for one marker per strain to allow only diploid cells to grow. After 2-3 days, diploids were picked and grown on the same medium for two more days. For sporulation, cells were freshly grown on YPD for 1 day and a small amount was transferred to liquid sporulation medium. After ~5 days at 25 °C, formation of tetrads was verified by light microscopy. To enzymatically digest the asci, 500 µl of the culture were centrifuged shortly for ~10 sec, the pellet was resuspended in 100 µl Zymolyase mix, and the sample was incubated at room temperature for 5 min. 25 µl of the digest were pipetted on a YPD plate and tetrads were dissected using a light microscope with micromanipulator.

4.5 Biochemical and immunological techniques

4.5.1 Protein sample preparation

E. coli and *S. cerevisiae* were grown in liquid medium supplemented with the appropriate antibiotics until the desired OD_{600} (see 4.3) and harvested by centrifugation at 4,000 rpm for *E. coli* and 3,000 rpm for *S. cerevisiae*. Cells were washed once with water and the pellet was frozen in liquid nitrogen prior to storage at -80 °C. Depending on the experiment, different protein extraction methods were applied.

4.5.1.1 Protein extraction under denaturing conditions (boiled extract)

In order to extract both soluble and insoluble proteins under denaturing conditions, cell pellets were resuspended in 15 µl 1x Laemmli lysis buffer (5x LLB: 0.3125 M Tris pH 6.8, 10 % SDS, 50 % glycerol, 0.00025 % bromophenol blue, 10 % β-mercaptoethanol) per OD_{600} unit. Samples were boiled at 99 °C for 5 minutes and centrifuged at 15,000 rpm for 1 minute to sediment the cell debris. Supernatant was ready to be used for analysis by SDS-PAGE.

4.5.1.2 Protein extraction by glass bead lysis (native extract)

In the case of small pellets, native protein extracts were obtained by lysing the cells with glass beads (≤ 106 µm for bacterial cells and 425-600 µm for yeast cells). Cells were resuspended in 15 µl cold *E. coli* lysis buffer (50 mM Tris-HCl pH 7.4, 150 mM NaCl, 5 mM $MgCl_2$, 15 % glycerol) supplemented with 0.1 % Triton X-100, 1x protease inhibitor, 10 µg/ml DNase I, 1 mg/ml lysozyme) or Yeast lysis buffer (50 mM Tris-HCl pH 7.5, 150 mM NaCl, 5 mM $MgCl_2$, 15 % glycerol) supplemented with 1x protease inhibitor per OD_{600} unit and 500 µl glass beads/ml suspension were added. Samples were incubated for 30 minutes on ice and vortexed for one minute at 4 °C. Extracts were centrifuged at 17,000 rpm for 10 minutes at 4 °C and the supernatant (crude extract) was transferred to a pre-cooled fresh tube. Proteins were directly used for downstream applications or frozen in liquid nitrogen and stored at -80 °C.

4.5.1.3 Protein extraction by sonication

For protein extraction of larger *E. coli* pellets, cells were resuspended in 15 µl *E. coli* lysis buffer (see above) per 1 OD_{600} unit. Lysates were incubated for 30 minutes on ice and sonicated for 6-8 minutes using short pulses (10 sec) with 10-sec interruptions. After sonication, cell debris was sedimented by centrifugation at 20,000 rpm and 4 °C for 45 minutes. Supernatant was transferred to a pre-cooled fresh tube and proteins were directly subjected to protein purification methods.

4.5.1.4 Protein extraction using a Mixer Mill MM400

For larger yeast pellets, cells were mechanically lysed with the help of the Mixer Mill MM400. The frozen cell pellet was placed in a grinding jar containing a grinding ball pre-cooled with liquid nitrogen. Radial oscillations were done in a horizontal position for 1 min at 30 Hz. Due to the short grinding time, samples did not warm up. The cell powder was transferred to a pre-cooled fresh tube and incubated with 2 ml Yeast lysis buffer (see above) per g wet weight for 30 minutes at 4 °C, rotating. Cell debris was removed by centrifugation at 20,000 rpm for 30 minutes at 4 °C and proteins were directly subjected to protein purification methods.

4.5.2 Protein purification

All purification steps were carried out at 4 °C. All buffers and solutions as well as materials were pre-cooled before getting in contact with any protein-containing solution. All purified proteins were analyzed by Western Blot or Coomassie staining before being used in downstream applications. For estimation of protein concentration, a Nanodrop spectrophotometer was used.

4.5.2.1 Purification of proteins from E. coli

Proteins were extracted using one of the methods described above. The crude extract was incubated with Ni^{2+}-NTA resin equilibrated with Wash buffer (50 mM Tris-HCl pH 7.4, 150 mM NaCl, 20 mM imidazole) for 1.5 hours at 4 °C, rotating. The resin was washed

3 times with 10 column bed volumes (CV) Wash buffer and bound proteins were eluted in two steps with each 5 ml Elution buffer (50 mM Tris-HCl pH 7.4, 150 mM NaCl, 15 % glycerol, 500 mM imidazole) for 15 minutes, rotating. In the case of Senp1, all buffers were additionally supplemented with 1-2 mM DTT and 1 mM EDTA. Afterwards, proteins were concentrated using Vivaspin Turbo 4 centrifugal concentrators (10,000 MWCO, Sartorius), aliquoted and snap frozen in liquid nitrogen. For proteins tagged with 8His-SUMO1, the following protocol was used to cleave the tag. After elution, samples were pooled and subjected to dialysis in Dialysis buffer (50 mM Tris-HCl pH 7.4, 150 mM NaCl) overnight to get rid of high imidazole concentrations and small molecules. Simultaneously, the 8His-SUMO1 tag was cleaved using Senp1 enzyme to obtain the pure protein. The next day, the cleaved 8His-SUMO1 tag, unspecific material and 6His-tagged Senp1 enzyme were removed by incubation for 1-2 hours with Ni^{2+}-NTA resin followed by incubation with TALON beads. No washing or elution steps were necessary at this point, unbound proteins simply needed to be collected after binding. Proteins were concentrated as described above, snap frozen in liquid nitrogen and stored at -80 °C.

4.5.2.2 Purification of 15S complexes from yeast – short version

For the purification of 15S complexes, the yeast strain MO27 (*pre4ΔC19 FLAG-6His-UMP1 blm10Δ* P_{GAL1}*-PBA1* P_{GAL1}*-PBA2*) was used. Cells were grown in complete medium (YP) containing 2 % galactose, harvested and pellets were frozen in liquid nitrogen. The cells were ground to powder using a Mixer and Mill MM400 (Retsch) for 1 min at 30 Hz. Afterwards, powder was incubated with 2 ml Yeast lysis buffer (50 mM Tris-HCl pH 7.5, 150 mM NaCl, 5 mM $MgCl_2$, 15 % glycerol) supplemented with 10 mM imidazole and protease inhibitors (cOmplete, EDTA-free, Roche) per g wet weight for 30 minutes at 4 °C, rotating. Cell debris was removed by centrifugation at 20,000 rpm for 30 min at 4 °C. Complexes were pulled down by their N-terminally FLAG-6His tagged Ump1. Therefore, the supernatant was incubated with Ni^{2+}-NTA resin equilibrated in Yeast lysis buffer for 2 hours at 4 °C with agitation. The resin was washed 3 times with 10 CV of Yeast lysis buffer supplemented with 10 mM imidazole. Bound complexes were eluted by enzymatic cleavage of the N-terminal FLAG-6His-tag using AcTEV™ protease (Thermo Fisher) in Protease buffer (50 mM Tris-HCl pH 7.5, 1 mM DTT, 0.5 mM EDTA) overnight. The latter

case provides simultaneously an additional highly specific purification step by removing material that non-specifically bound to the Ni^{2+} resin. After TEV cleavage, 15S complexes were concentrated using Vivaspin 6 centrifugal concentrators (50,000 MWCO, Sartorius) and directly used for downstream applications.

4.5.2.2 Purification of 15S and 20S complexes from yeast – long version

For the purification of 15S and 20S complexes, the yeast strains MO27 (*pre4ΔC19 FLAG-6His-UMP1 blm10Δ* P_{GAL1}*-PBA1* P_{GAL1}*-PBA2*) and MO24 (*PRE1-FLAG-6His*) were used, respectively. Cells were grown in complete medium (YP) containing 2 % galactose in case of MO27 cells and 2 % glucose for MO24 cells, harvested and pellets were frozen in liquid nitrogen. The cells were ground to powder using mortar and pestle. Afterwards, powder was incubated with 2 ml Buffer A (50 mM sodium phosphate, pH 8.0, 150 mM NaCl, 10 % glycerol) supplemented with protease inhibitors per g wet weight until powder was completely dissolved. Cell debris was removed by centrifugation at 20,000 rpm for 30 min at 4 °C. After incubation with Ni^{2+}-NTA resin for 1 hour at 4 °C, beads were washed 1x with Buffer A and 1x with Buffer B (50 mM sodium phosphate, pH 6.0, 150 mM NaCl, 10 % glycerol, 10 mM imidazole). Elution was done 3x in 1 ml Buffer C (Buffer A + 400 mM imidazole). Afterwards, eluted material was incubated with FLAG resin for 1 hour at 4 °C, washed 1x in Buffer A and eluted from the resin 3x in Buffer A containing FLAG peptide. Eluted material was snap frozen in liquid nitrogen and stored at -80 °C prior to usage.

4.5.3 Production of antisera against yeast proteasome components

Yeast proteasome components were expressed in *E. coli* and purification of representative proteins without tag was done as described above (see 4.5.2.1). To ensure the highest possible specificity of the antisera, pre-immune blood sera of different rabbits were tested concerning the background cross-reactivity to unspecific yeast proteins. Therefore, boiled extracts from wild-type yeast cells (JD47-13C) were separated by SDS-PAGE and after western blotting, each lane was probed with the individual rabbit blood sera in two different concentrations (1:1000 and 1:5000). Subsequent to washing and incubation with anti-rabbit secondary antibody, the membrane was developed, signals were analyzed, and one rabbit

was chosen for each antigen. Samples of 10 mg/ml in 100 µl total volume containing the desired protein in buffer (50 mM Tris-HCl pH 7.4, 150 mM NaCl, 5 mM $MgCl_2$, 20 mM imidazole) were sent for antibody production to Pineda Antikörper-Service Berlin (http://www.pineda-abservice.de).

4.5.4 Specificity improvement of antibodies against yeast proteasome components

To improve the specificity of antisera against yeast proteasome components, yeast cells lacking the desired protein were used. For nonessential proteasome genes such as *PBA3*, deletion strains were used. For essential genes such as *PUP2* and *PRE5*, shut off strains were used. Thereby, subunits were expressed under control of the galactose-inducible promoter P_{GALS}. After cells were grown in galactose, they were shifted to glucose medium overnight to repress transcription of the desired gene. The next day, cells were harvested, and proteins were extracted by boiling in 1x Laemmli lysis buffer (see above). 2 OD of the boiled extracts were loaded per lane on SDS-PAGE and proteins were transferred to a PVDF membrane. 1 ml of the respective antiserum was incubated with the membrane in 50 ml falcon tubes at 4 °C overnight to remove all material binding nonspecifically to yeast proteins. The next day, antiserum was transferred to another membrane, which treated the same way for several more hours. In the evening the antibody was removed and stored in aliquots at -80 °C.

4.5.5 Affinity purification of polyclonal antibodies from serum

To purify produced antisera, 250 µg of the *E. coli* purified target protein was loaded on SDS-PAGE containing only one well. Proteins were transferred to a methanol activated PVDF membrane and fixed on the membrane by boiling in water for 30 minutes. Ponceau S staining was performed for 5 minutes to visualize the band of the target protein, which was cut and incubated in blocking solution (5 % milk-TBST (10 mM Tris pH 8.0, 150 mM NaCl, 0.05 % Tween-20)) for 1 hour at room temperature. Afterwards, 1 ml immune serum was diluted in 5 % milk-TBST 1/25 and incubated with the membrane at 4 °C overnight. The next day, membrane was washed in TBST, and antibodies were eluted two times for three minutes using 1 ml Glycine elution buffer pH 2.8 (0.1 M glycine, 0.5 M NaCl, 0.05 %

Tween-20). For neutralization, antibody solution was transferred to 1 M Tris buffer pH 8.1 containing 10 % BSA and 6.5 % NaN_3. Finally, antibody was stored in aliquots at -80 °C.

4.5.6 *In vitro* binding assay using Ni-NTA pulldown

Ni-NTA Superflow resin (QIAGEN) was equilibrated 3x with 20 column volumes (CV) Lysis buffer. Pre-purified proteins or native extracts of *E. coli* cells transformed either with a plasmid expressing a Ump1-6His variant or an empty control vector were incubated with the resin in a total volume of 20 CV for 1 h at 4 °C, rotating. Afterwards, unspecific proteins were removed by washing 4x with Lysis buffer supplemented with 20 mM imidazole. Purified authentic β7 or β1 test variants were added in a total amount of 20 CV and binding was allowed for 1 h at 4 °C with rotation. Washing was performed as described above, and samples were transferred to fresh tubes. Proteins were eluted in Lysis buffer containing 250-500 mM imidazole for 30-60 min at 4 °C with shaking. Samples were analyzed by 12 % SDS-PAGE and western blotting.

4.5.7 *In vitro* binding assay on amylose resin

Amylose resin (New England Biolabs) was equilibrated 2x with 20 CV Buffer 1 (50 mM Tris-HCl pH 7.4, 150 mM NaCl, 10 % Glycerol, 1 mM DTT). Native protein extracts of 50 OD cells expressing MBP-β7-CTE or MBP control were incubated with the beads for 1.5 hours at 4 °C, rotating. Afterwards, samples were washed 2x with 20 CV Buffer 1 and 3x with 20 CV Buffer 2 (Buffer 1 + 1 mg/ml BSA). Binding was proceeded with native protein extracts of 50 OD cells expressing different Ump1 variants for 90 min at 4 °C, rotating. After washing 1x with 10 CV Buffer 2 and 2x with 10 CV Buffer 1, proteins were eluted in 40 µl 1x LLB at 99 °C for 5 min. Samples were analyzed by 12 % SDS-PAGE and immunoblot.

4.5.8 *In vitro* binding assay on HA resin

Equilibrated HA resin was incubated with 250 µg purified 8His-SUMO1-Pba3-Pba4-HA (protein purification from *E. coli* see 4.5.2.1) in a total volume of 1 ml Binding buffer (50

mM Tris-HCl pH 7.4, 150 mM NaCl, 5 mM EDTA, 1 % Triton X-100) for 1 hour at 4 °C. Afterwards, resin was washed 3x with 750 µl Binding buffer and shortly vortexed. 50 µg of purified test proteins (8His-SUMO1-α5/-α6/-α7/-Pba1-Pba2-FLAG) were added to the respective tubes together with 2 µl Senp1 enzyme to remove the 8His-SUMO1 tag. In a total volume of 1 ml Binding buffer, incubation was pursued for 1 hour at 4 °C. After washing 3x with 750 µl Binding buffer, samples were shortly vortexed, and elution was done in 100 µl Elution buffer (Binding buffer + 100 µM HA peptide) for 30 min at 4 °C. Samples were mixed with Laemmli lysis buffer and were ready to be analyzed by SDS-PAGE.

4.5.9 Fluorescence microscopy-based on-bead binding assay

Ni-NTA Superflow resin (QIAGEN) was equilibrated 3x with Binding buffer (50 mM Tris-HCl pH 7.4, 150 mM NaCl. 15 % glycerol), vortexed shortly and centrifuged at ~3,200 rpm for 30 secs at RT. Ump1-6His variant-containing or control protein extracts (EV) were incubated with the resin for 1 hour at 4 °C, rotating. Afterwards, unspecific proteins were removed 4x using Binding buffer containing 20 mM imidazole. Protein amounts of different mNeongreen (NG) fusion protein extracts were determined and adjusted by measuring the fluorescence using the Tecan Infinite F200 pro (filter 485 nm, 535 nm) prior to addition to the binding reaction. Binding was allowed for 1 hour at 4 °C with rotation. Proper washing was performed as described above. Samples were analyzed by fluorescence microscopy, which was carried out with the fluorescence microscope Zeiss Axioplan 2 and with the software AxioVision Rel 4.7 (Zeiss, Jena, Germany). For microscopy, a magnification of 10x was used, provided by the objective Zeiss Plan-Neofluar 10x/0.30 Ph1 (DIC I). For GFP, the following filter was used: F41-054 HQ-Cy2 HQ480/40 (excitation) Q505LP HQ527/30 (emission). Exposure times for image taking were 12 ms for brightfield and 1.5 s for GFP. For quantitative evaluation, images were analyzed using Fiji (ImageJ v1.53f, https://ij.imjoy.io).

4.5.10 Complex I to 15S PC shift assay

To check whether Pba1-Pba2 is capable of driving the formation from 15S PCs from Complex I, a shift assay was performed. Therefore, yeast native extracts of *pba1*Δ *UMP1*-

HA cells were mixed with native extracts of P_{GAL1}*PBA1* P_{GAL1}*PBA2* cells or different amounts of Pba1-Pba2 purified from *E. coli* containing a tag on the N- or C-terminus of the protein. Samples were incubated at room temperature or 4 °C for 12 minutes and analyzed by native-PAGE and anti-HA western blotting to detect Ump1-containing Complex I and 15S complexes.

4.5.11 *In vitro* assembly of Complex II

20 µg of proteins purified from *E. coli* (8His-SUMO1-α5/-α6/-α7/-Pba1-Pba2-FLAG-/Pba3-Pba4-HA) were mixed and incubated for 90 minutes at 4 °C in a total volume of 100 µl filled up with 26S Buffer (50 mM Tris-HCl pH 7.5, 1 mM DTT, 5 mM $MgCl_2$, 2 mM ATP, 15 % (v/v) glycerol). Additionally, samples contained 1 µl Senp1 enzyme to cleave the 8His-SUMO1 tag. Afterwards, samples were mixed with 1x Laemmli lysis buffer (5x LLB: 0.3125 M Tris pH 6.8, 10 % SDS, 50 % glycerol, 0.00025 % bromophenol blue, 10 % β-mercaptoethanol) or 1x Native buffer (4x NB: 240 mM Tris-HCl pH 8.8, 0.04 % (w/v) bromophenol blue, 80 % (v/v) glycerol) and analyzed by SDS-PAGE or native-PAGE, respectively.

4.5.12 *In vitro* dimerization of 15S precursor complexes

To check for dimerization of 15S PCs and resulting proteasomal activity, the release of fluorescent 7-amino-4-methylcoumarin (AMC) after cleavage from a specific substrate was measured. Specifically, the chymotryptic activity assay was based on the enzymatic processing of the substrate Suc-LLVY-AMC (N-succinyl-leucine-leucine-valine-tyrosine-AMC) (Kisselev and Goldberg, 2005). 10 or 20 µg of purified 15S PC and 1 or 25 µg of purified β subunits (β7, β1, β5 and β6) were mixed. 1 µl PMSF and 26S buffer (50 mM Tris-HCl pH 7.5, 1 mM DTT, 5 mM $MgCl_2$, 2mM ATP, 15 % (v/v) glycerol) were added to a total volume of 90 µl. Directly before the measurement was started, 10 µl substrate of a 1:10 diluted stock solution (10 mg/ml) were added. For a negative control 15S PC and β subunits were tested separately. The reactions were set up in a 96 well plate and measured using a fluorimeter (FluoStar Galaxy). Afterwards, samples were additionally analyzed by native- as well as SDS-PAGE and western blotting.

4.5.13 Protein gel electrophoresis

4.5.13.1 Denaturing polyacrylamide gel electrophoresis

Sodium dodecyl polyacrylamide gel electrophoresis (SDS-PAGE) was performed to separate proteins according to their size. Usually 12 % polyacrylamide resolving gels (12 % (w/v) acrylamide/bisacrylamide (37:5:1), 375 mM Tris-HCl pH 8.8, 0.1 % (w/v) SDS, 0.05 % (w/v) APS, TEMED) were used with 4 % stacking gels (4 % (w/v) acrylamide/bisacrylamide (37:5:1), 125 mM Tris-HCl pH 6.8, 0.1 % (w/v) SDS, 0.05 % (w/v) APS, TEMED). Samples were mixed with Laemmli lysis buffer and incubated at 99 °C for 5 min, before being loaded into the gel. Laemmli running buffer (25 mM Tris-HCl pH 8.3, 192 mM glycine, 0.1 % (w/v) SDS) was added to the cationic chamber and Laemmli running buffer with sodium acetate (0.1 M NaOAc) was added to the anionic chamber. PageRuler Plus Prestained protein ladder (Thermo Scientific) was used as marker for the molecular weight of separated proteins. The gels were exposed to an electric field and allowed to run until the bromophenol blue (front marker) reached the bottom of the gel (typically 90 V for about 2 hours).

4.5.13.2 Native polyacrylamide gel electrophoresis

Native polyacrylamide gel electrophoresis (native-PAGE) was performed for separating proteins under native conditions according to their size-charge ratio. Samples were kept on ice and mixed with cold Native buffer (4x NB: 240 mM Tris-HCl pH 8.8, 0.04 % (w/v) bromophenol blue, 80 % (v/v) glycerol). For native-PAGE, either self-made gels (6 % resolving gel: 6 % (w/v) acrylamide/bisacrylamide (37:5:1), 2.5 % (w/v) sucrose, 1x TBE (90 mM Tris, 80 mM boric acid, 0.1 mM EDTA pH 8.3), 0.05 % (w/v) APS, TEMED; 2.5 % stacking gel: 2.5 % (w/v) acrylamide/bisacrylamide (37:5:1), 2.5 % (w/v) sucrose, 50 mM (w/v) Tris, 0.1 % (w/v) APS, TEMED) or cold pre-casted gels (FastGene® PAGE Gels 4-12 % or 4-20 % from Nippon Genetics or nativePAGE™ 4-16 % Bis-Tris Gels from Invitrogen) were used. In the case of self-made and Invitrogen gels, cold Laemmli running buffer without SDS (25 mM Tris-HCl pH 8.3, 192 mM glycine) and for Nippon gels MOPS buffer (50 mM Tris, 50 mM MOPS, 1 mM EDTA) was used in both the cationic and anionic

chamber. Native-PAGE was performed in the cold room at 50 V/gel overnight or 16 mA/gel for up to 5 hours.

4.5.14 Coomassie staining

For visualization of proteins in a polyacrylamide gel, Coomassie Brilliant Blue R-250 (CBB-R250) staining was performed. Protein fixation and staining was typically carried out in 45 % (v/v) methanol, 10 % (v/v) acetic acid and 0.1 % CBB-R250 for 1 hour at room temperature. Destaining of the background was done up to 24 hours with 20 % (v/v) methanol and 10 % (v/v) acetic acid.

4.5.15 Silver staining

In comparison to the Coomassie staining, a silver staining of proteins in a polyacrylamide gel is more sensitive. After electrophoresis, the proteins in the gel were fixed in 40 % (v/v) ethanol, 10 % (v/v) acetic acid for at least 30 min. Following fixation, the gels were sensitized in 30 % (v/v) ethanol, 6.8 % (w/v) sodium acetate and 0.2 % (w/v) sodium thiosulfate for another 30 min. The gel was rinsed three times with Milli-Q water for 5 min and the staining was done using 0.5 % (w/v) silver nitrate for 30 min. Afterwards, the gel was rinsed once in Milli-Q water for 5 min and transferred to the developer solution consisting of 2.5 % (w/v) sodium carbonate, 0.05 % (v/v) formaldehyde and 0.0024 % (w/v) sodium thiosulphate. When the desired staining intensity was reached, the reaction was stopped with 0.5 % (w/v) glycine for 30 min and the gel was stored in Milli-Q water at 4 °C.

4.5.16 Western Blot analysis

After samples were separated by electrophoresis, specific proteins were identified by western blotting with the help of antibodies. Proteins were transferred to a methanol activated polyvinylidene fluoride (PVDF) membrane (pore size 0.45 µm, GE Healthcare) or nitrocellulose membrane (pore size 0.2 µm, GE Healthcare). Semi-dry blotting was performed for 1-2 hours (depending on the thickness of the gel and the size of the proteins

to be transferred) at 0.8 mA/cm^2 in Transfer buffer (25 mM Tris-HCl pH 8.3, 192 mM glycine, 0.1 % (w/v) SDS, 20 % (v/v) methanol). For native gels, eventually a 15-minute pre-incubation in Transfer buffer containing 0.2 % (w/v) SDS was done to allow the binding of SDS ions to improve the transfer efficiency of protein complexes. Afterwards, the membrane was incubated in Blocking solution (5 % (w/v) milk powder in PBS (phosphate-buffered saline: 137 mM NaCl, 2.7 mM KCl, 8.1 mM Na_2HPO_4, 1.5 mM KH_2PO_4, pH 7.4)) for 30-60 minutes at room temperature to prevent unspecific binding of antibodies. The primary antibody was diluted in blocking solution and applied overnight at 4 °C. The next day, the membrane was washed three times with PBS and the secondary antibody diluted in blocking solution was applied for 1 hour at room temperature. After incubation with the secondary antibody, membrane was washed again three times with PBS. In the case of fluorophore-bearing antibodies, the membrane was analyzed by using a LI-COR Odyssey Imager. The detections were made at 700 nm (shown in red) and 800 nm (shown in green). For peroxidase-coupled antibodies (POD), the membrane was detected using SuperSignal West Femto substrate from Thermo Scientific. The membrane was placed in a cassette and covered with an X-ray film (Fujifilm). After the desired exposure time, the film was placed in a developing machine AGFA Curix 60 and, by virtue of developer and fixer, the bands became visible.

4.5.17 Total protein staining

The Revert™ 700 Total Protein Stain from LI-COR is an alternative staining method, which can be quantified with the LI-COR Odyssey Imager and is done immediately after transfer and before blocking. The membrane was incubated in Revert™ Total Protein Stain solution for 5 minutes at room temperature. Then the membrane was washed with Revert™ 700 Wash solution (6.7 % (v/v) acetic acid, 30 % (v/v) methanol) for 5 minutes at room temperature. The total protein stain was imaged with the LI-COR Odyssey Imager in the 700 nm channel. After imaging, the staining was removed by incubation in Revert™ destaining solution (0.1 % sodium hydroxide, 30 % (v/v) methanol) for 10 minutes.

4.5.18 Ponceau staining

After transfer, membrane was shortly washed in PBS and, in the case of PVDF membranes, incubated in methanol for 5 minutes. Ponceau staining was done for 5 minutes at room temperature, and afterwards, the background was destained in PBS until the desired result was reached. Ponceau staining was removed by incubation in 0.2 M sodium hydroxide for 5 minutes. The membrane was shortly rinsed in PBS before being incubated in blocking solution.

4.5.19 Stripping of membranes

When detection of different antigens was necessary, antibodies were removed by incubating the respective blot two times for 15 minutes in 0.2 M sodium hydroxide. Afterwards, the membrane was rinsed three times for 15 minutes in PBS before being blocked and probed with the next antibody.

References

Abi Habib, J., Lesenfants, J., Vigneron, N., and Van den Eynde, BJ. (2022). Functional Differences between Proteasome Subtypes. Cells *11*, 421.

Amaya, C., Fader, CM., and Colombo, MI. (2015). Autophagy and proteins involved in vesicular trafficking. FEBS Lett. *589*, 3343–3353.

Amerik, AY., and Hochstrasser, M. (2004). Mechanism and function of deubiquitinating enzymes. Biochim. Biophys. Acta - Mol. Cell Res. *1695*, 189–207.

Amm, I., Sommer, T., and Wolf, DH. (2014). Protein quality control and elimination of protein waste: The role of the ubiquitin-proteasome system. Biochim. Biophys. Acta - Mol. Cell Res. *1843*, 182–196.

Arendt, CS., and Hochstrasser, M. (1999). Eukaryotic 20S proteasome catalytic subunit propeptides prevent active site inactivation by N-terminal acetylation and promote particle assembly. EMBO J. *18*, 3575–3585.

Arndt, V., Rogon, C., and Höhfeld, J. (2007). To be, or not to be - molecular chaperones in protein degradation. Cell. Mol. Life. Sci. *64*, 2525–2541.

Bartel, B., Wünning, I., and Varshavsky, A. (1990). The recognition component of the N-end rule pathway. EMBO J. *9*, 3179–3189.

Bashore, C., Dambacher, CM., Goodall, EA., Matyskiela, ME., Lander, GC., and Martin, A. (2015). Ubp6 deubiquitinase controls conformational dynamics and substrate degradation of the 26S proteasome. Nat. Struct. Mol. Biol. *22*, 712–719.

Baumeister, W., Walz, J., Zühl, F., and Seemüller, E. (1998). The proteasome: paradigm of a self-compartmentalizing protease. Cell *92*, 367–380.

Berndsen, CE., and Wolberger, C. (2014). New insights into ubiquitin E3 ligase mechanism. Nat. Struct. Mol. Biol. *21*, 301–307.

Beyer, A (1997). Sequence analysis of the AAA protein family. Protein Sci., *6*, 2043-2058.

Borissenko, L., and Groll, M. (2007). Diversity of proteasomal missions: Fine tuning of the immune response. Biol. Chem. *388*, 947–955.

Brannigan, JA., Dodson, G., Duggleby, HJ., Moody, PCE., Smith, JL., Tomchick, DR., and Murzin, AG. (1995). A protein catalytic framework with an N-terminal nucleophile is capable of self-activation. Nature *378*, 416–419.

Budenholzer, L., Cheng, CL., Li, Y., and Hochstrasser, M. (2017). Proteasome Structure and Assembly. J. Mol. Biol. *429*, 3500.

Burri, L., Höckendorff, J., Boehm, U., Klamp, T., Dohmen, RJ., and Lévy, F. (2000). Identification and characterization of a mammalian protein interacting with 20S proteasome precursors. Proc. Natl. Acad. Sci. U. S. A. *97*, 10348–10353.

Cagney, G., Uetz, P., and Fields, S. (2001). Two-hybrid analysis of the *Saccharomyces cerevisiae* 26S proteasome. Physiol. Genomics *7*, 27–34.

Canelas, AB. *et al*. (2010). Integrated multilaboratory systems biology reveals differences in protein metabolism between two reference yeast strains. Nat. Commun. *1*, 1–8.

Chen, P., and Hochstrasser, M. (1995). Biogenesis, structure and function of the yeast 20S proteasome. EMBO J. *14*, 2620.

Chen, P., and Hochstrasser, M. (1996). Autocatalytic Subunit Processing Couples Active Site Formation in the 20S Proteasome to Completion of Assembly. Cell *86*, 961–972.

Chitra, S., Nalini, G., and Rajasekhar, G. (2012). The ubiquitin proteasome system and efficacy of proteasome inhibitors in diseases. Int. J. Rheum. Dis. *15*, 249–260.

Chu-Ping, M., Vu, JH., Proske, RJ., Slaughter, CA., and DeMartino, GN. (1994). Identification, purification, and characterization of a high molecular weight, ATP-dependent activator (PA700) of the 20 S proteasome. J. Biol. Chem. *269*, 3539–3547.

Cozzi, M., and Ferrari, V. (2022). Autophagy Dysfunction in ALS: from Transport to Protein Degradation. J. Mol. Neurosci. *72*, 1456.

Crawford, LJ., Walker, B., and Irvine, AE. (2011). Proteasome inhibitors in cancer therapy. J. Cell. Commun. Signal *5*, 101–110.

Dikic, I., Wakatsuki, S., and Walters, KJ. (2009). Ubiquitin binding domains - from structures to functions. Nat. Rev. Mol. Cell Biol. *10*, 659.

Ditzel, L., Huber, R., Mann, K., Heinemeyer, W., Wolf, DH., and Groll, M. (1998). Conformational constraints for protein self-cleavage in the proteasome. J. Mol. Biol. *279*, 1187–1191.

Djaballah, H., and Rivett, J. (1992). Peptidylglutamyl-peptide hydrolase activity of the multicatalytic proteinase complex: evidence for a new high-affinity site, analysis of cooperative kinetics, and the effect of manganese ions. Biochemistry *31*, 4133–4141.

Dohmen, RJ., Willers, I., and Marques, AJ. (2007). Biting the hand that feeds: Rpn4-dependent feedback regulation of proteasome function. Biochim. Biophys. Acta - Mol. Cell Res. *1773*, 1599–1604.

Ellgaard, L., and Helenius, A. (2003). Quality control in the endoplasmic reticulum. Nat. Rev. Mol. Cell Biol. *4*, 181–191.

Elsasser, S., Gali, RR., Schwikart, M., Larsen, CN., Leggett, DS., Müller, B., Feng, MT., Tübing, F., Dittmar, GAG., and Finley, D. (2002). Proteasome subunit Rpn1 binds ubiquitin-like protein domains. Nat. Cell Biol. *4*, 725–730.

Emori, Y., Tsukahara, T., Kawasaki, H., Ishiura, S., Sugita, H., and Suzuki, K. (1991). Molecular cloning and functional analysis of three subunits of yeast proteasome. Mol. Cell Biol. *11*, 344–353.

Farré, JC., and Subramani, S. (2004). Peroxisome turnover by micropexophagy: an autophagy-related process. Trends Cell Biol. *14*, 515–523.

Finley, D., Ulrich, HD., Sommer, T., and Kaiser, P. (2012). The ubiquitin-proteasome system of Saccharomyces cerevisiae. Genetics *192*, 319–360.

Fleming, JA., Lightcap, ES., Sadis, S., Thoroddsen, V., Bulawa, CE., and Blackman, RK. (2002). Complementary whole-genome technologies reveal the cellular response to proteasome inhibition by PS-341. Proc. Natl. Acad. Sci. U. S. A. *99*, 1461–1466.

Frankland-Searby, S., and Bhaumik, SR. (2012). The 26S proteasome complex: an attractive target for cancer therapy. Biochim. Biophys. Acta *1825*, 64–76.

Frankowska, N., Lisowska, K., and Witkowski, JM. (2022). Proteolysis dysfunction in the process of aging and age-related diseases. Front. Aging *3*, 1-16.

Frentzel, S., Pesold-Hurt, B., Seelig, A., and Kloetzel, PM. (1994). 20 S proteasomes are assembled via distinct precursor complexes processing of LMP2 and LMP7 proproteins takes place in 13-16 S preproteasome complexes. J. Mol. Biol. *236*, 975–981.

Fricke, B., Heink, S., Steffen, J., Kloetzel, PM., and Krüger, E. (2007). The proteasome maturation protein POMP facilitates major steps of 20S proteasome formation at the endoplasmic reticulum. EMBO Rep. *8*, 1170–1175.

Fulop, T., Larbi, A., Kotb, R., and Pawelec, G. (2013). Immunology of Aging and Cancer Development. Interdiscip. Top. Gerontol. *38*, 38–48.

Galluzzi, L. *et al*. (2017). Molecular definitions of autophagy and related processes. EMBO J. *36*, 1811.

Gerards, WLH., Enzlin, J., Häner, M., Hendriks, ILAM., Aebi, U., Bloemendal, H., and Boelens, W. (1997). The human alpha-type proteasomal subunit HsC8 forms a double ringlike structure, but does not assemble into proteasome-like particles with the beta-type subunits HsDelta or HsBPROS26. J. Biol. Chem. *272*, 10080–10086.

Glickman, MH., Rubin, DM., Fried, VA., and Finley, D. (1998). The regulatory particle of the *Saccharomyces cerevisiae* proteasome. Mol. Cell Biol. *18*, 3149–3162.

Goldberg, AL., and Wittes, RB. (1966). Genetic Code: Aspects of Organization. Science *153*, 420–424.

Gomez, TA., Kolawa, N., Gee, M., Sweredoski, MJ., and Deshaies, RJ. (2011). Identification of a functional docking site in the Rpn1 LRR domain for the UBA-UBL domain protein Ddi1. BMC Biol. *9*, 33.

Gottesman, S., Wickner, S., and Maurizi, MR. (1997). Protein quality control: triage by chaperones and proteases. Genes Dev. *11*, 815–823.

Groll, M., Bochtler, M., Brandstetter, H., Clausen, T., and Huber, R. (2005). Molecular Machines for Protein Degradation. ChemBioChem *6*, 222–256.

Groll, M., Ditzel, L., Löwe, J., Stock, D., Bochtler, M., Bartunik, HD., and Huber, R. (1997). Structure of 20S proteasome from yeast at 2.4Å resolution. Nature *386*, 463–471.

Groll, M., Glickman, MH., Finley, D., Bajorek, M., Köhler, A., Moroder, L., Rubin, DM., and Huber, R. (2000). A gated channel into the proteasome core particle. Nat. Struct. Biol. *7*, 1062–1067.

Groll, M., Heinemeyer, W., Jäger, S., Ullrich, T., Bochtler, M., Wolf, DH., and Huber, R. (1999). The catalytic sites of 20S proteasomes and their role in subunit maturation: a mutational and crystallographic study. Proc. Natl. Acad. Sci. U. S. A. *96*, 10976–10983.

Grüning, NM., Lehrach, H., and Ralser, M. (2010). Regulatory crosstalk of the metabolic network. Trends Biochem. Sci. *35*, 220–227.

Gundogdu, M., and Walden, H. (2019). Structural basis of generic versus specific E2–RING E3 interactions in protein ubiquitination. Protein Sci. *28*, 1758–1770.

Hahn, JS., Neef, DW., and Thiele, DJ. (2006). A stress regulatory network for co-ordinated activation of proteasome expression mediated by yeast heat shock transcription factor. Mol. Microbiol. *60*, 240–251.

Hammack, LJ., Panfair, D., and Kusmierczyk, AR. (2020). A novel proteasome assembly intermediate bypasses the need to form α-rings first. Biochem. Biophys. Res. Commun. *525*, 107–112.

Harrigan, JA., Jacq, X., Martin, NM., and Jackson, SP. (2018). Deubiquitylating enzymes and drug discovery: emerging opportunities. Nat. Rev. Drug. Discov. *17*, 57.

Hartl, FU., and Hayer-Hartl, M. (2009). Converging concepts of protein folding i*n vitro* and *in vivo*. Nat. Struct. Mol. Biol. *16*, 574–581.

Heinemeyer, W., Fischer, M., Krimmer, T., Stachon, U., and Wolf, DH. (1997). The active sites of the eukaryotic 20 S proteasome and their involvement in subunit precursor processing. J. Biol. Chem. *272*, 25200–25209.

Heinemeyer, W., Ramos, PC., and Dohmen, RJ. (2004). The ultimate nanoscale mincer: assembly, structure and active sites of the 20S proteasome core. Cell Mol. Life Sci. *61*, 1562-1578.

Hermanns, T., and Hofmann, K. (2019). Bacterial DUBs: deubiquitination beyond the seven classes. Biochem. Soc. Trans. *47*, 1857–1866.

Hermanns, T., Pichlo, C, Woiwode, I., Klopffleisch, K., Witting, KF., Ovaa, H., Baumann, U., and Hofmann, K. (2018). A family of unconventional deubiquitinases with modular chain specificity determinants. Nat. Commun. *9*, 1-13.

Hershko, A. (1996). Lessons from the discovery ofthe ubiquitin system. Trends. Biochem. Sci. *21*, 445–449.

Hershko, A., and Ciechanover, A. (1986). The ubiquitin pathway for the degradation of intracellular proteins. Prog. Nucleic Acid. Res. Mo.l Biol. *33*, 19–56.

Hershko, A., and Ciechanover, A. (1992). The ubiquitin system for protein degradation. Annu. Rev. Biochem. *61*, 761-807.

Hershko, A., and Ciechanover, A. (1998). The ubiquitin system. Annu. Rev. Biochem. *67*, 425–479.

Hicke, L. (2001). Protein regulation by monoubiquitin. Nat. Rev. Mol. Cell Biol. *2*, 195–201.

Hill, CP., Masters, EI., and Whitby, FG. (2002). The 11S regulators of 20S proteasome activity. Curr. Top. Microbiol. Immunol. *268*, 73–89.

Hirano, Y., Hayashi, H., Iemura, S-I., Hendil, KB., Niwa, S-I., Kishimoto, T., Kasahara, M., Natsume, T., Tanaka, K., and Murata, S. (2006). Cooperation of multiple chaperones required for the assembly of mammalian 20S proteasomes. Mol. Cell *24*, 977–984.

Hirano, Y., Hendil, KB., Yashiroda, H., Iemura, S., Nagane, R., Hioki, Y., Natsume, T., Tanaka, K., and Murata, S. (2005). A heterodimeric complex that promotes the assembly of mammalian 20S proteasomes. Nature *437*, 1381–1385.

Hirano, Y., Kaneko, T., Okamoto, K., Bai, M., Yashiroda, H., Furuyama, K., Kato, K., Tanaka, K., and Murata, S. (2008). Dissecting beta-ring assembly pathway of the mammalian 20S proteasome. EMBO J. *27*, 2204–2213.

Ho, PWL., Leung, CT., Liu, H., Pang, SYY., Lam, CSC., Xian, J., Li, L., Kung, MHW., Ramsden, DB., and Ho, SL. (2020). Age-dependent accumulation of oligomeric SNCA/α-synuclein from impaired degradation in mutant LRRK2 knockin mouse model of Parkinson disease: role for therapeutic activation of chaperone-mediated autophagy (CMA). Autophagy *16*, 347.

Hochstrasser, M (1996). Ubiquitin-dependent protein degradation. Annu. Rev. Genet. *30*, 405–439.

Hofmann, K., and Bucher, P. (1996). The UBA domain: a sequence motif present in multiple enzyme classes of the ubiquitination pathway. Trends. Biochem. Sci. *21*, 172–173.

Horvitz, HR. (1999). Genetic control of programmed cell death in the nematode Caenorhabditis elegans. Cancer Res. *44*, 817-829.

Hu, G., Lin, G., Wang, M., Dick, L., Xu, RM., Nathan, C., and Li, H. (2006). Structure of the Mycobacterium tuberculosis proteasome and mechanism of inhibition by a peptidyl boronate. Mol. Microbiol. *59*, 1417–1428.

Huang, CJ., Wu, D., Khan, FA., and Huo, LJ. (2015). DeSUMOylation: An Important Therapeutic Target and Protein Regulatory Event. DNA Cell Biol. *34*, 652–660.

Huang, X., Luan, B., Wu, J., and Shi, Y. (2016). An atomic structure of the human 26S proteasome. Nat. Struct. Mol. Biol. *23*, 778–785.

Huber, EM., Basler, M., Schwab, R., Heinemeyer, W., Kirk, CJ., Groettrup, M., and Groll, M. (2012). Immuno- and Constitutive Proteasome Crystal Structures Reveal Differences in Substrate and Inhibitor Specificity. Cell *148*, 727–738.

Huibregtse, JM., Scheffner, M., Beaudenon, S., and Howley, PM. (1995). A family of proteins structurally and functionally related to the E6-AP ubiquitin-protein ligase. Proc. Natl. Acad. Sci. U. S. A. *92*, 2563.

Jäger, S., Groll, M., Huber, R., Wolf, DH., and Heinemeyer, W. (1999). Proteasome β-type subunits: unequal roles of propeptides in core particle maturation and a hierarchy of active site function. J. Mol. Biol. *291*, 997–1013.

Jelinsky, SA., Estep, P., Church, GM., and Samson, LD. (2000). Regulatory networks revealed by transcriptional profiling of damaged *Saccharomyces cerevisiae* cells: Rpn4 links base excision repair with proteasomes. Mol. Cell Biol. *20*, 8157–8167.

Johnson, PR., Swanson, R., Rakhilina, L., and Hochstrasser, M. (1998). Degradation Signal Masking by Heterodimerization of MATα2 and MATa1 Blocks Their Mutual Destruction by the Ubiquitin-Proteasome Pathway. Cell *94*, 217–227.

Ju, D., Wang, L., Mao, X., and Xie, Y. (2004). Homeostatic regulation of the proteasome via an Rpn4-dependent feedback circuit. Biochem. Biophys. Res. Commun. *321*, 51–57.

Ju, D., and Xie, Y. (2004). Proteasomal Degradation of RPN4 via Two Distinct Mechanisms, Ubiquitin-dependent and -independent. J. Biol. Chem. *279*, 23851–23854.

Ju, D., and Xie, Y. (2006). Identification of the preferential ubiquitination site and ubiquitin-dependent degradation signal of Rpn4. J. Biol. Chem. *281*, 10657–10662.

Kaplan, GS., Torcun, CC., Grune, T., Ozer, NK., and Karademir, B. (2017). Proteasome inhibitors in cancer therapy: Treatment regimen and peripheral neuropathy as a side effect. Free Rad. Biol. Med. *103*, 1-13.

Karpov, DS., Grineva, EN., Leinsoo, AT., Nadolinskaia, NI., Danilenko, NK., Tutyaeva, V., Spasskaya, DS., Preobrazhenskaya, OV., Lysov, YP., and Karpov, VL. (2016). Functional analysis of Debaryomyces hansenii Rpn4 on a genetic background of Saccharomyces cerevisiae. FEMS Yeast Res. *17*, 98.

Kaushik, S., and Cuervo, AM. (2012). Chaperone-mediated autophagy: a unique way to enter the lysosome world. Trends. Cell Biol. *22*, 407.

Kaushik, S., and Cuervo, AM. (2015). Proteostasis and aging. Nat. Med. *21*, 1406–1415.

Kimura, H., Caturegli, P., Takahashi, M., and Suzuki, K. (2015). New Insights into the Function of the Immunoproteasome in Immune and Nonimmune Cells. J. Immunol. Res. *2015*, 1-8.

Kisselev, AF., Garcia-Calvo, M., Overkleeft, HS., Peterson, E., Pennington, MW., Ploegh, HL., Thornberry, NA., and Goldberg, AL. (2003). The caspase-like sites of proteasomes, their substrate specificity, new inhibitors and substrates, and allosteric interactions with the trypsin-like sites. J. Biol. Chem. *278*, 35869–35877.

Kisselev, AF., and Goldberg, AL. (2005). Monitoring Activity and Inhibition of 26S Proteasomes with Fluorogenic Peptide Substrates. Methods Enzymol. *398*, 364–378.

Kock, M., Nunes, MM., Hemann, M., Kube, S., Dohmen, RJ., Herzog, F., Ramos, PC., and Wendler, P. (2015). Proteasome assembly from 15S precursors involves major conformational changes and recycling of the Pba1–Pba2 chaperone. Nat. Commun. *6*, 6123.

Komander, D., Clague, MJ., and Urbé, S. (2009). Breaking the chains: structure and function of the deubiquitinases. Nat. Rev. Mol. Cell Biol. *10*, 550–563.

Komander, D., and Rape, M. (2012). The ubiquitin code. Annu. Rev. Biochem. *81*, 203–229.

Kravtsova-Ivantsiv, Y., Cohen, S., and Ciechanover, A. (2009). Modification by single ubiquitin moieties rather than polyubiquitination is sufficient for proteasomal processing of the p105 NF-kappaB precursor. Mol. Cell *33*, 496–504.

Krogan, NJ. *et al*. (2006). Global landscape of protein complexes in the yeast *Saccharomyces cerevisiae*. Nature *440*, 637–643.

Kunau, WH., Beyer, A., Franken, T., Götte, K., Marzioch, M., Saidowsky, J., Skaletz-Rorowski, A., and Wiebel, FF. (1993). Two complementary approaches to study peroxisome biogenesis in *Saccharomyces cerevisiae*: Forward and reversed genetics. Biochimie *75*, 209–224.

Kunjappu, MJ., and Hochstrasser, M. (2014). Assembly of the 20S proteasome. Biochim. Biophys. Acta. - Mol. Cell Res. *1843*, 2–12.

Kusmierczyk, AR., Kunjappu, MJ., Funakoshi, M., and Hochstrasser, M. (2008). A multimeric assembly factor controls the formation of alternative 20S proteasomes. Nat. Struct. Mol. Biol. *15*, 237–244.

Kusmierczyk, AR., Kunjappu, MJ., Kim, RY., and Hochstrasser, M. (2011). A conserved 20S proteasome assembly factor requires a C-terminal HbYX motif for proteasomal precursor binding. Nat. Struct. Mol. Biol. *18*, 622–629.

Kwon, Y. Do, Nagy, I., Adams, PD., Baumeister, W., and Jap, BK. (2004). Crystal Structures of the Rhodococcus Proteasome with and without its Pro-peptides: Implications for the Role of the Pro-peptide in Proteasome Assembly. J. Mol. Biol. *335*, 233–245.

Lander, GC., Estrin, E., Matyskiela, ME., Bashore, C., Nogales, E., and Martin, A. (2012). Complete subunit architecture of the proteasome regulatory particle. Nature *482*, 186–191.

Leggett, DS., Hanna, J., Borodovsky, A., Crosas, B., Schmidt, M., Baker, RT., Walz, T., Ploegh, H., and Finley, D. (2002). Multiple Associated Proteins Regulate Proteasome Structure and Function. Mol. Cell *10*, 495–507.

Lehmann, A., Janek, K., Braun, B., Kloetzel, PM., and Enenkel, C. (2002). 20 S proteasomes are imported as precursor complexes into the nucleus of yeast. J. Mol. Biol. *317*, 401–413.

Li, X., Kusmierczyk, AR., Wong, P., Emili, A., and Hochstrasser, M. (2007). β-Subunit appendages promote 20S proteasome assembly by overcoming an Ump1-dependent checkpoint. EMBO J. *26*, 2339–2349.

Li, X., Li, Y., Arendt, CS., and Hochstrasser, M. (2016). Distinct Elements in the Proteasomal β5 Subunit Propeptide Required for Autocatalytic Processing and Proteasome Assembly. J. Biol. Chem. *291*, 1991–2003.

Lin, G. *et al*. (2006). Mycobacterium tuberculosis prcBA genes encode a gated proteasome with broad oligopeptide specificity. Mol. Microbiol. *59*, 1405–1416.

London, MK., Keck, BI., Ramos, PC., and Dohmen, RJ. (2004). Regulatory mechanisms controlling biogenesis of ubiquitin and the proteasome. FEBS. Lett. *567*, 259–264.

Löwe, J., Stock, D., Jap, B., Zwickl, P., Baumeister, W., and Huber, R. (1995). Crystal structure of the 20S proteasome from the archaeon *T. acidophilum* at 3.4 A resolution. Science *268*, 533–539.

Lundgren, J., Masson, P., Mirzaei, Z., and Young, P. (2005). Identification and Characterization of a Drosophila Proteasome Regulatory Network . Mol. Cell Biol. *25*, 4662–4675.

Mamnun, YM., Pandjaitan, R., Mahé, Y., Delahodde, A., and Kuchler, K. (2002). The yeast zinc finger regulators Pdr1p and Pdr3p control pleiotropic drug resistance (PDR) as homo- and heterodimers in vivo. Mol. Microbiol. *46*, 1429–1440.

Mannhaupt, G., and Feldmann, H. (2007). Genomic evolution of the proteasome system among hemiascomycetous yeasts. J. Mol. Evol. *65*, 529–540.

Mannhaupt, G., Schnall, R., Karpov, V., Vetter, I., and Feldmann, H. (1999). Rpn4p acts as a transcription factor by binding to PACE, a nonamer box found upstream of 26S proteasomal and other genes in yeast. FEBS. Lett. *450*, 27–34.

Marques, AJ., Glanemann, C., Ramos, PC., and Dohmen, RJ. (2007). The C-terminal Extension of the β7 Subunit and Activator Complexes Stabilize Nascent 20 S Proteasomes and Promote Their Maturation. J. Biol. Chem. *282*, 34869–34876.

Marques, AJ., Palanimurugan, R., Matias, AC., Ramos, PC., and Dohmen, RJ. (2009). Catalytic Mechanism and Assembly of the Proteasome. Chem. Rev. *109*, 1509–1536.

Martinez-Fonts, K., Davis, C., Tomita, T., Elsasser, S., Nager, AR., Shi, Y., Finley, D., and Matouschek, A. (2020). The proteasome 19S cap and its ubiquitin receptors provide a versatile recognition platform for substrates. Nat. Commun. *11*, 1-16.

Matias, AC., Matos, J., Dohmen, RJ., and Ramos, PC. (2022). Hsp70 and Hsp110 Chaperones Promote Early Steps of Proteasome Assembly. Biomolecules *13*, 1-18.

Matias, AC., Ramos, PC., and Dohmen, RJ (2010). Chaperone-assisted assembly of the proteasome core particle. Biochem. Soc. Trans. *38*, 29–33.

Matias, A.C. (2010). Dissection of the early steps in the assembly of the 20S proteasome in *Saccharomyces cerevisiae*. PhD thesis, University of Algarve, Portugal.

Matyskiela, ME., and Martin, A. (2013). Design principles of a universal protein degradation machine. J. Mol. Biol. *425*, 199–213.

Maupin-Furlow, JA., Humbard, MA., Kirkland, PA., Li, W., Reuter, CJ., Wright, AJ., and Zhou, G. (2006). Proteasomes from Structure to Function: Perspectives from Archaea. Curr. Top. Dev. Biol. *75*, 125–169.

Maytal-Kivity, V., Reis, N., Hofmann, K., and Glickman, MH. (2002). MPN+, a putative catalytic motif found in a subset of MPN domain proteins from eukaryotes and prokaryotes, is critical for Rpn11 function. BMC Biochem. *3*, 28.

Meierhofer, D., Wang, X., Huang, L., and Kaiser, P. (2008). Quantitative analysis of global ubiquitination in HeLa cells by mass spectrometry. J. Proteome Res. *7*, 4566–4576.

Meiners, S., Heyken, D., Weller, A., Ludwig, A., Stangl, K., Kloetzel, PM., and Krüger, E. (2003). Inhibition of Proteasome Activity Induces Concerted Expression of Proteasome

Genes and de Novo Formation of Mammalian Proteasomes. J. Biol. Chem. *278*, 21517–21525.

Metzger, MB., Pruneda, JN., Klevit, RE., and Weissman, AM. (2013). RING-type E3 ligases: master manipulators of E2 ubiquitin-conjugating enzymes and ubiquitination. Biochim. Biophys. Acta. *1843*, 47–60.

Mizuno, K., Nakamura, T., Takada, K., Sakakibara, S., and Matsuo, H. (1987). A membrane-bound, calcium-dependent protease in yeast alpha-cell cleaving on the carboxyl side of paired basic residues. Biochem. Biophys. Res. Commun. *144*, 807–814.

Morawe, T., Hiebel, C., Kern, A., and Behl, C. (2012). Protein Homeostasis, Aging and Alzheimer's Disease. Mol. Neurobiol. *46*, 41.

Mülleder, M., Capuano, F., Pir, P., Christen, S., Sauer, U., Oliver, SG., and Ralser, M. (2012). A prototrophic deletion mutant collection for yeast metabolomics and systems biology. Nat. Biotechnol. *30*, 1176–1178.

Mullooly, M., McGowan, PM., Crown, J., and Duffy, MJ. (2016). The ADAMs family of proteases as targets for the treatment of cancer. Cancer Biol. Ther. *17*, 870.

Mumberg, D., Muller, R., and Funk, M. (1994). Regulatable promoters of *Saccharomyces cerevisiae*: comparison of transcriptional activity and their use for heterologous expression. Nucleic Acids Res. *22*, 5767.

Murata, S., Sasaki, K., Kishimoto, T., Niwa, SI., Hayashi, H., Takahama, Y., and Tanaka, K. (2007). Regulation of CD8+ T cell development by thymus-specific proteasomes. Science *316*, 1349–1353.

Murata, S., Takahama, Y., Kasahara, M., and Tanaka, K. (2018). The immunoproteasome and thymoproteasome: functions, evolution and human disease. Nat. Immunol. *19*, 923–931.

Murata, S., Yashiroda, H., and Tanaka, K. (2009). Molecular mechanisms of proteasome assembly. Nat. Rev. Mol. Cell Biol. *10*, 104–115.

Nunes, M.N. (2015). Characterization of proteasome precursor complexes. PhD thesis, University of Cologne.

Owsianik, G., Balzi, L., and Ghislain, M. (2002). Control of 26S proteasome expression by transcription factors regulating multidrug resistance in *Saccharomyces cerevisiae*. Mol. Microbiol. *43*, 1295–1308.

Ozkaynak, E., Finley, D., and Varshavsky, A. (1984). The yeast ubiquitin gene: head-to-tail repeats encoding a polyubiquitin precursor protein. Nature *312*, 663–666.

Peng, J., Schwartz, D., Elias, JE., Thoreen, CC., Cheng, D., Marsischky, G., Roelofs, J., Finley, D., and Gygi, SP. (2003). A proteomics approach to understanding protein ubiquitination. Nat. Biotechnol. *21*, 921–926.

Perry, JJP., Tainer, JA., and Boddy, MN. (2008). A SIM-ultaneous role for SUMO and ubiquitin. Trends Biochem. Sci. *33*, 201–208.

Pronk, JT. (2002). Auxotrophic yeast strains in fundamental and applied research. Appl. Environ. Microbiol. *68*, 2095–2100.

Ramos, PC., and Dohmen, RJ. (2008). PACemakers of proteasome core particle assembly. Structure *16*, 1296–1304.

Ramos, PC., Höckendorff, J., Johnson, ES., Varshavsky, A., and Dohmen, RJ. (1998). Ump1p Is Required for Proper Maturation of the 20S Proteasome and Becomes Its Substrate upon Completion of the Assembly. Cell *92*, 489–499.

Ramos, PC., Marques, AJ., London, MK., and Dohmen, RJ. (2004). Role of C-terminal extensions of subunits beta2 and beta7 in assembly and activity of eukaryotic proteasomes. J. Biol. Chem. *279*, 14323–14330.

Ravid, T., and Hochstrasser, M. (2008). Diversity of degradation signals in the ubiquitin–proteasome system. Nat. Rev. Mol. Cell Biol. *9*, 679–689.

Rechsteiner, M., and Hill, CP. (2005). Mobilizing the proteolytic machine: cell biological roles of proteasome activators and inhibitors. Trends Cell Biol. *15*, 27–33.

Sá-Moura, B. *et al*. (2013). Biochemical and biophysical characterization of recombinant yeast proteasome maturation factor ump1. Comput. Struct. Biotechnol. J. *7*,1-9.

Sadre-Bazzaz, K., Whitby, FG., Robinson, H., Formosa, T., and Hill, CP. (2010). Structure of a Blm10 complex reveals common mechanisms for proteasome binding and gate opening. Mol. Cell *37*, 728–735.

Saeki, Y., and Tanaka, K. (2012). Assembly and function of the proteasome. Methods Mol. Biol. *832*, 315–337.

Sahu, I., and Glickman, MH. (2021). Structural Insights into Substrate Recognition and Processing by the 20S Proteasome. Biomolecules *11*, 1–15.

Saibil, H. (2013). Chaperone machines for protein folding, unfolding and disaggregation. Nat. Rev. Mol. Cell Biol. *14*, 630.

Schmidt, M., Haas, W., Crosas, B., Santamaria, PG., Gygi, SP., Walz, T., and Finley, D. (2005). The HEAT repeat protein Blm10 regulates the yeast proteasome by capping the core particle. Nat. Struct. Mol. Biol. *12*, 294–303.

Schnell, HM. *et al*. (2021). Structures of chaperone-associated assembly intermediates reveal coordinated mechanisms of proteasome biogenesis. Nat. Struct. Mol. Biol. *28*, 418–425.

Schoenheimer, R. (1942). Dynamic State of Body Constituents. Cambridge Harvard Univ. Press.

Schwab, S. (2017). Assembly and Regulation of the Yeast 20S Proteasome. PhD thesis, University of Cologne.

Seemüller, E., Lupas, A., and Baumeister, W. (1996). Autocatalytic processing of the 20S proteasome. Nature *382*, 468–470.

Seemüller, E., Lupas, A., Stock, D., Löwe, J., Huber, R., and Baumeister, W. (1995). Proteasome from Thermoplasma acidophilum: a threonine protease. Science *268*, 579–582.

Shirozu, R., Yashiroda, H., and Murata, S. (2015). Identification of minimum Rpn4-responsive elements in genes related to proteasome functions. FEBS. Lett. *589*, 933–940.

Sitia, R., and Braakman, I. (2003). Quality control in the endoplasmic reticulum protein factory. Nat. 2003 4266968 *426*, 891–894.

Sooparb, S., Price, SR., Shaoguang, J., and Franch, HA. (2004). Suppression of chaperone-mediated autophagy in the renal cortex during acute diabetes mellitus. Kidney Int. *65*, 2135–2144.

Sorimachi, H., Hata, S., and Ono, Y. (2011). Calpain chronicle - an enzyme family under multidisciplinary characterization. Proc. Jpn. Acad. Ser. B. Phys. Biol. Sci. *87*, 287.

Stadtmueller, BM., Kish-Trier, E., Ferrell, K., Petersen, CN., Robinson, H., Myszka, DG., Eckert, DM., Formosa, T., and Hill, CP. (2012). Structure of a proteasome Pba1-Pba2 complex: implications for proteasome assembly, activation, and biological function. J. Biol. Chem. *287*, 37371–37382.

Stein, RL., Melandri, F., and Dick, L. (1996). Kinetic characterization of the chymotryptic activity of the 20S proteasome. Biochemistry *35*, 3899–3908.

Suppahia, A., Itagi, P., Burris, A., Kim, FMG., Vontz, A., Kante, A., Kim, S., Im, W., Deeds, EJ., and Roelofs, J. (2020). Cooperativity in Proteasome Core Particle Maturation. IScience *23*, 1-29.

Suresh, HG., Pascoe, N., and Andrews, B. (2020). The structure and function of deubiquitinases: lessons from budding yeast. Open Biol. *10*, 1-18.

Tagwerker, C., Flick, K., Cui, M., Guerrero, C., Dou, Y., Auer, B., Baldi, P., Huang, L., and Kaiser, P. (2006). A Tandem Affinity Tag for Two-step Purification under Fully Denaturing Conditions: Application in Ubiquitin Profiling and Protein Complex Identification Combined with *in vivo* Cross-Linking. Mol. Cell Proteomics *5*, 737–748.

Takagi, K., Saeki, Y., Yashiroda, H., Yagi, H., Kaiho, A., Murata, S., Yamane, T., Tanaka, K., Mizushima, T., and Kato, K. (2014). Pba3–Pba4 heterodimer acts as a molecular matchmaker in proteasome α-ring formation. Biochem. Biophys. Res. Commun. *450*, 1110–1114.

Le Tallec, B., Barrault, M-B., Courbeyrette, R., Guérois, R., Marsolier-Kergoat, M-C., and Peyroche, A. (2007). 20S proteasome assembly is orchestrated by two distinct pairs of chaperones in yeast and in mammals. Mol. Cell *27*, 660–674.

Tanahashi, N., Murakami, Y., Minami, Y., Shimbara, N., Hendil, KB., and Tanaka, K. (2000). Hybrid proteasomes. Induction by interferon-gamma and contribution to ATP-dependent proteolysis. J. Biol. Chem. *275*, 14336–14345.

Tian, G., Park, S., Lee, MJ., Huck, B., McAllister, F., Hill, CP., Gygi, SP., and Finley, D. (2011). An asymmetric interface between the regulatory and core particles of the proteasome. Nat. Struct. Mol. Biol. *18*, 1259–1267.

Tomko, RJ., and Hochstrasser, M. (2013). Molecular Architecture and Assembly of the Eukaryotic Proteasome. Annu. Rev. Biochem. *82*, 415–445.

Toste Rêgo, A., and da Fonseca, PCA. (2019). Characterization of Fully Recombinant Human 20S and 20S-PA200 Proteasome Complexes. Mol. Cell *76*, 138-147.

Uekusa, Y., Okawa, K., Yagi-Utsumi, M., Serve, O., Nakagawa, Y., Mizushima, T., Yagi, H., Saeki, Y., Tanaka, K., and Kato, K. (2014). Backbone 1H, 13C, and 15N assignments of yeast Ump1, an intrinsically disordered protein that functions as a proteasome assembly chaperone. Biomol. NMR Assign. *8*, 383–386.

Unno, M., Mizushima, T., Morimoto, Y., Tomisugi, Y., Tanaka, K., Yasuoka, N., and Tsukihara, T. (2002). The structure of the mammalian 20S proteasome at 2.75 A resolution. Structure *10*, 609–618.

Ustrell, V., Hoffman, L., Pratt, G., and Rechsteiner, M. (2002). PA200, a nuclear proteasome activator involved in DNA repair. EMBO J. *21*, 3516–3525.

Uttenweiler, A., and Mayer, A. (2008). Microautophagy in the yeast *Saccharomyces cerevisiae*. Methods Mol. Biol. *445*, 245–259.

Vabulas, RM., and Hartl, FU. (2005). Protein synthesis upon acute nutrient restriction relies on proteasome function. Science *310*, 1960–1963.

Varshavsky, A. (1996). The N-end rule: functions, mysteries, uses. Proc. Natl. Acad. Sci. U. S. A. *93*, 12142–12149.

Varshavsky, A. (2012). The Ubiquitin System, an Immense Realm. Annu. Rev. Biochem. *81*, 167-76.

Van Der Veen, AG, and Ploegh, HL (2012). Ubiquitin-Like Proteins. Annu. Rev. Biochem. *81*, 323-357.

Velichutina, I., Connerly, PL., Arendt, CS., Li, X., and Hochstrasser, M. (2004). Plasticity in eucaryotic 20S proteasome ring assembly revealed by a subunit deletion in yeast. EMBO J. *23*, 500–510.

Vembar, SS., and Brodsky, JL. (2008). One step at a time: endoplasmic reticulum-associated degradation. Nat. Rev. Mol. Cell Biol. *9*, 944.

Verma, R., Aravind, L., Oania, R., McDonald, WH., Yates, JR., Koonin, E. V., and Deshaies, RJ. (2002). Role of Rpn11 Metalloprotease in Deubiquitination and Degradation by the 26S Proteasome. Science *298*, 611–615.

Wang, X., Xu, H., Ha, SW., Ju, D., and Xie, Y. (2010). Proteasomal degradation of Rpn4 in *Saccharomyces cerevisiae* is critical for cell viability under stressed conditions. Genetics *184*, 335–342.

Wang, Z., Li, H., Guan, W., Ling, H., Wang, Z., Mu, T., Shuler, FD., and Fang, X. (2010). Human SUMO fusion systems enhance protein expression and solubility. Protein Expr. Purif. *73*, 203–208.

Wani, PS., Rowland, MA., Ondracek, A., Deeds, EJ., and Roelofs, J. (2015). Maturation of the proteasome core particle induces an affinity switch that controls regulatory particle association. Nat. Commun. *6*, 6384.

Watanabe, A., Yashiroda, H., Ishihara, S., Lo, M., and Murata, S. (2022). The Molecular Mechanisms Governing the Assembly of the Immuno- and Thymoproteasomes in the Presence of Constitutive Proteasomes. Cells *11*, 1-16.

Witt, E., Zantopf, D., Schmidt, M., Kraft, R., Kloetzel, P-M., and Krüger, E. (2000). Characterisation of the newly identified human Ump1 homologue POMP and analysis of LMP7(β5i) incorporation into 20 S proteasomes. J. Mol. Biol. *301*, 1–9.

Woese, CR. (1970). Codon recognition: The allosteric ribosome hypothesis. J. Theor. Biol. *26*, 83–88.

Xie, Y., and Varshavsky, A. (2001). RPN4 is a ligand, substrate, and transcriptional regulator of the 26S proteasome: A negative feedback circuit. Proc. Natl. Acad. Sci. U. S. A. *98*, 3056–3061.

Xu, G., and Jaffrey, SR. (2013). Proteomic Identification of Protein Ubiquitination Events. Biotechnol. Genet. Eng. Rev. *29*, 73.

Xu, P., Duong, DM., Seyfried, NT., Cheng, D., Xie, Y., Robert, J., Rush, J., Hochstrasser, M., Finley, D., and Peng, J. (2009). Quantitative Proteomics Reveals the Function of Unconventional Ubiquitin Chains in Proteasomal Degradation. Cell *137*, 133.

Yan, C., Gao, N., Cao, X., Yao, L., Zhou, YJ., and Gao, J. (2023). Auxotrophs compromise cell growth and fatty acid production in *Saccharomyces cerevisiae*. Biotechnol J. *18*, 1-8.

Yang, Z., and Klionsky, DJ. (2010). Eaten alive: a history of macroautophagy. Nat. Cell Biol. *12*, 814.

Yao, T., and Cohen, RE. (2002). A cryptic protease couples deubiquitination and degradation by the proteasome. Nature *419*, 403–407.

Yao, Y., Toth, CR., Huang, L., Wong, ML., Dias, P., Burlingame, AL., Coffino, P., and Wang, CC. (1999). alpha5 subunit in Trypanosoma brucei proteasome can self-assemble to form a cylinder of four stacked heptamer rings. Biochem. J. *344*, 349–358.

Yashiroda, H. *et al*. (2008). Crystal structure of a chaperone complex that contributes to the assembly of yeast 20S proteasomes. Nat. Struct. Mol. Biol. *15*, 228–236.

Yoshimura, T. *et al*. (1993). Molecular Characterization of the "26S" Proteasome Complex from Rat Liver. J. Struct. Biol. *111*, 200–211.

Zaiss, DMW., Standera, S., Kloetzel, P-M., and Sijts, AJAM. (2002). PI31 is a modulator of proteasome formation and antigen processing. Proc. Natl. Acad. Sci. U. S. A. *99*, 14344–14349.

Zimmermann, J., Ramos, PC., and Dohmen, RJ. (2022). Interaction with the Assembly Chaperone Ump1 Promotes Incorporation of the β7 Subunit into Half-Proteasome Precursor Complexes Driving Their Dimerization. Biomolecules *12*, 1-15.

Ziv, I. *et al*. (2011). A Perturbed Ubiquitin Landscape Distinguishes Between Ubiquitin in Trafficking and in Proteolysis. Mol Cell Proteomics *10*, 1-22.

Zühl, F., Seemüller, E., Golbik, R., and Baumeister, W. (1997). Dissecting the assembly pathway of the 20S proteasome. FEBS. Lett. *418*, 189–194.

Zwickl, P., Kleinz, J., and Baumeister, W. (1994). Critical elements in proteasome assembly. Nat. Struct. Biol. *1*, 765–770.

Peters, J-M., Harris, JR., Finley, D. (1998). Ubiquitin and the Biology of the Cell, New York.

List of abbreviations

°C	Degree Celsius
µg	Microgram
µl	Microliter
µm	Micrometer
µM	Micromolar
a.a.	Amino acid
AAA+	ATPases associated with various cellular activities
ADAM	A desintegrase and metalloproteinase
ALP	Autophagy-lysosome pathway
AMC	7-amino-4-methylcoumarin
AMP	Adenosine-monophosphate
AP	Alkaline phosphatase
APG-LYS	Autophagosome-lysosome
APS	Ammonium persulfate
Asn	Asparagine
Asp	Aspartic acid
ATP	Adenosine-triphosphate
bp	Base pair
BSA	Bovine serum albumin
C	Concentrated and senp1 cleaved
CBB	Coomassie Brilliant Blue
CE	Crude extract
cm^2	Square centimeter
CMA	Chaperone-mediated autophagy
Co-IP	Co-immunoprecipitation

CP	Core particle
CTE	C-terminal extension
CV	Column bed volumes
DNA	Deoxyribonucleic acid
dNTP	Deoxynucleotide triphosphate
DTT	Dithiothreitol
DUB	Deubiquitylating enzyme
E	Elution
E. coli or *Ec*.	*Escherichia coli*
e.g.	For example
EDTA	Ethylenediaminetetraacetic acid
EM	Electron microscopy
ER	Endoplasmic reticulum
ERAD	Endoplasmic reticulum-associated degradation
EV	Empty vector
FD	Fast digest
FLAG or F	FLAG epitope (DYKDDDDK)
FT	Flow through
FW	Forward
g	Gram
Gal	Galactose
GFP	Green fluorescent protein
Gln	Glutamine
Glu	Glucose
Gly	Glycine
h	Hour
HA	Hemagglutinin epitope (YPYDVPDYA)
HbYX	Hydrophobic amino acid/ tyrosine/ random amino acid
HECT	Homologous to the E6-AP Carboxyl Terminus
HF	High-fidelity
His or H	Histidine
HRP	Horseradish peroxidase

HSC70	Heat-shock cognate protein of 70 kDa
HSF	Heat-shock transcription factor
Hsp	Heat-shock protein
Hz	Hertz
IN	Input
JAMM	JAB1, MPN, MOV34 family
kb	Kilobase
kDa	Kilodalton
L2A	Lysosome-associated membrane protein type 2A
LB	Luria-Bertani
Leu	Leucine
LLB	Laemmli lysis buffer
LRR	Leucine-rich-repeat
LS	Leader sequence
Lys	Lysine
M	Molar
MA	Macroautophagy
mA	Milliampere
MBP	Maltose binding protein
MDa	Megadalton
mg	Milligram
MHC	Major Histocompatibility Complex
min	Minute
MINDY	Motif-interacting with ubiquitin-containing novel DUB family
MJD	Machado-Josephin domain-containing novel DUB
ml	Milliliter
mm	Millimeter
mM	Millimolar
mRNA	Messenger ribonucleic acid
MS	Mass spectrometry
ms	Millisecond
MWCO	Molecular weight cut-off

NAT1	Nα-acetyltransferases
NB	Native Buffer
NG	Neongreen
Ni	Nickel
nm	Nanometer
NTE	N-terminal extension
OD	Optical density
OTU	Ovarian tumor protease
PA28	Proteasome activator of apparent subunit molecular weight 28 kDa
PAC	Proteasome assembly chaperone
PACE	Proteasome associated control elements
PAGE	Polyacrylamide gel electrophoresis
Pba	Proteasome biogenesis associated protein
PBS	Phosphate-buffered saline
PC	Precursor complex
PCR	Polymerase chain reaction
PEG	Polyethylene glycol
PMSF	Phenylmethylsulfonylfluorid
POD	Peroxidase
POMP	Proteasome maturation protein
PPi	Pyrophosphate
Pro	Propeptide
PTM	Post-translational modification
PVDF	Polyvinylidene fluoride
qPCR	Quantitative polymerase chain reaction
RBR	RING-between-RING
REG	11S regulator
RING	Really interesting new gene
RNA	Ribonucleic acid
RP	Regulatory particle
Rpm	Revolutions per minute
RT	Room temperature

RV	Reverse
S. cerevisiae or *Sc.*	*Saccharomyces cerevisiae*
SD	Synthetic medium
SDS	Sodium dodecyl sulfate
sec or s	Second
SENP	Sentrin/SUMO-specific protease
Senp	Sentrin-specific protease
SL	Soluble
STUbLs	SUMO-targeted ubiquitin ligase
Suc-LLVY	N-succinyl-leucine-leucine-valine-tyrosine
SUMO	Small ubiquitin-like modifier
T	Total
TEMED	Tetramethylethylenediamine
TEV	Tabbaco etch virus
Thr	Threonine
Tm	Melting temperature
Trp	Tryptophan
Ub	Ubiquitin
UB	Unbound
UBA	Ubiquitin association domain
UBL	Ubiquitin-like protein
UCH	Ubiquitin C-terminal hydrolase
Ump1	Underpinning maturation of proteasome
UPS	Ubiquitin-proteasome system
URA	Uracil
USP/UBP	Ubiquitin-specific protease
V	Volt
v/v	Volume per volume
w/v	Weight per volume
WT	Wild-type
ZUFSP	Zinc finger with UFM1-specific peptidase domain protein protease
Δ	Deletion

Acknowledgement

First of all, I want to thank **Prof. Dr. Jürgen Dohmen** for giving me the opportunity to work on this project. Scientific research often feels like a roller coaster, but you have the impressive ability to keep people positive and motivated. Your passion for science is enviable. I appreciate very much that you put so much effort and time in each person of your lab. Your kind and humorous personality made me always feel comfortable.

I thank Prof. Dr. Kay Hofmann, Prof. Dr. Ulrich Baumann and Dr. Karsten Klopffleisch for accepting to be my thesis committee members. I really enjoyed the supportive and helpful conversations and discussions. Furthermore, I would like to thank Dr. Thomas Hermanns for the gift of the Senp1 plasmid (and the purified Senp1 before I had to do it myself).

Paula. Your enthusiasm for everything is incredible. Thanks for all the scientific and non-scientific conversations, your encouraging words and well-intentioned advices. To do handicrafts with you was always a lot of fun. I am very happy that I could work with you together on the big puzzle of the proteasome.

To all the current and former members of the lab: I could not imagine to spend my PhD time with other people than you. The working atmosphere was always respectful and pleasant. Everyone is extremely cheerful and patient. Each day was a lot of fun.

Especially, I want to thank you guys: Stefan, LENNY, **Friederike**, Max & *Kai*. I barely know how to put into words how much I appreciated the last years with you. I enjoyed all the lunch breaks, table football matches, afternoon coffees, cakes and ice-creams, discussions about useless and curious stuff, Mauerbiere, Gins, rounds of beerpong, smoking breaks without smoking, parties, days and nights. For me, you are not only colleagues, but friends. With you, it wasn't work but spending time with people I love. I will never forget the time we spent together. Each of you has a piece of my heart.

How lucky am I to have something that makes saying goodbye so hard. ~Winnie the Pooh.

Eidesstattliche Erklärung

Hiermit versichere ich an Eides statt, dass ich die vorliegende Dissertation selbstständig und ohne die Benutzung anderer als der angegebenen Hilfsmittel und Literatur angefertigt habe. Alle Stellen, die wörtlich oder sinngemäß aus veröffentlichten und nicht veröffentlichten Werken dem Wortlaut oder dem Sinn nach entnommen wurden, sind als solche kenntlich gemacht. Ich versichere an Eides statt, dass diese Dissertation noch keiner anderen Fakultät oder Universität zur Prüfung vorgelegen hat; dass sie - abgesehen von unten angegebenen Teilpublikationen und eingebundenen Artikeln und Manuskripten - noch nicht veröffentlicht worden ist sowie, dass ich eine Veröffentlichung der Dissertation vor Abschluss der Promotion nicht ohne Genehmigung des Promotionsausschusses vornehmen werde. Die Bestimmungen dieser Ordnung sind mir bekannt. Darüber hinaus erkläre ich hiermit, dass ich die Ordnung zur Sicherung guter wissenschaftlicher Praxis und zum Umgang mit wissenschaftlichem Fehlverhalten der Universität zu Köln gelesen und sie bei der Durchführung der Dissertation zugrundeliegenden Arbeiten und der schriftlich verfassten Dissertation beachtet habe und verpflichte mich hiermit, die dort genannten Vorgaben bei allen wissenschaftlichen Tätigkeiten zu beachten und umzusetzen. Ich versichere, dass die eingereichte elektronische Fassung der eingereichten Druckfassung vollständig entspricht.

Teilpublikationen:

Zimmermann, J., Ramos, P. C. and Dohmen, R. J. (2022) 'Interaction with the Assembly Chaperone Ump1 Promotes Incorporation of the β7 Subunit into Half-Proteasome Precursor Complexes Driving Their Dimerization', *Biomolecules*. MDPI, 12(2), p. 253.

Köln, den 14.08.2023 Jessica Zimmermann

J. Zimmermann